Bulletin No. 56

Deformed Lower Cretaceous coal-bearing strata

of the Grande Cache area, Alberta

C.W. Langenberg,
W. Kalkreuth, C.B. Wrightson

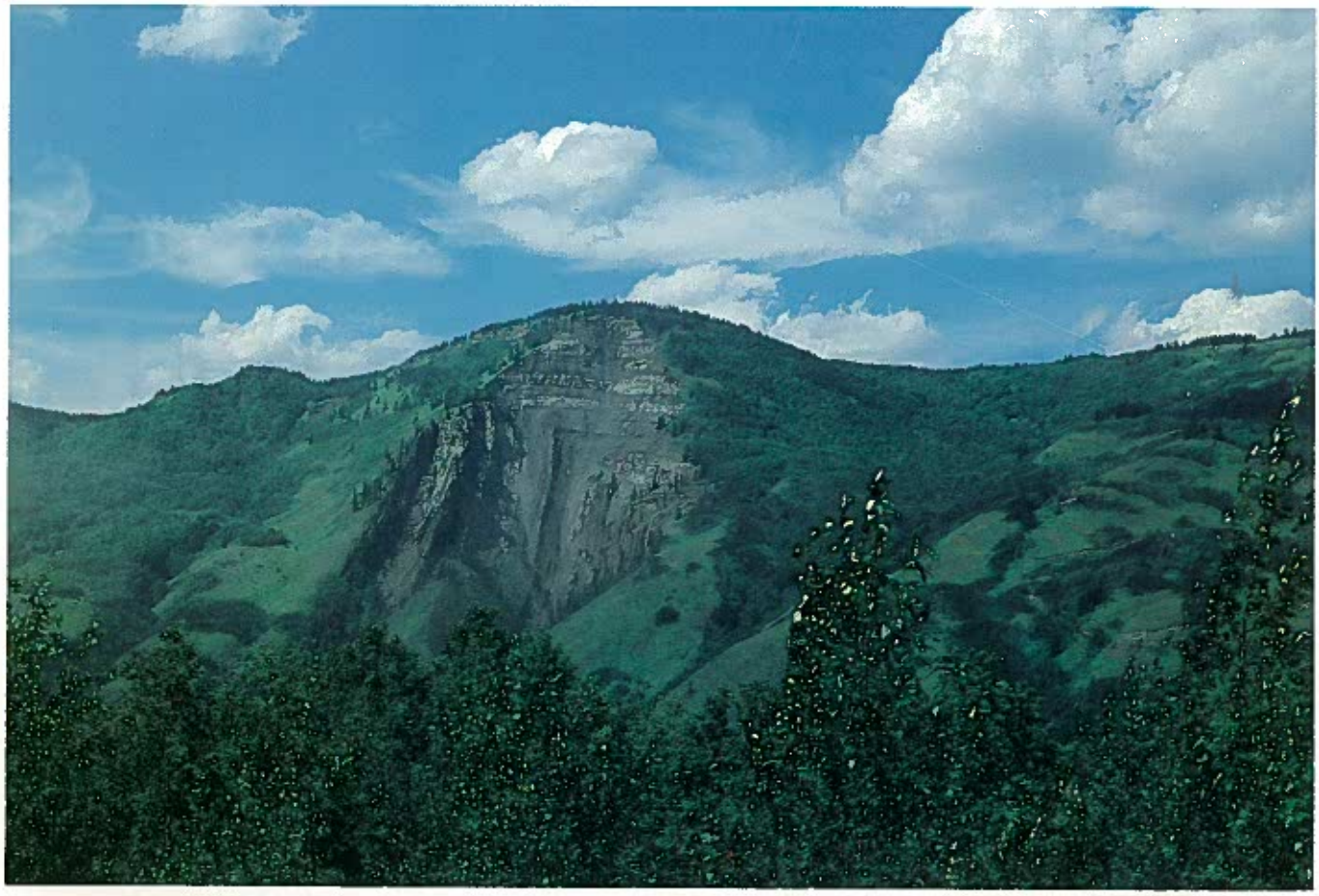

ALBERTA RESEARCH COUNCIL
Alberta Geological Survey

Deformed Lower Cretaceous coal-bearing strata

of the Grande Cache area, Alberta

C.W. Langenberg
Alberta Geological Survey,
Alberta Research Council, Edmonton

W. Kalkreuth
Institute of Sedimentary
and Petroleum Geology, Calgary

C.B. Wrightson
B.C. Geological Survey Branch, Victoria

Cover photo:

Overview of the Barrett Anticline, containing the major economic coal seams (cf. figure 8).

GEOLOGICAL SURVEY DEPARTMENT, ALBERTA RESEARCH COUNCIL
EDMONTON, ALBERTA, CANADA 1987

Preface

The foothills and mountains of Alberta contain most of the province's exportable coal resources. For this reason, the Alberta Research Council has been developing techniques that provide a basis for the establishment of exploration targets. From detailed studies of deformed coal-bearing strata of the Grande Cache area, a detailed geological map and cross sections were constructed. It is anticipated that the techniques used in this study will be applicable to the development of other coal fields along Alberta's deformed coal belt.

Jan Boon, Head
Alberta Geological Survey
December 1987

Acknowledgments

Smoky River Coal Limited is thanked for allowing access to their property and for releasing mine plans and drill hole data to the Alberta Research Council. This study greatly benefited from continuing discussions with Smoky River Coal Limited staff, especially Richard Dawson and Dave Fawcett. Steve Brownridge and Chuck James ably assisted with fieldwork, and Doug Grimes with data analysis. Shell Canada Limited is thanked for making a seismic section available to the Alberta Research Council.

Further thanks are due to Dr. J.H. Wall of the Geological Survey of Canada, Calgary, for providing a micropaleontology report, to Dr. S.G. Pemberton for identifying trace fossils in the field, to Dr. C.R. Stelck for identifying fossils in hand specimen, and to Dr. H.A.K. Charlesworth (all from the University of Alberta, Department of Geology) for the use of the TRIPOD computer program. Dr. R.A. Rahmani is thanked for his help in sedimentological methods. The manuscript was critically read by Drs. P.J. McCabe and M.E. McMechan. Their helpful comments are greatly appreciated. Permission was obtained from the Bulletin of Canadian Petroleum Geology and the Canadian Journal of Earth Sciences to reproduce illustrations that were published in Langenberg and McMechan (1985) and Kalkreuth and Langenberg (1986).

Copies of this report are available from:

Edmonton:
Alberta Research Council
Publications Sales
250 Karl Clark Road
Edmonton, Alberta
Canada

Phone (403)450-5111

Mailing address:
Alberta Research Council
Publications Sales
PO Box 8330
Postal Station F
Edmonton, Alberta
Canada T6H 5X2

Calgary:
Alberta Research Council
Publications Sales
3rd Floor
6815 - 8 Street NE
Calgary, Alberta
Canada T2E 7H7

Phone (403)297-2600

Contents

Tables

Figures

Abstract

Deformed coal-bearing strata of the Grande Cache area were studied to obtain techniques that could be used in exploration and development of the Smoky River coal field and other coal fields of Alberta's foothills and mountains. The strongly folded and thrusted, exposed rocks of the Grande Cache area can be divided into three thrust sheets—the Syncline Hills, Mason, and Muskeg thrust sheets. The oldest rocks are marine and non-marine strata of the Jurassic/Cretaceous Nikanassin Formation. The Lower Cretaceous Luscar Group includes a thin basal conglomerate (Cadomin Formation), a predominantly non-marine sandstone and shale unit that locally contains coal (Gladstone Formation), a shallow marine shale and sandstone unit (Moosebar Formation), and an upper non-marine sandstone and shale unit that contains thick commercial coal seams (Gates Formation). The thick coals of the Gates Formation were probably deposited on a coastal or delta plain. That formation is overlain by marine shales of the Albian/Cenomanian Shaftesbury Formation, largely marine sandstones and shales of the Dunvegan Formation, and marine shales of the late Cenomanian Kaskapau Formation. These strata are complexly deformed by the Laramide Orogeny, between early Campanian and late Eocene. The deformation proceeded from southwest to northeast. It is estimated that the main deformation in the Grande Cache area took place at the end of the Paleocene.

Shortening of these rocks, estimated from balanced downplunge cross sections, averages 31 percent. This shortening is accomplished by folding and faulting. Folds in the area are generally of the chevron variety, caused by shortening of a multilayered sequence of alternating competent and incompetent strata, where the thickness of the competent layers is fairly constant. The folds are cylindrical and maintain their shapes over distances of up to 2 km along the trend. However, at their tapering ends, they are conical. The majority of faults are southwest-dipping thrusts, displaying ramps that cut up stratigraphic section and flats that are parallel to bedding. Close connection between thrusting and folding is shown by fault-to-fold displacement transfer. The deformation model for the Grande Cache area is a series of fold-thrust structures with cylindrical chevron folds, which become conical at their tapering ends.

Incompetent material, such as coal, has flowed into dilation zones, which develop in the hinges of chevron folds. Another process of structural thickening of coal is duplex thrusting, where the roof thrust is the top and the floor thrust the bottom of the coal seam. Both structural situations are important coal exploration targets in the Grande Cache area. The rank of the coals, as determined by measuring mean maximum vitrinite reflectances, ranges from medium to low volatile bituminous. The rank data indicate that the degree of coalification was largely established during burial from Albian to late Paleocene times, before folding and faulting started.

Most joints are extensional with preferred orientations that conform to regional patterns of foothills and plains. They probably result from erosional unloading and uplift. Other joints show effects of compressive stress across the fracture plane, as indicated by slickensides. Some of these can be related to the regional movement picture of the fold and thrust belt; others are probably a result of gravitational sliding of blocks into valleys after erosional unloading and resulting uplift.

Introduction

Structural position is an important factor in the mineability of coal in Alberta's foothills and mountains. For this reason, the Alberta Research Council, in cooperation with the University of Alberta and the Geological Survey of Canada, has studied deformed coal-bearing rocks in the foothills of the Grande Cache area. Some of the results of the studies have been published recently in scientific journals (Langenberg, 1984 and 1985; Langenberg and McMechan, 1985; Kalkreuth and Langenberg, 1986). The purpose of this publication is to integrate findings from those studies into a general description of the geology of the Grande Cache area. On a detailed geological map and nine cross sections (figures 1 and 2, in pocket) are the locations of coal seams and information that define models for coal exploration in the Grande Cache area and other regions of Alberta's foothills and mountains.

Study area

The study area is located in west-central Alberta, between latitudes 53°55′ and 54°03′N, and longitudes 119°01′ and 119°15′W. The area forms part of the Grande Cache (NTS 83E/14) and Copton Creek (NTS 83L/3) mapsheets and covers approximately 140 km². Direct access to the area is obtained through Highway 40, which connects Hinton with Grande Cache. This highway extends toward the offices and plant facilities of Smoky River Coal Limited near the center of the study area. From there, several well-maintained mine property roads and a forestry road result in easy access to most corners of the study area.

The area consists mainly of forested mountains. However, some of these mountains reach altitudes higher than 1800 m. Consequently, they often extend above timberline and have little or no vegetation on rocky peaks. Topographic relief is greatest and bed rock exposure best on mountain slopes adjacent to the Smoky River, an antecedent river flowing northeastward. Additional outcrops are found on exposed ridges, along tributary streams of the Smoky River, and at coal mining sites. The area is situated on coal leases held by Smoky River Coal Limited. Consequently, permission should be obtained from that company before entering the area.

Previous work

Outcrops of thick coal seams are evident at many localities along the Smoky River; hence, the presence of coal in the area was likely known to the earliest travellers. Short reports by MacVicar (1917, 1920) provide the first documentation of coal occurrences. Later, MacVicar (1924) published a more extensive report on the Smoky River area, which included a geological sketch map and data on coal quality. He cor-

related the coal-bearing strata of the Smoky River with the coal-bearing Kootenay Formation of southern Alberta. Several coal claims had been staked at that time along the Smoky River and Sheep Creek.

McEvoy (1925) briefly described the coal-bearing sections, large structural features, and the quality of the coal near the Smoky River. MacKay's (1930) description of the stratigraphy and structure of coal fields in the vicinity of Jasper Park included a short section on the Smoky River coal field, extending stratigraphic nomenclature from the Cadomin area toward Grande Cache.

Thorsteinsson mapped the geology of the 15-minute quadrangle that is now referred to as Grande Cache East (83E/14 east half). His results were combined with work to the west by Irish and published as the Grande Cache mapsheet (Irish and Thorsteinsson, 1957). Irish (1951 and 1955) also mapped areas to the east (Pierre Greys Lakes mapsheet), and to the north (Copton Creek mapsheet), respectively. He then published a bulletin that summarized the geology of the northern foothills of Alberta (Irish, 1965).[1] Pearson (1960) analyzed coal from adit samples obtained along the Smoky River and from an outcrop along Sheep Creek.

Winder (*in* Landes, 1963) reported on detailed geological mapping, using information from outcrop and shallow drill holes on the coal leases held by McIntyre Mines Limited. His report included geological maps at a scale of 1:15 840. That exploration led to the opening of coal mines, and, in 1970, the first shipment of clean metallurgical coal from the Grande Cache area.

In a review article on the structural geology of the eastern margin of the Canadian Rocky Mountains, Dahlstrom (1970, his figure 36) used the Sterne Creek Anticline on Hells Creek as an example of a box fold. A regional geological map, compiled by Mountjoy (1978), extends to the Grande Cache area. McLean (1977, 1982) studied the Lower Cretaceous along the foothills, including the Grande Cache area and he introduced several new lithostratigraphic units.

General geology

The Grande Cache area is situated in the Inner Foothills[2] of the Rocky Mountains fold and thrust belt. In this area, the Inner Foothills are bounded on the southwest by the Rocky Pass Thrust and on the northeast by the Muskeg Thrust (Mountjoy, 1978). Because of a general northwesterly plunge of Paleozoic carbonate rocks, the Inner Foothills are much wider along the Smoky River than along the Athabasca River.

The Inner Foothills in the Grande Cache area are characterized by exposures of Upper Jurassic and Cretaceous clastic rocks. They are outcrops of a 1200-m thick succession that was deposited in a molasse basin (Eisbacher et al., 1974). The lowermost unit is the Nikanassin Formation. It is overlain by the Luscar Group, which is about 550 m thick and contains the thick economic coal seams. The rank of this coal ranges from medium to low volatile bituminous. The top of the succession comprises the Shaftesbury, Dunvegan and Kaskapau formations.

Strata in the region are complexly folded and cut by numerous thrust faults. The main deformation took place between early Campanian and late Eocene and is thought to have proceeded from southwest to northeast (Bally et al., 1966; Price, 1981). It is estimated that it reached the Grande Cache area during the Paleocene (Kalkreuth and McMechan, 1984). The major thrusts (e.g., the Cowlick, Syncline Hills, Mason and Muskeg thrusts) are rooted in a common floor thrust at the top of the Precambrian basement, which is estimated to be at a depth of 5500 m below sea level (Mountjoy, 1978). The shortening accomplished by folding and thrusting is about 30 percent, and fault-to-fold displacement transfer has been documented along the Mason Thrust (Langenberg, 1985).

[1] The northern foothills extend from the Athabasca River to the British Columbia-Alberta border.

[2] In this publication, the Inner Foothills are defined as that area of the foothills that has a predominance of Lower Cretaceous rocks at the surface; the Outer Foothills show a predominance of Upper Cretaceous and Paleocene outcrops.

Data collection

Fieldwork was done by C.B. Wrightson in 1978, and by C.W. Langenberg in 1981, 1982 and 1983, to gather data on the stratigraphy and structural geology of the study area. The area between Mt. Hamell and Grande Mountain was mapped by Wrightson as part of the requirements of the degree of Master of Science at the University of Alberta (Wrightson, 1979).

To analyze the relationship between structural events and coal rank, samples were collected by C.W. Langenberg and W. Kalkreuth from laterally continuous coal seams, and their mean maximum vitrinite reflectances were determined. This petrographic work was performed at the Institute of Sedimentary and Petroleum Geology in Calgary.

Three sources of information about the geology of the area were used. They are outcrops, drill holes and underground mine plans that show the location of exploited coal seams. Information from these sources was collected using data sheets that were formatted to be processed by the computer package TRIPOD (Charlesworth et al., 1987).

Outcrop data

Structural and stratigraphic data were collected in the field by finding exposures along traverses, plotting their positions on aerial photographs and recording lithological observations at each locality. The term outcrop is used in this bulletin for the locality of individual exposures. In addition, certain stratigraphic marker horizons were followed on the ground and on stereoscopic pairs of photographs. The surface traces of

stratigraphic marker horizons and faults were mapped on the aerial photographs and then transferred with the outcrops to a base map. These traces were continually modified throughout the investigation as more information became available and as knowledge of the structure and stratigraphy improved.

The aerial photographs and enlargements were obtained from Alberta Energy and Natural Resources. Smoky River Coal Limited supplied detailed 1:6000-scale topographic base maps. The grid system on these maps is the 3 degrees Universal Transverse Mercator grid, which will be referred to as the 3TM grid. This map projection is one of the provincial standard projections and is similar to the standard 6 degrees Universal Transverse Mercator projection (UTM). The 3TM grid is centered on the 120°W meridian (figure 1). On the original base maps, the grid is rectangular with about 300-m (1000-ft) spacing, and the topographic elevation is represented by contours of about 3-m (10-ft) intervals.

The eastings and northings of outcrops were recorded from the base maps using an engineer's scale, and the elevation was estimated from the nearest 10 foot contour. Outcrops were numbered consecutively. Altogether, 2200 outcrops were visited; 800 by Wrightson in 1978 and the remainder by Langenberg in 1981, 1982, and 1983. At each outcrop, the following lithological information was recorded on the formatted data sheets: rock type, grain size, sorting, weathering, bed thickness, color, kind of fossils present and type of sedimentary structures observed. A note was made if rock samples were collected or if a photograph was taken. Some space was available on the data sheets to make additional comments or draw a sketch of the outcrop.

Five main types of mesoscopic structural elements were measured and recorded (if present) at each outcrop: bedding, cleavage, folds, faults and joints. The pitch of slickenside striae on bedding, faults or joints with a sense of relative movement was recorded. If folds were present, the trace of the axial plane was also recorded. In general, these measurements were taken within an area of about 10 m^2, although, in the case of a fold or a fault, a larger area was sometimes sampled. If possible, at least five repeated measurements of planar bedding were taken on different bedding planes at each outcrop.

Drill hole data

Data were collected from a total of 335 selected drill holes. These holes were selected from all drill holes completed in the area before 1984. Drill holes not included are largely from areas where the coal has been mined out. The locations of collars of the drill holes used in this study are shown on figure 3 (in pocket).

All drill holes were numbered consecutively, but the numbering used by Smoky River Coal was also recorded for reference. At each drill hole, the geographic location, orientation, stratigraphic horizons intersected and depths to these horizons were recorded.

For most drill holes, the 3TM coordinates were available; however, for many drill holes in the active mining areas, the so-called McEvoy grid was used. This grid is parallel to the McEvoy Anticline and makes an angle of 27.15728° with the 3TM grid. The origin of the McEvoy grid has coordinates of 18 967.6 m east and 5 989 087.3 m north in the 3TM grid. A FORTRAN computer program was written to convert McEvoy coordinates into 3TM coordinates.

Several drill holes deviate substantially from being straight. For these holes, the orientation of the drill hole was measured at regular intervals (often every 15 m (50 ft)). On the data sheets, the trend of the drill hole and its deviation from the vertical were recorded together with the depth at which these measurements were taken.

The stratigraphic horizons used in this study were generally those picked by the Smoky River Coal geologists. Their selections were based on geophysical logs and drillers' reports. For a minority of the holes, core descriptions were used to pick stratigraphic boundaries more accurately. The majority of the horizons were from coal seams and were numbered from 1 to 11, according to the numbering system introduced by Landes (1963). However, if other stratigraphic horizons could be recognized they were entered in the data base as well.

Underground mines

Detailed plans of seven underground mines in the study area were made available by Smoky River Coal Limited in 1983. These are the Nos. 2-4, RT2-4, 5, 9A and 9G mines, which are all situated along the No.4 coal seam, and the Nos. 2-11 and RT2-11 mines, which are situated along the No.11 seam. All mines are now worked out, except No.9A and No.9G.

The locations of the mines of the No.4 seam, as of July 1983, are shown on figure 3 (in pocket). Nos. 2-11 and RT2-11 mines are situated above Nos. 2-4 and RT2-4. On these detailed mine maps, the contours in feet above sea level of the top of the coal seam are shown, based on underground surveying. A grid with 150-m spacing was selected to collect elevation data of the coal seam from these maps. The coordinates and the elevation of the coal seam at the grid nodes were recorded as outcrops without orientation measurements. These underground exposures were numbered in a range outside the numbering of regular outcrops to easily differentiate these two types of outcrop.

Stratigraphy

Some 1200 m of late Jurassic to late Cretaceous clastic sediments are present in the study area (figure 4). The formations and members are discussed separately.

Nikanassin Formation

This formation was introduced by MacKay (1929a and b), but no type section was described. Some 400 m of Nikanassin sandstone and shale are exposed in the Syncline Hills Thrust sheet. In the Mason and Muskeg thrust sheets, only the top 120 m of the formation is exposed. The gradual contact with the underlying Fernie Formation is not exposed in the study area.

Lithology

The upper 160 m of the formation is non-marine, as indicated by plant remains, carbonaceous shale and thin lenticular coal seams. Marine trace fossils *(Scalarituba, Diplocraterion, Skolithos, Gordia* and *Planolites,* G. Pemberton, pers. comm., 1982) and crinoids indicate the marine origin of the lower part of the formation.

The lower, marine part consists predominantly of medium to very thick bedded orange-gray weathering sandstone, interbedded with minor amounts of shale, silty shale and shaley sandstone. The upper, non-marine section consists of thin to thick bedded gray and orange weathering sandstones. Interbedded with the sandstone are gray and dark gray (sometimes carbonaceous) shales, silty shales, shaley sandstones and, in some places, thin coal seams. Some beds contain wood fragments and plant debris. Ripple cross-stratification is fairly common.

The Nikanassin is disconformably overlain by the Cadomin Formation of the Luscar Group. Using the method described by Cruden and Charlesworth (1966), bedding orientations on both sides of the contact were measured at six localities to determine the angularity of the disconformity and the dip direction of Nikanassin strata in Cadomin times. At two localities, there was no significant angularity. Apparent angularities of 28°, 22°, 9° and 8° were observed at the other localities with inferred dip directions for Nikannassin strata in Cadomin times of N293°E, N321°E, N72°E and N90°E, respectively. It is concluded from the variation in angularity and dip directions that the contact is not angular and that the apparent angularities suggest an irregular erosional surface with cross bedding. This is also indicated by Cadomin channels cutting into the Nikanassin Formation. However, it cannot be excluded that some folding took place before deposition of the Cadomin Formation.

Age

The crinoid *Pentacrinus* from the lower, marine part suggests a late Jurassic age for this part of the formation. Irish (1965) reports Lower Cretaceous plants from the upper part of the formation, found in an area south of the Athabasca River.

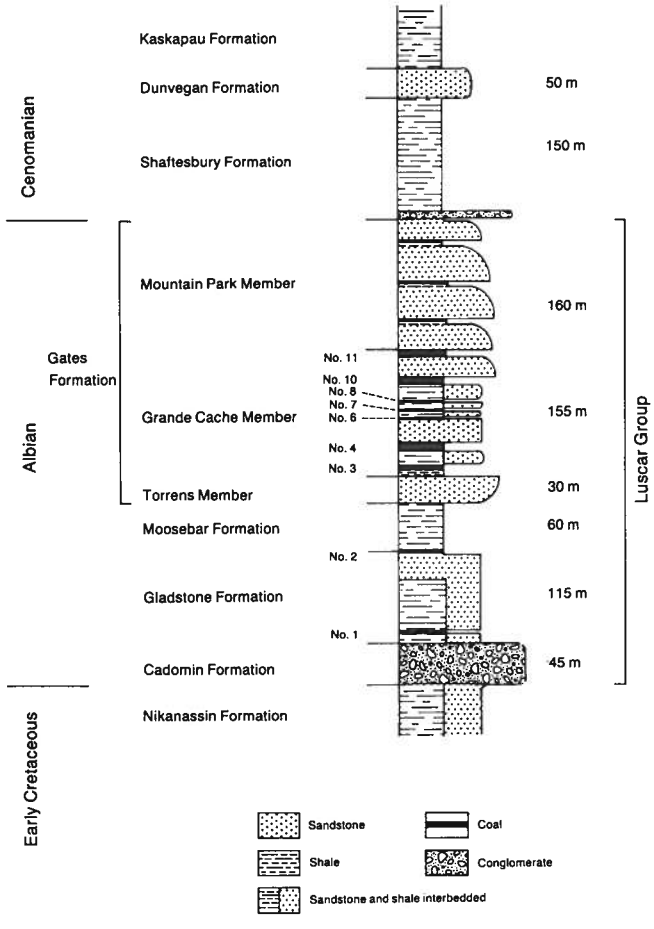

Figure 4. Simplified columnar stratigraphic section of study area with position of coal seams Nos. 1-11.

Luscar Group

The Luscar Group (Langenberg and McMechan, 1985) comprises 555 m of sandstone, shale, and lesser conglomerate and coal, deposited in predominantly non-marine environments. The type section is along the railroad tracks near Cadomin. Sections 81-1, 81-2 and 81-4 of the Grande Cache area (appendix A) were designated as reference sections for the Luscar Group (Langenberg and McMechan, 1985). Nomenclature for the Luscar Group and equivalent strata is shown in figure 5.

The strata in the Grande Cache area are readily subdivided into formations consisting of a basal conglomerate (Cadomin), predominantly non-marine sandstone and shale (Gladstone), marine shale and sandstone (Moosebar), and non-marine sandstone, shale and coal (Gates).

Cadomin Formation

The formation was introduced by MacKay (1929a and b), but no type section was described. However, Cadomin can be considered the type area. For an extensive

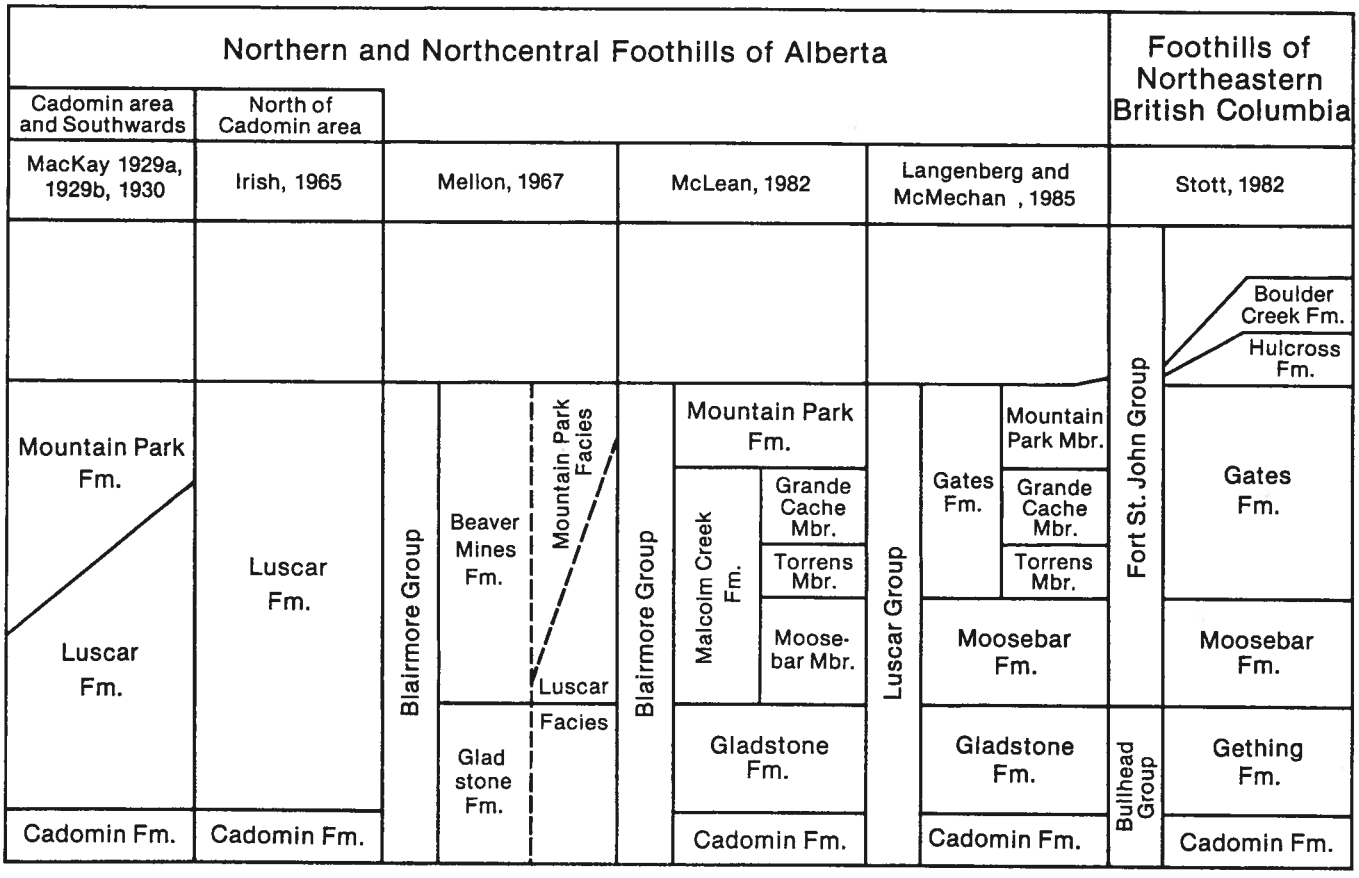

Figure 5. Stratigraphic nomenclature for parts of the Lower Cretaceous in the northern and north-central Alberta Foothills and northeast British Columbia.

description of the Cadomin Formation, the reader is referred to McLean (1977).

The Cadomin Formation is more resistant than nearby beds; thus, it outcrops more extensively and has been the key to unravelling the structure in many areas of the foothills. The conglomerates of the Cadomin Formation have been one of the most useful stratigraphic markers in the foothills, particularly during early coal exploration. Once the conglomerate is accurately mapped and the relative position of coal to the conglomerate is known, it is possible to locate and trace coal seams (MacKay, 1930). For this reason some early workers called the Cadomin the "coal conglomerate."

Lithology

In the study area, the Cadomin Formation is up to 45 m thick. It comprises a lower conglomerate, a middle sandstone and an upper conglomerate. The clasts of the conglomerate are generally of pebble size, averaging 1 to 3 cm in diameter; however, they also range from coarse sand to boulders as much as 30 cm in diameter. The clasts are generally subrounded to well rounded and consist mainly of chert and quartzite. Most of the chert is white, gray or black, but some characteristic pale green pebbles occur. The conglomerate beds are generally gray, although the sand matrix is commonly brownish gray.

Carbonaceous material occurs in small lenses of coalified plant fragments. Along the Smoky River, a 40- to 80-cm thick coal seam occurs in this formation at the top of the lower conglomerate (section 81-2 of appendix A). The sequence of a lower and upper conglomerate with a middle sandstone unit is characteristic of the Smoky River area. The lower conglomerate tends to be coarser and to have more green chert clasts than the upper conglomerate. The middle sandstone unit is generally fine to medium grained with abundant cross bedding. Minor amounts of shale are also present.

Depositional environments

McLean (1977), in a regional study on the Cadomin Formation, concluded that a long period of pedimentation accompanied the deposition of the sediments. Extensive areas covered by a single thin bed of conglomerate are interpreted as the remnants of the pediment surface, whereas thicker conglomerate and sandstone sequences are interpreted as alluvial fans. The Cadomin Formation in the Grande Cache area forms part of the Smoky River alluvial fan (McLean, 1977).

Age

The age of sedimentation of the Cadomin Formation is estimated to be Neocomian-Albian (Stott, 1968).

Gladstone Formation

The Gladstone Formation was introduced by Mellon (1967). Its type section is in southern Alberta along the Gladstone Creek west of Pincher Creek. McLean (1982) extended the delineation of the formation into the northern foothills. The best sections of the Gladstone Formation in the study area are along the Smoky River (e.g., sections 81-1 and 81-2, appendix A; they are reference sections for the Luscar Group).

The Gladstone Formation is correlative with the Gething Formation of northeast British Columbia (Stott, 1968). That formation is characterized by the presence of thick (more than 1 m) coal seams, while such are generally absent in the Gladstone Formation. Langenberg and McMechan (1985) proposed that the change in nomenclature occurs at the Kakwa River.

Lithology

In the Grande Cache area, the Gladstone Formation is represented by 115 m of fining-upward sequences of sandstone, shale and minor coal. The contact with the underlying Cadomin Formation is gradational; by contrast, the contact with the overlying Moosebar Formation is abrupt.

The majority of sandstones are lithic arenites. Their matrix consists of quartz, carbonate or clay minerals. Detrital grains found in thin section are mainly quartz, chert and carbonate, but other rock fragments are present. Potassium feldspar is absent or present in only minor amounts, and plagioclase is never encountered. This latter feature makes the Gladstone sandstones distinctive from the stratigraphically higher sandstones of the Gates Formation, which contain detrital plagioclase.

The gray colors of fresh sandstone originate from chert and quartz grains. Brownish weathering shades result from iron oxide, generally in the form of limonite, produced by various alteration processes. Limonite forms rims around most grains. Most sandstones are well cemented and show diagenetic quartz and carbonate overgrowth on their grains.

Depositional environments

The lower part of the Gladstone Formation has well-defined fining-upward sequences with relatively thin mudrock intervals, which are interpreted as braided river deposits of the Platte type (Miall, 1977). Along Sheep Creek, pebble conglomerates are present in this part of the Gladstone Formation. The upper part of the formation contains shallow marine bivalves (*Protocardium*), marine trace fossils and possibly slightly brackish water foraminifera. These observations agree with the estuarine environment proposed by McLean and Wall (1981) for the upper Gladstone Formation north of the North Saskatchewan River.

Age

Microfossils indicate an early Albian age for the upper part of the formation (McLean and Wall, 1981).

Moosebar Formation

The Moosebar Formation was defined by McLearn (1923). Its type section is along the Peace River Canyon in British Columbia (Stott, 1968). McLean (1982) extended the term Moosebar into the northern and north-central foothills of Alberta as a member of his Malcolm Creek Formation. Langenberg and McMechan (1985) elevated the Moosebar Member to a formation in Alberta, based on its mappability.

Recessive weathering and the dark gray marine shales in the lower part make the Moosebar Formation one of the more-distinctive units in the Lower Cretaceous succession of the northern and north-central foothills. It can be easily recognized as far south as the Clearwater River. The contact with the underlying Gladstone Formation is abrupt, while the contact with the overlying Torrens Member of the Gates Formation is gradational.

Lithology

A good section of the Moosebar Formation is found at section 81-1 (appendix A), which is easily accessible along the railroad. Here it is 60 m thick, while in section 81-7 the formation is 63 m thick. The dominant lithology in the lower part of the Moosebar is marine dark gray shale. Some ironstone and bentonite layers are interbedded with the dark shales. The bentonites can probably be correlated with those described from the Moosebar Formation in northeastern British Columbia (Spears and Duff, 1984; Kilby, 1985). They are most likely of volcanic origin.

Some of the shales in the lower part of the Moosebar have a characteristic greenish hue. This has been ascribed to the presence of glauconite (McLean, 1982, his pg.12). However, in samples from the present study area, the only green mineral present in thin sections of greenish shales is chlorite. Thus, it is concluded that the greenish color of shales in the lower part of the Moosebar is a result of the presence of chlorite.

Interbedded layers of generally fine-grained sandstone and shale are present in the middle and upper part of the formation. Those in the upper part of the formation form two coarsening-upward sequences, and hummocky cross-stratification is common. The top of the highest coarsening-upward sequence is the Torrens Member. These sequences can probably be correlated with the Wilrich A and B cycles of Cant (1983).

Depositional environment

Burrows and traces of a marine, deposit-feeding fauna (G. Pemberton, pers. comm., 1982) and the presence of foraminifera indicate a shallow shelf setting (see also McLean and Wall, 1981). This is furthermore indicated by the hummocky cross-beds that indicate storm wave activity in a shallow marine environment below average wave base.

A good description of sedimentary structures, fossils and depositional environments of the Moosebar Formation in the north-central foothills of Alberta is provided by Taylor and Walker (1984). Although their reference section at Crescent Falls is about 250 km southeast of Grande Cache, depositional environments deduced

from sedimentary structures, microfossils and trace fossils are similar.

Age
Based on foraminifera (appendix D), an age of early Albian can be assigned to this formation (see also McLean and Wall, 1981).

Gates Formation

The Gates Formation (Stott, 1982) is represented by a 345-m thickness of sandstone, shale and coal. Its type section is along the Peace River in British Columbia. However, two reference sections at Dokie Ridge and Bullmoose Mountain (sections 60-9 and 60-5 in Stott, 1968) are more typical of the sequence in the foothills. Section 81-4 (appendix A) is a good reference section for the Gates Formation in the northern foothills of Alberta (see also Langenberg and McMechan, 1985, their figures 7 and 8). Another good section was created in 1986 by highway construction northeast of the mine plant; however, the top of the formation is not exposed in this section.

In the Grande Cache area, the Gates Formation can be divided into three members—the Torrens, Grande Cache and Mountain Park members.

Torrens Member
The type section of the Torrens Members is near Mount Torrens, which is close to the border of Alberta and British Columbia (McLean, 1982). The contact between the Moosebar Formation and the Torrens Member of the Gates Formation is gradational and is placed at the base of the first massive sandstone bed, above which few or no shales occur.

Lithology
The Torrens Member is, in most sections, about 30 m thick (sections 81-1 and 81-7, appendix A) and consists of fine-grained sandstone that often shows parallel laminations. However, some cross-bedding is present, and pebble conglomerate beds form part of the member in minor amounts. Burrows of a marine suspension feeding fauna are present in distinct layers, and one outcrop contains a bed of oyster (*Ostrea* sp.) shells. The sandstones are generally lithic arenites. However, lithic wackes are also present (nomenclature of Dott, 1964). Detrital grains, determined in thin section, are mainly quartz, chert, feldspar (including plagioclase), carbonate and other rock fragments.

The matrix of the sandstone commonly constitutes more than 10 percent of the rock. It can be clay minerals, micaceous minerals, organic material or quartz. The gray color of fresh sandstone results from the presence of chert and quartz grains. The typical gray-orange weathering color results from the presence of iron oxide, generally in the form of limonite. Most sandstones are well cemented and show diagenetic quartz and carbonate overgrowth on their grains. These overgrowths may have prevented the formation of an extensive matrix. Brown siderite freckles are probably of local origin, formed through breakup and resedimentation of siderite-rich muds in penecontemporaneously deposited sandstones, as suggested by Mellon (1967).

Depositional environment
The Torrens Member represents a relatively high energy shoreline environment from wave base to slightly above sea level. Consequently, the coarsening-upward sequence is caused by a prograding beach complex (McLean, 1982).

Age
No fossils useful for age determinations were found, but the gradational contact with the Moosebar Formation suggests an early Albian age.

Grande Cache Member
The Grande Cache Member was introduced by McLean (1982). The type section is a bulldozer cut in the Cowlick Thrust sheet, 750 m southwest of the trace of the Cowlick Thrust on the Smoky River. A good reference section is No. 81-4 (appendix A).

The Grande Cache Member is characterized by thick, economic coal seams. All lower Cretaceous coal mined in the central and northern Alberta foothills has come from the Grande Cache Member. These economically viable coal seams (within the Luscar Group) were one of the main reasons to retain the term Luscar as a group name for Lower Cretaceous coal-bearing strata in the north-central and northern Alberta foothills (Langenberg and McMechan, 1985).

The boundary between the Grande Cache Member and the overlying Mountain Park Member is placed at the base of the first prominent sandstone unit with an abrupt basal contact above the highest major coal seam in the Grande Cache Member (McLean, 1982, his pg.15).

Lithology
Five complete sections of the Grande Cache Member were measured (appendix A, sections 81-3, 81-4, 81-5, 81-6 and 81-8). The thicknesses range from 145 m to 162 m, with an average of 151 m. Shale and fine-grained sandstone are the main constituents of this member, besides coal. Sandstone above the No. 4 coal seam (known as Super 4 Sandstone) changes facies laterally and locally, shales occur in this interval (for example section 81-3, appendix A). The numbering of coal seams (figure 4) is according to Landes (1963). Higher up in the section, fine- to medium-grained channel sandstones are present, especially in the interval between Nos. 10 and 11 seams.

The sandstones are similar to those of the Mountain Park Member; however, the Grande Cache Member shows a higher percentage of fine-grained sandstone. These sandstones are generally lithic arenites, although lithic wackes are present. Detrital grains are mainly quartz, chert, feldspar (including plagioclase), carbonate and rock fragments. Volcanic rock fragments were probably derived from west of the Rocky Mountain Trench (Leckie, 1986). Brown siderite freckles are found, especially in the channel sandstones. The gray color of fresh sandstone results from the presence of chert and quartz grains, whereas the

gray-orange weathering color (typical for Gates sandstones) results from the presence of iron oxide, generally in the form of limonite. Limonite coats many of the detrital grains. The matrix comprises clay minerals, micaceous minerals (including chlorite), organic material and quartz. The matrix may have formed by breakdown of unstable detrital particles, such as volcanic debris (a process suggested by Pettijohn, 1975). Other lithic sandstones have a pervasive diagenetic quartz or carbonate cement.

Remnants of conifers and ferns are present through the whole member. Good specimens of such remains can be collected in the open pit mines of Smoky River Coal Limited in the overburden material of the No. 4 coal seam (the Super 4 Sandstone). Figure 6 shows two examples of fossil plants from this horizon. Although flowering plant remains have been reported from the Gates Formation in northeastern British Columbia (Stott, 1968, his pg.76), none were found in the Grande Cache area.

Nos. 4 and 10 coal seams are the only laterally continuous seams in the study area. A 5-cm thick tonstein parting occurs in the upper part of No. 4 coal seam. No. 11 seam is absent in the Syncline Hills Thrust sheet (section 81-8, appendix A). No. 3 seam, which occurs immediately above the Torrens Member in the Syncline Hills Thrust sheet, is expressed as (locally coaly) carbonaceous shales in the Mason and Muskeg Thrust sheets. Some shell layers immediately above the No. 3 coal seam (and its carbonaceous shale equivalents) are laterally continuous. Bivalves from these layers include *Unio douglassi* and *Murraia naiadiformis* (C.R. Stelck, pers.comm., 1982). The latter bivalve is indicative of brackish water conditions.

Depositional environment

Shallow, brackish marine conditions are substantiated by microfossils from the shales associated with the shell layers above the No. 4 seam (appendix D). Microfossils indicative of shallow, brackish marine conditions are also found in shales above the No. 4 and No. 10 seams. A marine trace fossil assemblage was found in the footwall rocks of the No. 4 seam. Coal associated with a shallow, brackish marine fauna points to a low-energy, coastal or delta plain environment behind shoreline deposits (see also McLean, 1982). The trough cross-bedded sandstones in fining-upward sequences with erosional bases in the upper part of the member are indicative of the presence of fluvial channel deposits.

Age

From the occurrence of ostracods *(Cytheridea bonaccordensis*), the age of the Grande Cache Member is estimated to be early Albian (J.H. Wall, pers. comm., 1982).

Mountain Park Member

This lithostratigraphic unit was defined as a formation by MacKay (1929a,b) in the Mountain Park area. No type section was described. McLean (1982) presented two reference sections—one along Malcolm Creek just across the Smoky River from Grande Cache, and the other along Wabiabi Creek. Another good, accessible reference section is available along the railroad across from the mine plant (section 81-4, appendix A).

The mappability of the Mountain Park Formation has been a problem in certain areas, and, for that reason, it was reduced to member status by Langenberg and McMechan (1985). The boundary with the overlying marine shales of the Shaftesbury Formation is abrupt and is marked by a pebble conglomerate bed.

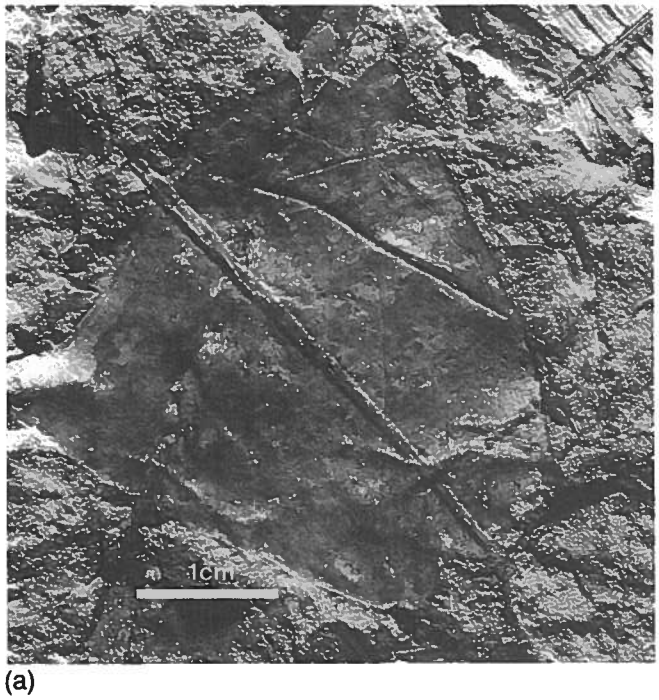

(a)

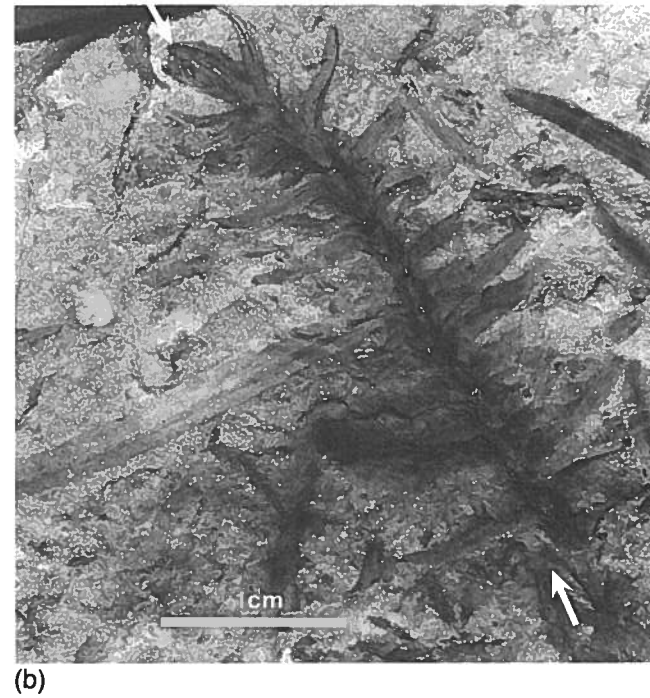

(b)

Figure 6. Fossil plants from the sandstone overlying the No. 4 coal seam. (a) *Nilsonia canadensis* (b) *Elatides* sp.

Lithology

Three complete sections of the Mountain Park Member were measured (appendix A; sections 81-3, 81-4 and 81-8). The thicknesses range from 156 m to 193 m, with an average of 174 m. A fourth section was measured (appendix A, section 81-5), although its total thickness could not be determined because the top of the member was covered. However, it was measured to be at least 153 m thick at this locality. The thickest section (193 m in section 81-8) is in the most westerly location. This may indicate that the member thickens to the southwest (McLean, 1982, his pg.19). There are also indications that the member thins towards the northwest (Richard Dawson, pers. comm., 1987).

The Mountain Park Member is characterized by very fine to medium-grained, grayish orange weathering sandstones. They occur in thick to massive beds, with abrupt bases and a decrease in grain size upward. They are often cross-bedded and generally show scour surfaces at the base, typical for channel sandstones. Between the sandstones are units of shale, or interbedded shale and sandstone that contain minor thin coal seams.

Sandstones of the Mountain Park Member are generally arenites, but lithic wackes are also present. They are microscopically similar to the sandstones of the Grande Cache Member. A description of detrital grains, matrix and cement is found in the lithology section of the Grande Cache Member.

Siderite freckles are pervasive in the medium-grained Mountain Park sandstones. They were mapped as Upper Freckled, Lower Freckled and Sub Freckled sandstone by Landes (1963). The Lower Freckled Sandstone is generally the basal sandstone of the Mountain Park Member. But in other cases, a sandstone from the Grande Cache Member, between Nos. 10 and 11 coal seams, was picked as the Lower Freckled sandstone. Because it can be expected that channel sandstones are not laterally continuous, this terminology is not recommended. However, the fining-upward sandstones (generally medium grained near the base) can be mapped for certain distances. They are shown as 'mappable sandstone bodies' on figure 1. In most sections, four or five fining-upward sequences, from medium-grained sandstone to shale and minor coal, can be distinguished. Another distinctive feature of the Mountain Park Member is the presence of greenish to olive-gray weathering sandstone. Thin sections show that this greenish color is from chlorite grains, which may be of volcanic origin (Mellon, 1967). Fine-grained sandstones with quartz cement near the top of the member have characteristic reddish brown weathering colors, resulting from the presence of biotite and limonite. The presence of dark, olive-green and brick-red weathering colors in sandstones overlying the coal-bearing sequence in the Cadomin area was one of the main reasons for the introduction of the Mountain Park Formation (MacKay, 1930, his pg.1310). Although the colors in the Grande Cache area are not as vivid as in the Cadomin area, their similarity is a good indication of equivalent beds.

Depositional environment

Thick, fining-upward sandstones are interpreted as fluvial channel deposits laid down by meandering streams. The intervening finer-grained sediments are considered floodplain deposits (McLean, 1982). Near the top of the formation, some marine trace fossils are found, together with possibly brackish bivalve fossils (*Elliptio* sp.). This may indicate an estuarine environment, signalling the advance of the Boreal Sea.

Age

Angiosperm pollen recovered from the upper 50 m of the Mountain Park Member along Malcolm Creek have affinities to the microflora from the Hulcross and Boulder Creek Formations of northeastern British Columbia and indicate a late Middle Albian age (A.R. Sweet, Geological Survey of Canada, Calgary, unpubl. rept., 1982).

Shaftesbury Formation

About 150 m of dark gray marine shale belonging to the Shaftesbury Formation (Irish, 1965) are present in the study area. The base of the formation is marked by a pebble conglomerate bed that often shows large wave ripples. The age of the formation is late Albian to early Cenomanian (Stott, 1968).

Dunvegan Formation

Brown to reddish weathering quartzitic sandstones with interbedded shale and thin coal seams above the Shaftesbury shales define the largely marine Dunvegan Formation (Stott, 1982). The type section of this formation is at Dunvegan, Alberta. In the Grande Cache area, the formation is about 50 m thick, as estimated from cross sections (figure 2), although at the Syncline Hills the thickness is 85 m (see also Irish, 1965, pg.164). The sandstones are lithic arenites with predominantly detrital quartz and chert grains and a quartz cement. Micaceous and argillaceous rock fragments occur only in minor amounts. Feldspar grains were not encountered. Specimens of *Inoceramus athabaskensis* have been recovered from these sandstones. The formation has been assigned a Cenomanian age based on the occurrence of such fauna and a distinctive flora (Stott, 1982).

Kaskapau Formation

Dark gray marine shales above the Dunvegan Formation belong to the Kaskapau Formation (Irish, 1965). Only the lower part of the formation is present in the study area. Because of internal folding, a thickness cannot be determined. The lower part of the formation, in which a specimen of *Dunveganoceras* was found, is late Cenomanian in age (Irish, 1965).

Stratigraphic thickness of coal seams

Economically, the viable coal seams (figure 1) have been found only in the Grande Cache Member of the Gates Formation. The Nos. 4 and 10 coal seams are the

only laterally continuous seams in the area. Thicknesses in outcrop of the economically viable coal seams were tabulated (appendices A and C); additional information, obtained from drill holes, is summarized in the following descriptions.

No. 3 seam
This seam is present only in the Syncline Hills Thrust sheet. From the limited exposure and drilling, it can be estimated that the thickness ranges from 1.5 m to 3 m. It is expressed as (locally coaly) carbonaceous shales in the Mason and Muskeg thrust sheets. The carbonaceous shales have a very conspicuous signature on geophysical logs and form a useful marker horizon. It should be noted that this zone is referred to as No. 3 seam in Smoky River Coal Limited reports of the No. 9 Mine area north of Sheep Creek (Richard Dawson, pers. comm., 1987).

No. 4 seam
This coal seam is the most extensively exploited and explored coal seam of the area and is laterally continuous over the study area (figure 3, in pocket). Its thickness ranges from 4 m to 7 m, with an average of 6 m. In the Mason Thrust sheet its thickness decreases east of 61 000 E (east of Goat Cliffs), because of a 2-m thick shale split. This split results in two 1.5-2 m thick seams.

No. 10 seam
This seam is also laterally continuous over the study area. It is 2 m to 5 m thick, averaging about 3 m. The greater thickness is generally found in the Goat Cliffs area southeast of the Smoky River.

No. 11 seam
This seam is present only in the Muskeg and Mason thrust sheets. It generally consists of an upper and lower seam (appendix A). The cumulative thickness ranges from 1.5 m to 5 m, individual seams being from 0.5 m to 4 m thick.

Structural geology

Geological maps, cross sections and structure contour maps form a model depicting the geometry of the deformed rocks. Litho-stratigraphic formations and members described in the stratigraphy section are the building stones of this model. Prominent macroscopic structural elements are four major thrust faults: from southwest to northeast, the Cowlick, Syncline Hills, Mason and Muskeg thrusts (Irish and Thorsteinsson, 1957; see also figure 1). As a result, the area can be divided into thrust sheets, where a thrust sheet is defined as a rock mass that is thrusted over another rock mass. Each thrust sheet is named after the thrust fault over which it moved. Consequently, the study area comprises parts of the Syncline Hills, Mason, and Muskeg thrust sheets (figure 7). Other prominent structural elements are macroscopic folds (figure 1). They are, from southwest to northeast: Sterne Creek Anticline (Irish and Thorsteinsson, 1957); Two Camp Creek Anticline, Fox Creek Syncline and Syncline Hills Syncline (Landes, 1963); Susa Creek Anticline (Irish and Thorsteinsson, 1957); Flood Mountain Syncline and Westridge Anticline (new names); and McEvoy Anticline, Winder Syncline, Barrett Anticline and Muskeg Anticline (Landes, 1963).

Cross sections and shortening

In folded terrains, the downplunge projection method can be used to construct cross sections. The study area has to be divided into domains, within which folding is considered cylindrical. The procedure is as follows (see also Charlesworth et al., 1976). The area is, by trial-and-error, divided into the smallest number of subareas within which folds appear cylindrical, and the orientation of the fold axis in each subarea is calculated from bedding plane measurements. The cylindricity of the folds in each subarea is statistically tested. On the basis of these tests, subareas are grouped or subdivided into cylindrical domains. This procedure resulted in 60 domains being identified for the Grande Cache area (figure 7 and appendix B).

The concentration parameter K for these domains, as calculated from repeated orientation measurements of bedding, ranges from 129 to 366, with an average of 213. This parameter is needed in the test for co-planarity. Cylindricity is most times rejected with this test; however, with the F-test for coaxiality it can be shown that the domains are cylindrical. This indicates that the values of K underestimate total roughness errors and are too high for use in the co-planarity test (Charlesworth et al., 1976, his pg.56). Consequently, the F-test for coaxiality was the main test used for determining the cylindrical domains.

In some areas, lack of outcrop prevented the use of bedding orientations for establishing domains. However, information from drill holes was used to find the direction of the fold axis in these areas. A trial-and-error method was used in combination with interactive graphics. Various plots with different fold axis directions were produced until certain stratigraphic horizons (mainly coal seams) lined up in a coherent manner on the cross section. Examples of these areas are domains 48, 49, 50, 53 and 60 (figure 7 and appendix B).

Trends and plunges of the best fitting cylindrical fold axes of the 60 domains were plotted (figure 7). The fold axes generally trend southeast, with shallow plunges either to the southeast or northwest. The average fold axis (assuming a spherical normal distribution of the 60 directions) is plunging 1 degree in direction N124°E. Plunge variation in the Muskeg Thrust sheet defines a dome-shaped culmination along the Barrett Anticline near Sheep Creek. Variation in the fold axis orientation

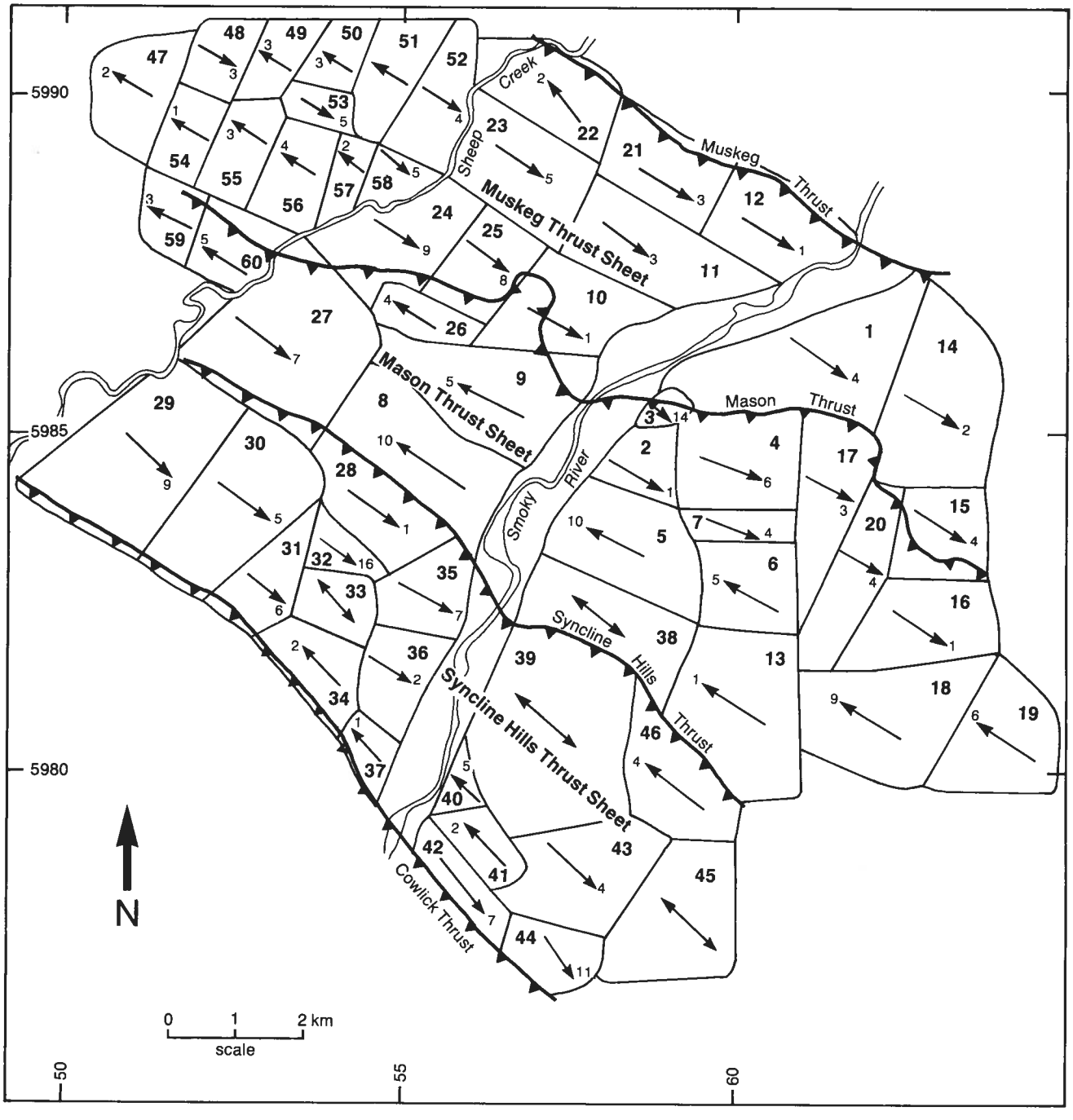

Figure 7. Map showing the domains within which folding is statistically cylindrical, together with the orientation of the fold axes. The domains are listed in appendix B.

of the Susa Creek Anticline is shown by domains in the Mason Thrust sheet. The domains in the Syncline Hills Thrust sheet are largely a result of changes in geometry of the Sterne Creek Anticline along its trend.

The domain boundaries shown on figure 7 are by no means the only possible solution. Folds change geometry along their trends, and, for that reason, cylindrical domains should not be wider than approximately 2 km. Where more information is available, the geometry is shown to be better constrained and the domains tend to be narrower in the trend direction. For example, in the area northwest of Sheep Creek, where large open pit mines, underground mines and many drill holes exist, the domains are only 1 km wide. Originally, domain boundaries were chosen where a change in geometry was apparent from the preliminary map. Afterwards, these boundaries were adjusted and refined. Other natural domain boundaries are areas with a lack of information. An example is the valley of the Smoky River, where Quaternary sediments conceal bedrock for up to 1 km along the general trend.

Once the area was divided into statistically cylindrical domains, downplunge cross sections were obtained by the TRIPOD computer package (Charlesworth et al., 1976; Charlesworth et al., 1987). Elliott (1983) emphasized the importance of using downplunge projection in the construction of balanced, retrodeformable cross sections. The geological map (figure 1) is based on computer plots of orientation of bedding in outcrop, location of drill holes and traces of stratigraphic horizons transferred from aerial photos. Construction of this map required a continuous interaction between downplunge cross section and map. Both map and cross sections had to be mutually consistent. The map was completed after cross sections of all individual domains were examined.

Nine cross section lines were chosen, which are shown on figure 1 (in pocket). Data points in domains situated near the section lines were projected downplunge along their respective fold axes from their location onto the plane of section. On resulting plots, the stratigraphic units and faults were drawn as shown in figure 2 (in pocket). The sections were completed to an elevation of 500 m, based on stratigraphic thicknesses and the model of flexural slip folding. Section HH′ was extended downward to -750 m, based on a seismic section made available by Shell Canada Limited.

One of the most striking features of the cross sections are chevron folds with relatively straight limbs and narrow hinge areas. Chevron folds can be expected where regularly bedded sequences of alternating competent and incompetent layers are shortened (Ramsay, 1974). The competent sandstone layers have a constant thickness throughout the structure and the ratio of layer thickness to limb length is less than 1 to 10. The competent layers form buckles resulting from concentric folding (Ramsay, 1967; Dahlstrom, 1970). This suggests that the deformation in sandstone is mainly taken up by shear parallel to the layer boundaries. This process of flexural slip is substantiated by the occurrence of slickenside striae on bedding planes, which are oriented approximately perpendicular to the fold axis. The incompetent layers show thickening in the fold hinge areas by simple shear, which results in disharmonious folding. This type of folding is closer to a similar fold model. Coal thickened in this way forms exploration targets in the area (see section on structurally thickened coal).

Because the predominant process of folding in the foothills is considered to be flexural slip (Dahlstrom, 1970), the deformation in the plane of the section is plane strain. In this type of folding, the bed length in the original and in the deformed cross section is the same. In fact, the bed length measured around the fold at different stratigraphic levels remains the same, so that bed lengths balance. The sections (figure 2) can be restored to an unstrained state, which shows that they are balanced (Dahlstrom, 1969). We can now use well-constrained horizons to calculate the amount of shortening, where shortening is defined as original length of section minus present length, divided by the original length (Hossack, 1979). The best constrained horizon is the top of the No. 4 coal seam as a result of exploration and exploitation. Dahlstrom (1969, pg.754) emphasized that shortening should be calculated on only one horizon because of possible disharmony between horizons. The cross sections (figure 2) show that disharmony indeed occurs.

The shortening was calculated between the Muskeg and Cowlick thrusts. Displacement along the Cowlick Thrust was not included because it is considered to be part of shortening of the Cowlick Thrust sheet, which is outside the map area. Some uncertainty exists about displacement along the Muskeg Thrust, because no marker horizon can be matched across the fault. Based on cross sections by Irish (1965) and Mountjoy (1978), a minimum displacement of 1 km along this fault was included in the reconstruction of the original length of Sections DD′, EE′, FF′ and GG″ (table 1). The original length of the top of No. 4 coal seam was measured with a planimeter. The present length of the section can be measured with a ruler. The amount of shortening of nine cross sections of figure 2 are shown in table 1. Because erosion of the banks of the Smoky River is fairly deep along Section FF′, the top of the Cadomin Formation was used as a shortened horizon for this section. Sections AA′ and BB′ are restricted to McEvoy and Barrett Anticlines, and show less shortening than the other sections. Section CC′ does not cross the Muskeg Thrust. If 1 km of shortening by the Muskeg Thrust is added, the shortening of Section CC′ would be 29 percent.

For four cross sections through the Muskeg, Mason and Syncline Hills thrust sheets (Sections DD′, EE′, FF′ and GG″), shortening ranges from 28 to 33 percent with an average of 31 percent. Assuming that this longitudinal strain occurs perpendicular to the trend of the foothills in a northeast direction and no strain takes place along the trend of the foothills, maximum extension would be taking place in a vertical direction. This is expressed by thickening of the section. These strain directions are known as the principal axes of finite strain X, Y and Z (Ramsay and Huber, 1983), which are parallel to the principal strains of values e_1, e_2 and e_3 (whereby $e_1 \geq e_2 \geq e_3$). Consequently, in the Grande Cache area, X is vertical, Y is parallel to the trends of the folds,

Table 1. Shortening in the Grande Cache area as calculated from cross sections using the top of No.4 coal seam as reference horizon.

Section	Original length (km)	Present length (km)	Shortening
AA′	4.2	3.6	14%
BB′	5.5	4.4	20%
CC′	12.6	9.6	24%
DD′	15.2*	10.2	33%
EE′	14.9*	10.2	32%
FF′	15.2*	11.0	28%+
GG″	17.8*	12.1	32%
HH′	9.1	6.4	30%
II′	2.5	1.7	32%

* These lengths include 1 km of shortening along the Muskeg Thrust, which had to be added to the original length.
+ For section FF′, the top of the Cadomin Formation was used as reference horizon because the level of erosion is deep along this section.

and Z is perpendicular to both X and Y. The shortening in the Z direction is 31 percent. This means that a unit length is reduced to 0.69. Because of plane strain, the extension in the X direction is 45 percent (unit length is thickened to 1.45). Consequently, the finite strain ellipsoid has axial ratios of 1.45:1.00:0.69. Thus the X:Z strain ratios are 2.1:1.

Other estimates for shortening in the Rocky Mountains are available, but they were calculated on much longer cross sections. For example, Thompson (1981) calculated 30 percent shortening for the whole foothills belt in northeastern British Columbia, while Price and Mountjoy (1970) calculated 54 percent shortening for the southern Canadian Rocky Mountains. The average shortening of 31 percent for the Grande Cache area has to be included with determinations on shortening of a complete cross sections through the Rocky Mountains along the Smoky River to estimate shortening of the northern Alberta Rocky Mountains.

Structure-contour maps

Additional information about the structure of the area can be obtained from structure-contour maps. No. 4 coal seam is the thickest seam of the area; therefore, the top of this seam was selected as the horizon to be contoured. The three main sources of information are available to prepare structure-contour maps of No. 4 seam (i.e., outcrop data, data from underground mines and intersections in drill holes). This information is shown in summarized form on figure 3 (in pocket). The best information is present along the McEvoy and Barrett anticlines.

In areas where no mining has taken place and where drilling is scarce or absent, there were insufficient data points for contouring. The cylindrical fold model was used to generate a set of inferred elevation points on the coal seam in those areas that are shown to form cylindrical domains (Wrightson et al., 1979). The computer-based procedure is as follows. On the profiles (cross sections perpendicular to the fold axes) of the cylindrical areas, the coal seam is drawn and digitized. A model of the coal seam is generated by moving a line parallel to the fold axis of the domain through the profile of the coal seam. The elevation of the modelled coal seam is calculated at the nodes of a square grid. In the present example, a grid with 150-m spacing is used.

For computational purposes, the rectangular grid is generated first. Grid points with zero elevation are projected parallel to the fold axis onto the plane of the profile. These projections are performed numerically by rotating axes (Charlesworth et al., 1976). X and Y are the coordinate axes in the profile plane, where X is horizontal and Y perpendicular to X, and B is the distance along the Y axis between projected grid point and the digitized profile of the coal seam. If the plunge of the fold axis is P, then the elevation of the modelled coal seam at the grid point is B/cos P. These elevation points of the coal seam are added to a computer file containing positional data from outcrops and drill holes.

It should be realized that data generated from the profile are only as good as the model they are based on. Folds are statistically cylindrical in the established domains and generally maintain their geometry over distances of up to 2 km along trend. However, they can be expected to deviate from an ideal cylindrical fold. Consequently, the modelled surface should be adjusted when additional drill hole or mining data become available. Care should be taken that points from the profile are not projected over too great a distance.

Areas where modelled elevation points were obtained comprise the northeast limb of the Barrett Anticline, the area northeast of underground No. 5 Mine, the northeast limb of the Two Camp Creek Anticline, the southwest limb of the Sterne Creek Anticline on Mt. Hamell and the general area of the Sterne Creek Anticline on Grande Mountain.

In the area north of underground No. 2-4 Mine, the hinge of the Barrett Anticline was projected 1 km northwestward while points on its limbs were projected over a distance of up to 2 km. Additional elevation points were obtained by projecting a profile of the Barrett Anticline on Sheep Creek southeastward. A gap was kept between the modelled grid points because the geometry of the Barrett Anticline along Sheep Creek differs from that along Smoky River (compare Sections DD′ and EE′, figure 2). This gap is necessary to smooth contours between the cylindrical domains 11 and 23 (figure 7). The profile of the No. 4 seam in the Barrett Anticline southeast of the Smoky River was projected 1 km southeastward. Because of the absence of drill holes and because of the conical nature of the folding, the modelled elevation points are highly speculative in this particular area.

Very few drill holes are available in the Flood Creek and Flood Mountain area; therefore, the contours that are shown should be considered tentative. Similarly, the contours on Grande Mountain should be considered tentative. In the Goat Cliffs area, no structure contours are shown because of the complicated structure and lack of drill hole data. Similarly, near the Muskeg and Fox Creek anticlines, insufficient exploration data are available to warrant any structure contours.

Both hand-made and machine-contoured maps were produced. Machine contouring was done by the SURFACE II Graphics System (Sampson, 1975). SURFACE II produced unrealistic contours near the map edges and in areas with gaps in the data points, where it tended to produce closed contours. These contours were ignored in the final presentation of figure 3.

The structure contours of the top of No. 4 coal seam, as shown in figure 3, very clearly outline the geometry of this horizon. Individual folds can be followed along their trend for considerable distance. Their plunge is shown by the intersection of the contours with the fold axes. Some of these folds will be discussed in greater detail in the next section.

Cylindrical and conical folds

The folds can generally be classified as chevron folds, as discussed earlier. The Barrett Anticline is a prominent chevron fold and extends for a considerable distance along its trend, both on the surface (figure 1) and in the subsurface (figure 3). The fold is well exposed on

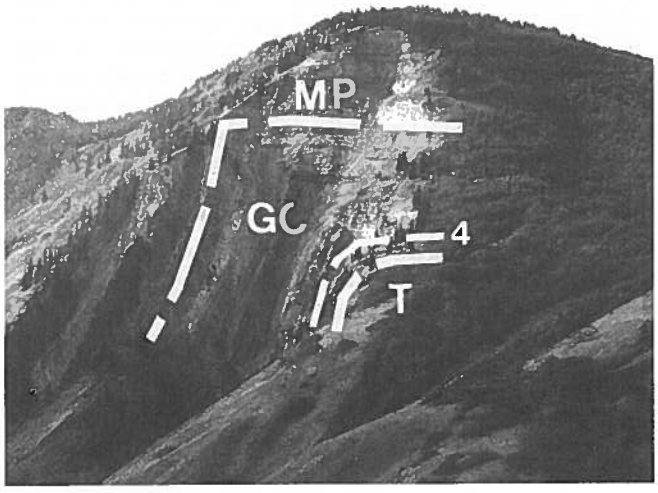

Figure 8. Overview of the Barrett Anticline, which is a chevron fold. T = Torrens Member, 4 = No. 4 coal seam, GC = Grande Cache Member, MP = Mountain Park Member.

the northwest side of the Smoky River (figure 8). The Torrens, Grande Cache and Mountain Park members are exposed in the cliff, while the Moosebar and Gladstone formations are exposed in the lower slopes.

The structure contours (figure 3), and cross sections BB′, CC′, DD′, EE′, FF′ and GG″ (figure 2), show the variable geometry of the Barrett Anticline. The fold is not present along Section AA′; only a slight flexure exists. On Section BB′, the fold is well defined and is plunging to the northwest. Near Section CC′, the fold in No. 4 seam reaches its highest elevation at 4500 feet (1372 m), marking a culmination. East of here, the plunge is southeastward. The fold gradually tightens toward the southeast, as shown by narrowing of the structure contours. Along Section EE′, the shortening in the Barrett Anticline using the No. 4 seam as datum horizon, is 28 percent. Southeast of section EE′, the fold opens up, as shown in Sections FF′ and GG″, and by the widening of contours. Along Section GG″, there are two gentle anticlines (exposed along the Smoky River) instead of the one prominent anticline elsewhere. The shortening of No. 4 seam horizon is only 10 percent in this part of the cross section. Although these chevron folds are generally cylindrical, they do not persist for long distances but taper out, as shown by the Barrett Anticline and other folds in the area. At their tapering end, folds can be expected to be noncylindrical (Dubey and Cobbold, 1977).

The tapering can be studied in a little more detail because of good exposure of the Barrett Anticline on both sides of the Smoky River. On the northwest side of the Smoky River, the fold forms part of domain 11, and, on the southeast side of the river, it is part of domain 1 (figure 7). Using the methodology of Kelker and Langenberg (1982), the folds were tested for conicity. Although folding of the Barrett Anticline in domain 11 is shown to be statistically cylindrical, the normals or poles to the bedding can also be fitted to a cone with a half apical angle of 85 degrees (figure 9a). This test of conicity is valid because the limbs show some curvature. Chevron folds with perfect straight limbs would not be susceptible to this procedure. Consequently, the folded surfaces in domain 11 fit a cone with a half apical angle of 5 degrees. The cone is closing toward the southeast. This is based on 38 stations where five repeated measurements of the bedding were taken.

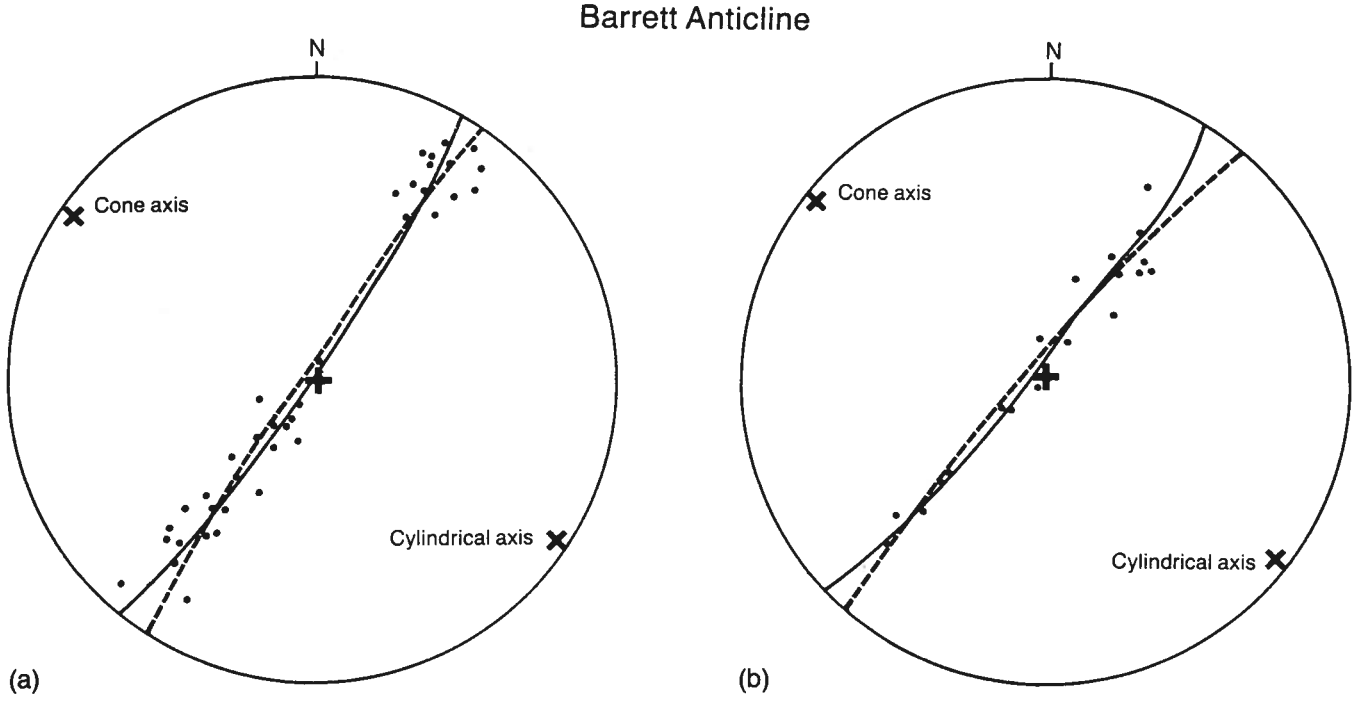

Figure 9. Equal area projections of poles to bedding in the Barrett Anticline: (a) in domain 11 and (b) southeast of the Smoky River in domain 1. The best fitting small circle (conical model) is shown by a solid curve, the best fitting great circle (cylindrical model) is shown by a dashed curve.

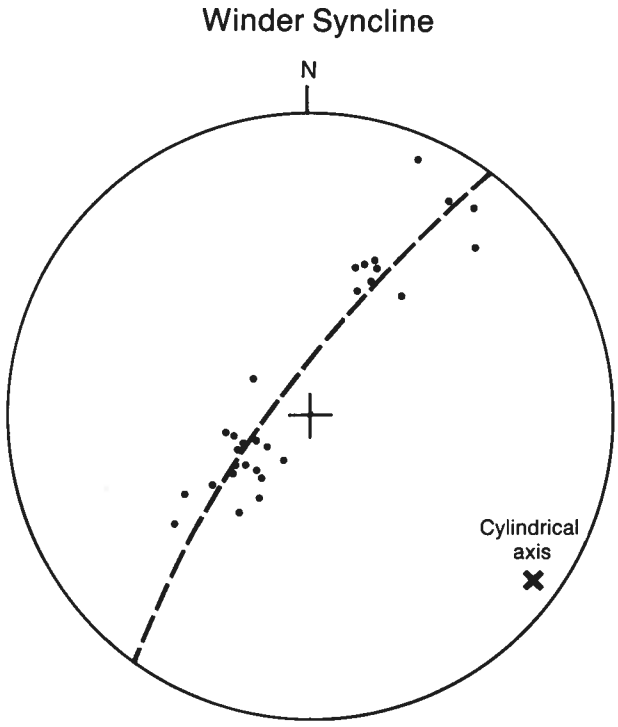

Figure 10. Equal area projections of poles to bedding in the Winder Syncline near Sheep Creek. The best fitting great circle (cylindrical model) is shown by the dashed curve.

Thus, a total of 190 bedding plane measurements is used in the fitting procedure. The mean precision parameter K of the individual stations (assuming spherical normal distributions for the five repeated measurements) is 235. This value of K is used in a statistical test, which indicates that the small deviation from the conical surface can be attributed to small inaccuracies in measurements of the 38 mean bedding orientations. Another statistical test shows that the conical model can be accepted with 95 percent confidence over the cylindrical model. The cone axis is plunging 4 degrees in direction N307°E. The stereoplot shows that conical folds with small apical angles may easily go unnoticed without the numerical approach.

The Barrett Anticline on the southeast side of the Smoky River forms part of the statistically cylindrical domain 1 (figure 7). However, the poles to the bedding measured in 19 stations (19 mean bedding orientations from a total of 95 measurements) can also be fitted to a cone with a half apical angle of 83 degrees (figure 9b). The mean precision parameter K in this area is 258, and the statistical test shows that the conical model is accepted with 90 percent confidence over the cylindrical model, but not with 95 percent confidence. The lower degree of confidence is probably caused by the relatively few mean bedding orientations (i.e., 19). It follows that the folded surface fits a southeasterly closing cone with a half apical angle of 7 degrees. The cone axis is plunging 4 degrees in direction N307°E. There is good agreement on the orientation and tightness of the cone on opposite sides of the river (figure 9). Consequently, the geometry represents the tapering end of a cylindrical fold, where the folding is conical. Still further to the southeast, the Barrett Anticline is predicted to terminate. However, this cannot be verified because of the disharmonious nature of shales above the Gates Formation southeast of Section GG″. At the termination, in the northwest between Sections AA′ and BB′, the Barrett Anticline is probably also conical, but because of limited exposure, this cannot be verified with orientation data.

The Winder Syncline extends from Section FF′ to Sheep Creek. It is plunging southeast in the No. 5 Mine area and slightly northwest in the vicinity of No. 2-4 Mine area. This northwesterly plunge can be expected in connection with the nearby conical Barrett Anticline, which has a southeasterly plunging hinge and a northwesterly plunging cone axis (figure 9). On Sheep Creek, the Winder Syncline is well exposed and is close to an ideal cylindrical fold, plunging 8 degrees towards N126°E (figure 10). Northwest of section CC′, the Winder Syncline is split into two synclines with an intermediate anticline. The northern syncline changes from a southeastern to a northwestern plunge near Section BB′ before terminating. The southern syncline probably terminates just east of Section AA′, but insufficient data are available to substanstiate this.

Another major fold that extends for a considerable distance is the McEvoy Anticline, which can be followed from the No. 9 Mine area to the Smoky River. The largest open pit mine in the area is along this anticline (No. 9 Mine). The overburden and No. 4 coal seam have been stripped, exposing the footwall of No. 4 seam over a large area. This footwall probably forms one of the largest exposed single folded surfaces in the world. Natural erosion generally tends to result in cross sections through folds, where individual surfaces are only exposed over a limited area. However, the stripping operation offers structural geologists a unique opportunity to observe and measure a single folded surface over about 2 km² (figure 11).

The orientation of the footwall of the No. 4 seam was measured in 29 stations spread out over domains 47, 54 and 55 (figure 7). At every station, five repeated measurements of bedding were taken. The 29 mean

Figure 11. Exposure of the footwall of the No. 4 coal seam along the McEvoy Anticline in the No. 9 Mine. The view is along the fold axis in southeastern direction.

bedding orientations are shown in figure 12, which clearly indicates the cylindrical nature of the fold. The normalized eigen values are 0.8917, 0.1075 and 0.0008, and the eigenvector related to the minimum eigenvalue is dipping 2 degrees in direction N300°E. This is the direction of the best-fitting cylindrical fold axis. All the tests show that this is an ideal cylindrical fold. The fold can be predicted to extend for a certain distance northwestward of the study area. Toward the southeast, the McEvoy Anticline is decapitated by the Mason Thrust (Sections DD′ and EE′). Across the Smoky River, the McEvoy Anticline cannot be correlated with certainty with any of the numerous folds present in that area.

The next fold of interest is the Westridge Anticline. This fold can only be recognized between Sheep Creek and just east of Section DD′. It has disappeared along Section EE′. From the contours on figure 3, it is shown that the anticline is plunging southeastward in the area southeast of section DD′ and is plunging northwest in the area northwest of section DD′. Consequently, the Westridge Anticline is doubly plunging and forms a culmination. The Westridge Anticline has reasonable exposure northwest of Section DD′.

The orientation of bedding was measured in several stratigraphic horizons, including the No. 4 coal seam. These measurements defined domain 26 (figure 13). A test for conicity shows that the normals to the bedding can be fitted to a cone with a half apical angle of 81 degrees. Consequently, the folded surfaces in domain 26 fit a cone with a half apical angle of 9 degrees. The cone axis is plunging 18 degrees in direction N299°E, and the hinge line, which is the cylindrical axis, plunges 4 degrees in direction N300°E. The cone is closing towards the southeast. This geometry is supported by the fact that the Westridge Anticline is not present along Section EE′. The syncline between the Westridge and McEvoy anticlines terminates in the same general area. This example shows that a conical fold explains the termination of individual cylindrical folds along their trends.

The Two Camp Creek Anticline is a well-defined structure along Sections CC′ and DD′. However, it is not present along Section EE′. There is good exposure of the fold in domain 32. The stereoplot of figure 14 shows 20 mean bedding orientations of the fold in the western part of domain 32. The best fit cylindrical fold axis (as estimated from eigenvectors) is plunging 18 degrees in direction N130°E. However, a better fit is made to the data using a cone with a half apical angle of 77 degrees. As with the Barrett Anticline, a statistical test shows that the conical model is accepted with 90 percent confidence over the cylindrical model, but not with 95 percent confidence. It follows that the folded surfaces fit a southeasterly closing cone with a half apical angle of 13 degrees. The cone axis is plunging 3 degrees in direction N127°E. The closing of the cone toward the southeast explains why the Two Camp Creek Anticline is not present along Section EE′.

Sterne Creek Anticline extends from the slopes of Mt. Hamell toward Grande Mountain across the Smoky River. It is doubly plunging at the level of the No. 4 coal seam on Mt. Hamell, forming a slight depression. On

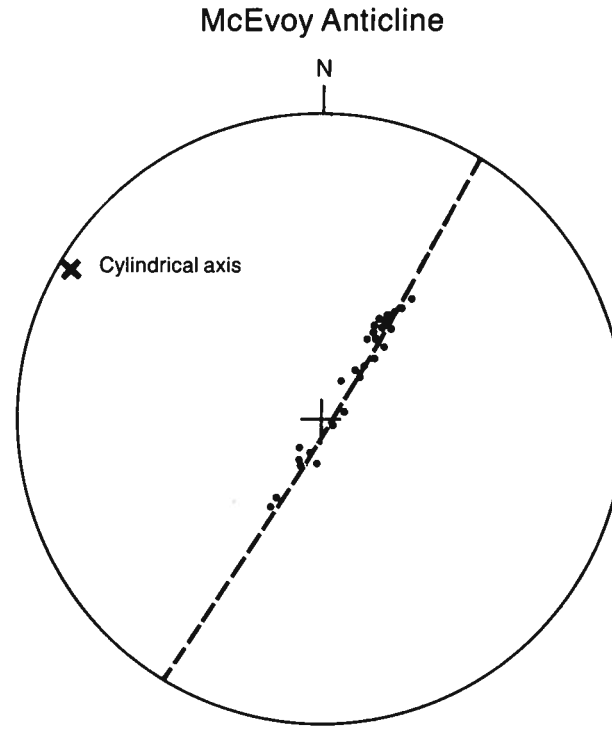

Figure 12. Stereoplot showing the orientation of the footwall of the No. 4 coal seam in domains 47, 54 and 55. The cylindrical fit (great circle) is shown by the dashed curve.

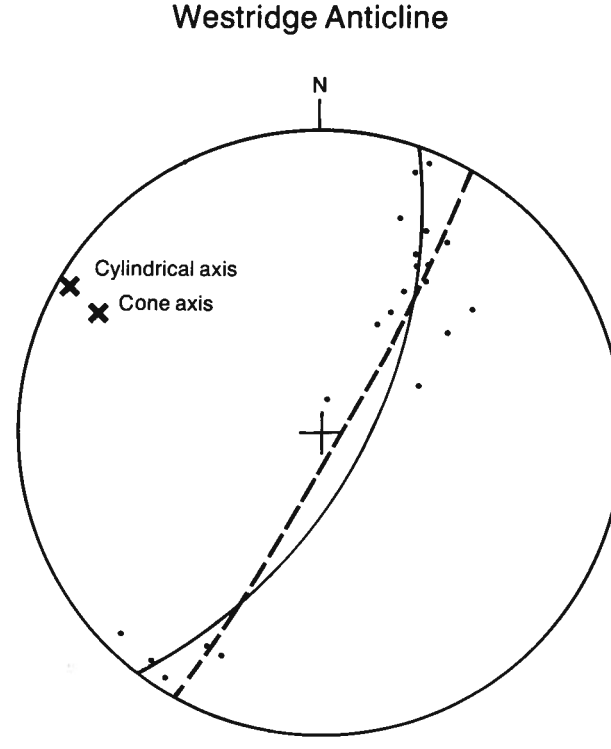

Figure 13. Stereoplot showing the orientation of the poles to bedding along the Westridge Anticline in domain 26. The conical fit is shown by the solid curve and the cylindrical fit by the dashed curve.

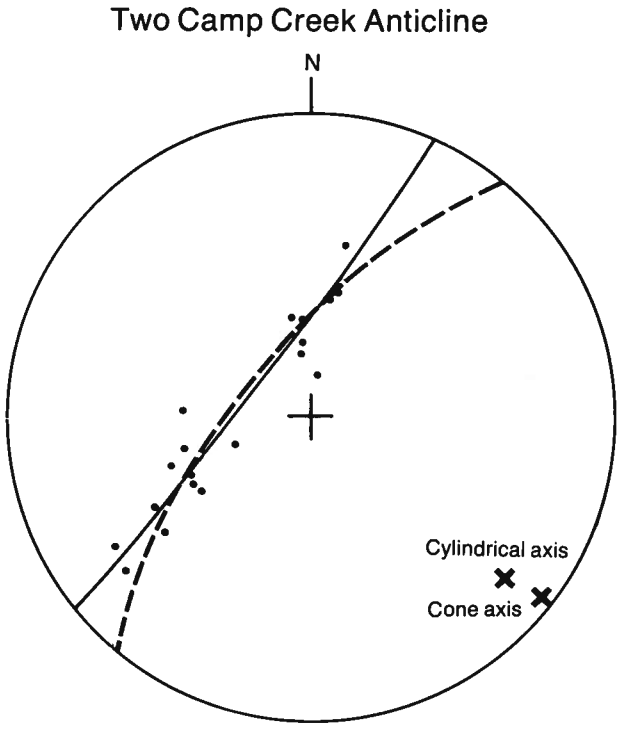

Figure 14. Stereoplot of the orientation of the poles to bedding along the Two Camp Creek Anticline in domain 32. The conical fit is shown by the solid curve and the cylindrical fit by the dashed curve.

Grande Mountain, it is plunging slightly eastward. At Sheep Creek, the fold has terminated, and the main fold is the Two Camp Creek Anticline. From Grande Mountain, the fold extends for about 30 km southeast (Irish, 1965), indicating its cylindrical character.

It is concluded that a good deformation model for this part of the foothills includes cylindrical chevron folding, with conical folds at the tapering ends.

Fold-thrust structures

The four major thrust faults in the area are, from southwest to northeast, the Cowlick, Syncline Hills, Mason and Muskeg Thrusts (figure 15). The Mason Thrust is very well exposed in domain 10 where the No. 4 coal seam is thrusted over the No. 11 seam (figure 15c), defining a ramp as shown on section EE′. Other good exposures are above the No. 5 underground mine along the railway southeast of the Smoky River, where the thrust forms the boundary between domains 1 and 3. Here, the thrust forms two thrust surfaces with a 30 m thick thrust slice in between. The thrust is a ramp in both the hanging wall and the footwall. Between domains 1 and 4, it is largely a flat bedding plane thrust, except farther east where it forms a ramp through Dunvegan sandstones in the footwall (figure 1). In this area, the fault is again defined by one (and sometimes two) 20-m thick thrust slice.

From the information shown in figure 15c and from a downplunge cross section, the displacement along the Mason Thrust in domain 10 is measured to be 150 m. The shortening by folding between the Mason Thrust and the northeast limb of the Barrett Anticline, as estimated using the No. 4 seam as datum horizon along Section EE′, is 20 percent or 550 m. These numbers add up to a combined shortening of 700 m, or 25 percent.

Across the Smoky River, in the western part of domain 1 between the Mason Thrust and the northeast limb of the Barrett Anticline, the shortening by folding is estimated from the No. 4 seam to be 10 percent or 210 m. Displacements along the Mason Thrust are observed from the separation of the No. 4 coal seam (see Section GG″) and amount to 500 m. The combined shortening is estimated as 710 m, which is in good agreement with the shortening obtained from the other side of the river.

About 750 m east of Section GG″, the displacements along the Mason Thrust are estimated to have increased to 1000 m by movements along flat bedding plane surfaces. These observations indicate that there is a close connection between thrust displacement and folding in the footwall. A decrease in shortening by folding is compensated by an increase in fault displacement. Changes in the amount of shortening by folding are accomplished by conical folds as described in the previous section. These changes are reflected by changes in the amount of thrust displacement and are a result of fault-to-fold displacement transfer (Dahlstrom, 1969; Gardner and Spang, 1973). It is concluded that folding of the Barrett Anticline and faulting of the Mason Thrust was contemporaneous.

Another indication of fault-to-fold displacement transfer is given by the continuation to depth of the Mason Thrust. At the surface of Section HH′, there is about 1000 m of displacement along the Mason Thrust and its splay. The displacement along the thrust increases to 3000 m or more at the top of the Paleozoic, as shown by a seismic section in this area (information made available by Shell Canada Limited). In the relatively rigid carbonates, very little folding occurs; shortening is mainly by thrusting. This is also shown on cross section 2 of Mountjoy (1978). This situation is similar to that described along the Turner Valley Thrust, where diminishing fault displacement is likely compensated by increased shortening due to folding (Dahlstrom, 1970, pg.359; Williams and Chapman, 1983). The displacement along the Muskeg Thrust decreases from 1000 m in the study area to 0 m at its termination 30 km to the southeast. Consequently, the transfer may be part of a fault-to-fold-to-fault displacement transfer between the Mason and Muskeg thrusts.

Along Section DD′, the shortening by folding between the Mason Thrust and the northeast limb of the Barrett Anticline is 15 percent or 480 m. The displacements along the Mason Thrust have decreased to 20 m. The rest of the shortening is apparently taken up by the McEvoy and Westridge anticlines in the hanging wall of the Mason Thrust. The Mason Thrust is inferred to terminate just west of section AA′. Consequently, it does not extend as far northwest as suggested by Irish (1965). In domain 10, the Mason Thrust cuts downsection and then upsection in the direction of displacement of the hanging wall as it crosses the McEvoy Anticline (see section EE′). That is, it decapitates the McEvoy Anticline, although there are problems making the

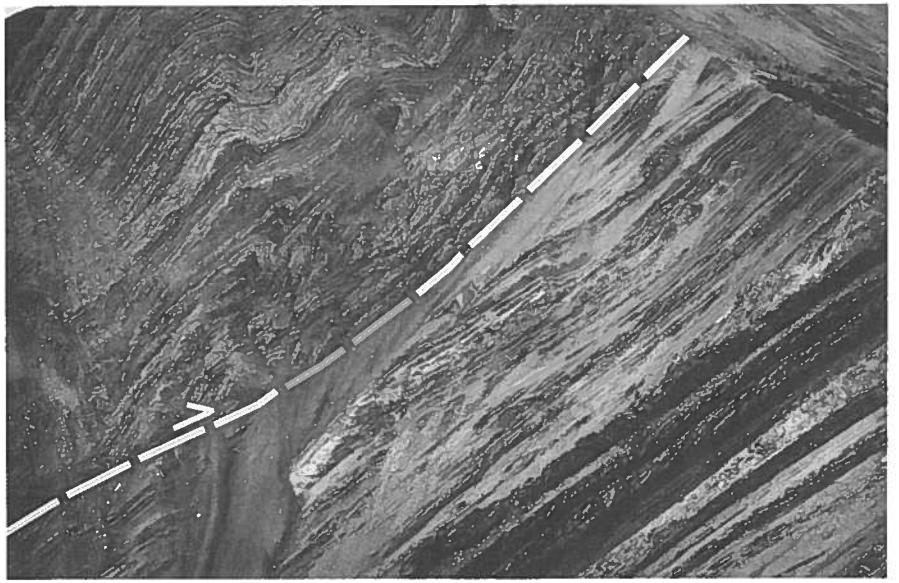

(a)

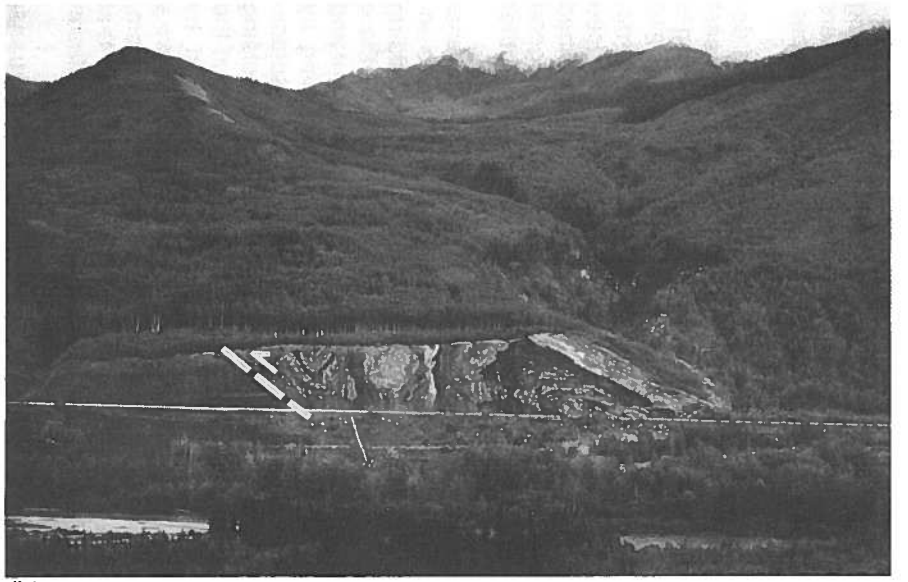

(b)

(c)

(d)

Figure 15. Exposure of the major thrust faults of the area. (a) Cowlick Thrust below Mt. Hamell, which places Nikanassin Formation on top of Mountain Park Member and Shaftesbury Formation. (b) Syncline Hills Thrust along railroad, which places Grande Cache Member on top of Shaftesbury Formation. (c) Mason Thrust in domain 10. The traces of the No. 4, No. 10 and No. 11 coal seams of the Grande Cache Member are indicated. (d) Muskeg Thrust along Sheep Creek, which places Torrens and Grande Cache members on top of Kaskapau Formation.

cross section completely balanced at this locality. This indicates that folding was present before the initiation of the Mason Thrust in this particular area. Once the fold became locked, shortening was accomplished by the Mason Thrust. Additional folding may have occurred after thrusting, as shown by the curved nature of the Mason Thrust along section EE′. These observations point to contemporaneity of folding of the McEvoy Anticline and faulting of the Mason Thrust.

Folds with related thrusts are termed fold-thrust structures (Chapman and Williams, 1984) and are a common feature of foreland fold and thrust belts. Similar structures are described as fault-propagation folds by Suppe (1985); however, this term implies that the folds are secondary structures that form in response to faulting. The term fold-thrust structure is used in the Grande Cache area because it emphasizes that folding and thrusting are roughly contemporaneous.

Williams and Chapman (1983) describe back thrusts in examples of fold-thrust structures. Back thrusts are fairly common in the Grande Cache area on a mesoscopic scale (see next section) and five are found on the scale of the 1:15 000 map (figure 1). One is located in the core of a prominent anticline north of the Flood Mountain Syncline at 61000 E and 5984000 N. Two are located on the western slopes of Grande Mountain at 56300 E, 5978800 N and at 57100 E, 5977700 N. A fourth is present on the north limb of Two Camp Creek Anticline at 54300 E and 5983400 N; and the fifth is near the hinge of the Susa Creek Anticline.

The deformation model for the Grande Cache area can now be extended to include fold-thrust structures in areas where thrusting occurs.

Mesoscopic structural elements

Mesoscopic structural elements are useful in describing the geometry of deformed rocks. In this section, they will be described under the headings of bedding, folds, cleavage, faults and joints. Slickenside striae are sometimes present on planar structures such as bedding, faults or joints. Their orientations are plotted on stereonets together with a portion of the great circle which passes through the pole of the shear surface and the slickenside stria. Where the sense of relative movement is determined, the direction of relative motion of the hanging wall is shown by an arrowhead. The normals to the planes defined by slickenside stria and normal to shearplane are referred to as slipnormals (sometimes called axes of slip) and are also shown on these plots. Together, the orientations of shearplanes, slickenside striae and slipnormals give a movement picture of the deformation.

Bedding

Bedding was measured in almost all outcrops visited. Generally, five repeated measurements of bedding were taken. Figure 1 (in pocket) shows the orientation of bedding (estimated from the mean bedding orientation) of a representative number of outcrops. From the repeated measurements, a precision parameter K for the cylindrical domains was calculated. The values of K

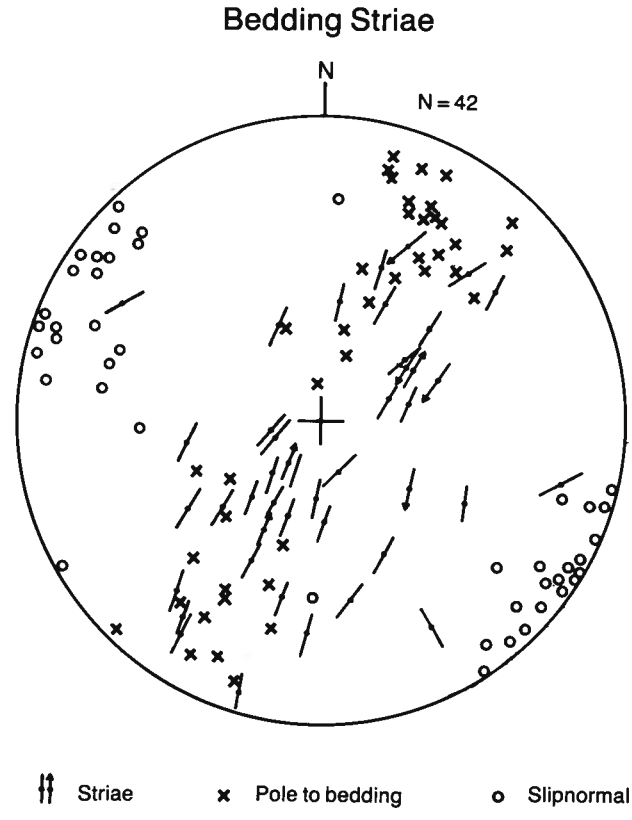

Figure 16. Stereoplot showing the orientation of all measured slickenside striae on bedding (N = 42), the bedding on which they are present and the slipnormals (axes of slip).

range between 129 and 366, with an average of 231 (appendix B). They indicate relatively little roughness on the bedding planes.

Slickensides were observed on bedding planes in 42 stations, seven of which showed the sense of relative movement. The sense was determined where slickenside straie, which are generally formed by fibrous calcite, show accretion steps. The orientation of slickenside striae, the bedding on which they occur and the slipnormals are shown in figure 16. The slipnormals show a preferred orientation parallel to the average fold axis of the area, which is plunging 1 degree in direction N124°E. Of seven stations where the sense of movement is known, five show that the hanging wall moved up relative to the footwall. These observations are consistent with a flexural-slip model of folding around axis N124°E/1° and a movement direction of N30°E with shallow plunge. Four axes of slip deviate from this direction. They may represent younger movements, as indicated by an outcrop with two superimposed directions of slickensiding. In this outcrop, the older direction shows a horizontal axis of slip near the average fold axis. The younger direction has a 40 degrees plunging axis of slip in direction N268°E. These younger movements may be related to erosion and resulting stress release, with possible sliding into the valleys.

Folds

Mesoscopic folds are present in many outcrops. They are minor folds in the cores or limbs of macroscopic

folds. Figure 17a shows the preferred orientation of 104 mesoscopic fold axes from the whole study area. The highest concentration (over 15 percent per 1 percent area) of orientations is centered around N124°E/1°, which is the average fold axis calculated from the macroscopic fold axes in 60 cylindrical domains (listed in appendix B). Because of a slightly skewed distribution, the average of the 104 mesoscopic fold axes is plunging 2 degrees in direction N116°E.

In 57 outcrops, the axial plane of these mesoscopic folds was measured (figure 17b). Both northerly and southerly dipping axial planes are present, which is the same pattern as shown by the macroscopic folds (see cross sections of figure 2).

Cleavage

A spaced cleavage was found in one location, just above the Mason Thrust in domain 10. It is axial planar to a mesoscopic fold in a shaley sandstone.

Faults

All 29 mesoscopic faults measured were reverse faults, which show the same movement pattern as the major thrust faults of the area. The majority of these faults are south dipping (figure 18), but northward dipping back thrusts are also present. Three of these back thrusts are north dipping reverse faults in the south limb of the McEvoy Anticline, with 3-10 cm displacements. Faults with striae (N = 8) have slipnormals parallel to the average fold axis of the area (figure 18), showing that the mesoscopic faults conform to the fold-thrust structures described in the previous section.

Joints

At most outcrops, the orientation of two to three joint sets was measured, generally in sandstone. They were selected after a brief visual inspection of all joints in the outcrop. The joints are generally perpendicular to bedding. This does not imply that the joints necessarily formed prior to tilting of beds, but attests to the control that sedimentary stratification exerts over development of joints. Consequently, the preferred orientation of joint sets have only significance in structurally simple areas (i.e., in individual limbs of macroscopic folds). For this reason only two areas will be discussed with regard to joints: the area of the Barrett Anticline in domains 11 and 23, and the south limb of the McEvoy Anticline in domains 47, 54 and 55.

The orientation of 89 joint sets together with the mean bedding orientation in the north limb of the Barrett Anticline (figure 19a) clearly shows that most joints are perpendicular to bedding and that there are two preferred orientations—one dipping steeply northwest and the other dipping southwest. The south limb (figure 19b) has 48 joint sets, which are generally perpendicular to bedding and which have two (possibly three) preferred orientations. One is dipping steeply northwest and southeast, the other is dipping 40 degrees toward the northwest.

To get a better appreciation of the preferred orientations, the joints were represented with respect to bedding rotated to horizontal around its strike. For this purpose the area was divided into four sub-areas, representing the north and south limb in domains 11 and 23. In these four sub-areas, the mean bedding orientation was calculated, and all joints were rotated around the mean bedding strike in such a way that bed-

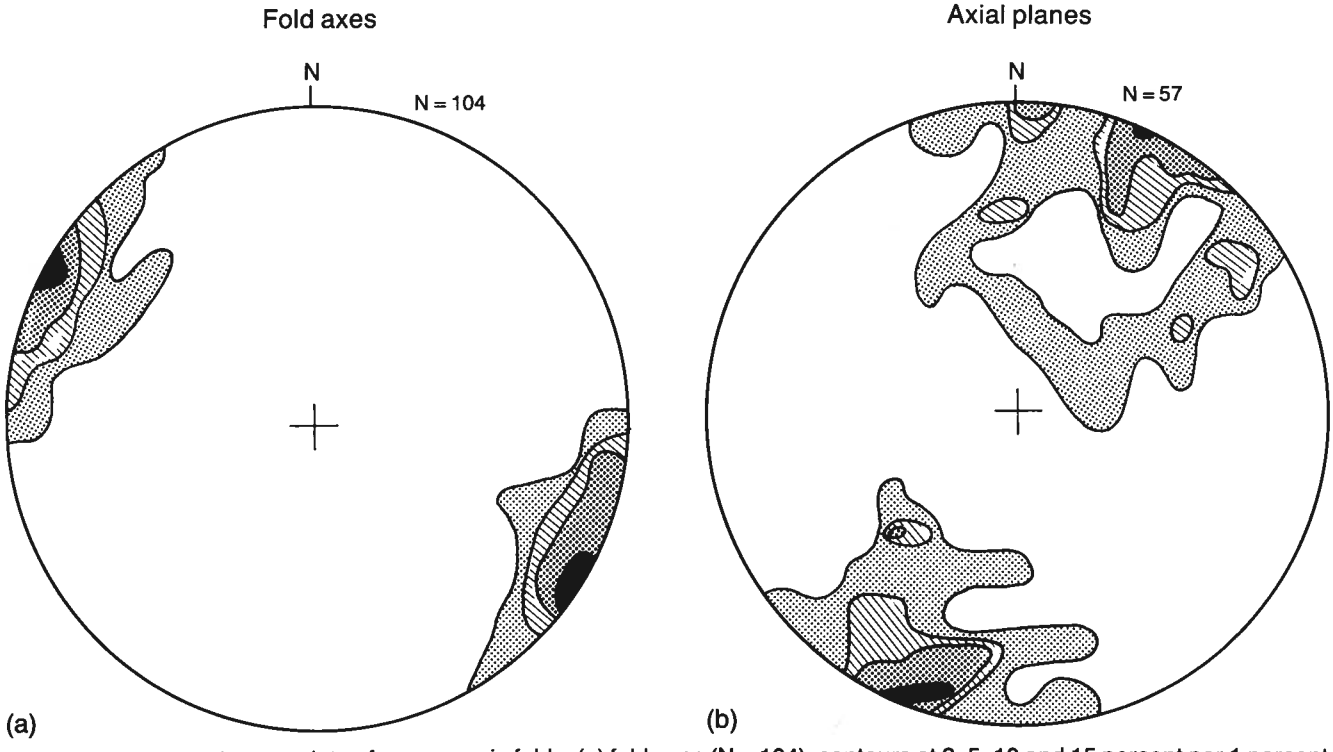

Figure 17. Contoured stereoplots of mesoscopic folds. (a) fold axes (N = 104), contours at 2, 5, 10 and 15 percent per 1 percent area. (b) axial planes (N = 57), contours at 1, 3, 5 and 10 percent per 1 percent area.

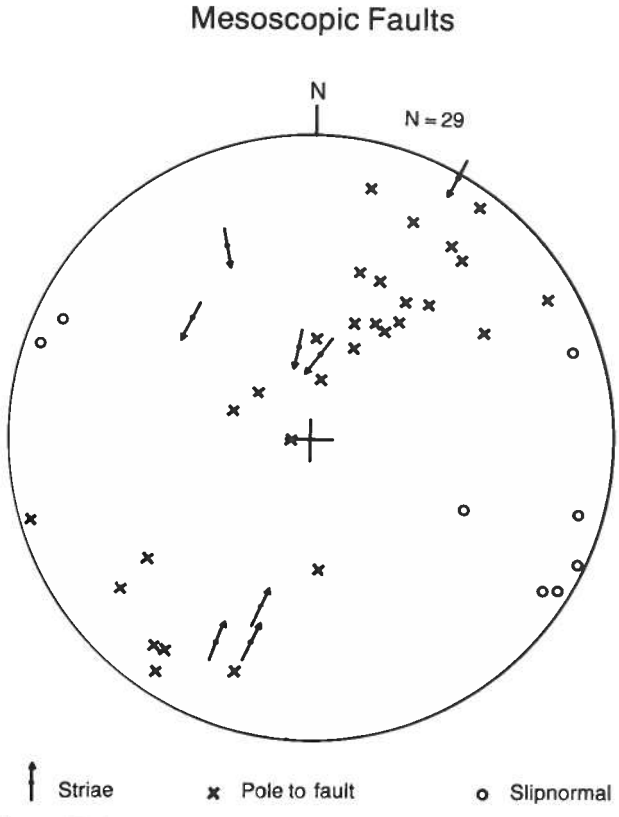

Figure 18. Stereoplot showing the orientation of all measured mesoscopic faults (N = 29), slickenside striae (N = 8) and slip-normals (N = 8).

ding became horizontal. All 137 rotated joint sets were plotted together (figure 20a). About 90 percent of the joint sets lie within 20 degrees of being normal to bedding. Some of the deviation from normality can be attributed to variable bedding orientations in the limbs of this chevron fold. The north limb of the Barrett Anticline is not completely straight (figure 9).

Because the rotated joints are near vertical, they can be displayed in a two-dimensional rose diagram. The rose diagram is smoothed by a technique developed by Ramsden (1975). In this diagram, every measurement is represented not by a spike but by a bell-shaped curve. The shape of this curve is controlled by the precision parameter k of the von Mises density function (Mardia, 1972). Consequently, k is used as a smoothing parameter. The larger the value of k, the spikier the resulting curve will be.

The value of the smoothing parameter k was obtained by taking repeated measurements of joints belonging to the same set. This was done for 20 different sets in 20 different outcrops. An overall precision parameter of 35 was estimated from these measurements, and a rose diagram was drawn from the results (figure 20b). Clearly, two preferred orientations of jointing are significant; one parallel to the fold axis, and the other, which is slightly more prevalent, perpendicular to that direction. A similar pattern is shown by 13 joint sets measured on the south limb of the McEvoy Anticline in the footwall of the No. 4 coal seam (figure 21). The most prominent direction strikes perpendicular to the fold axis and the other direction strikes roughly parallel to the fold axis (which is N302°E/4°).

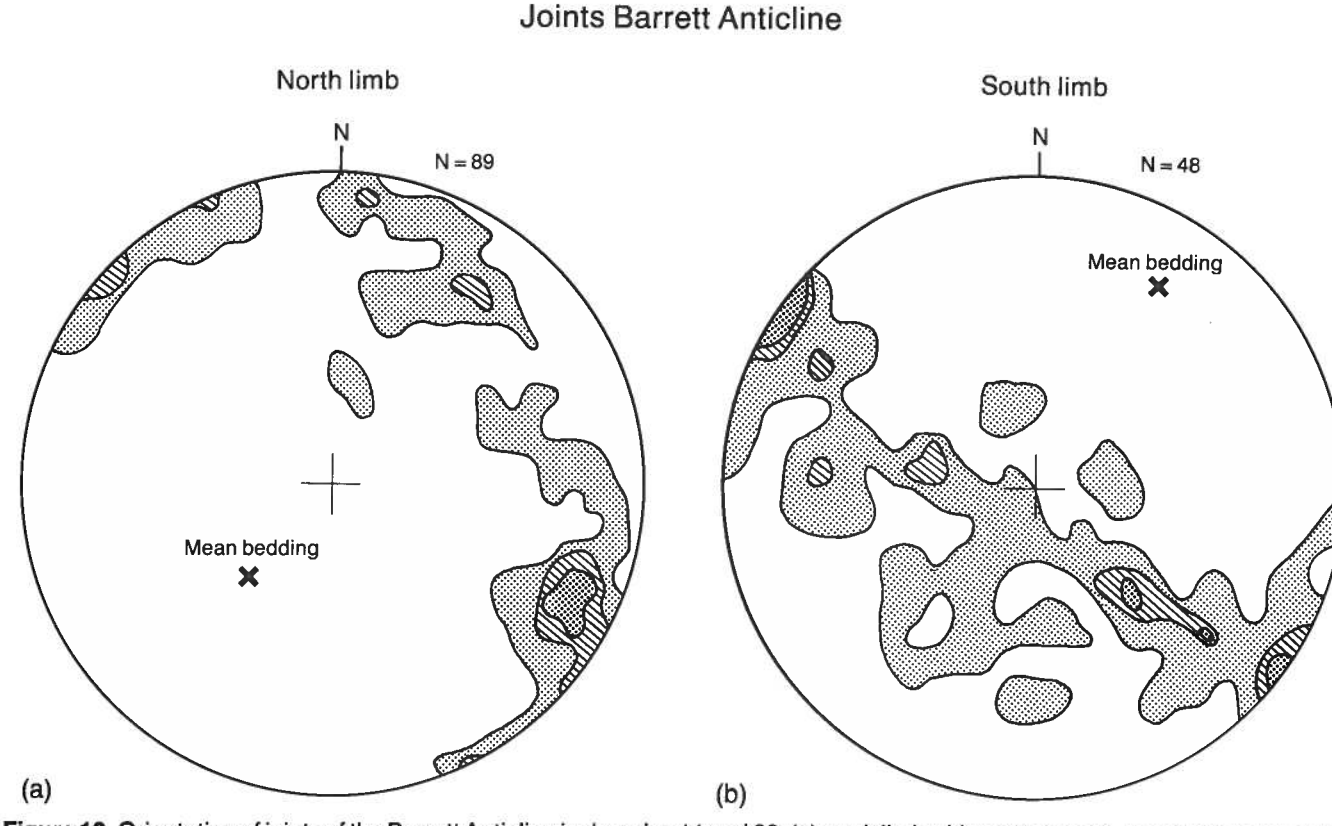

Figure 19. Orientation of joints of the Barrett Anticline in domains 11 and 23. (a) north limb with contours at 2, 5 and 7 percent per 1 percent area for a total of 89 joints. (b) south limb with contours at 2, 5 and 7 percent per 1 percent area for a total of 48 joints.

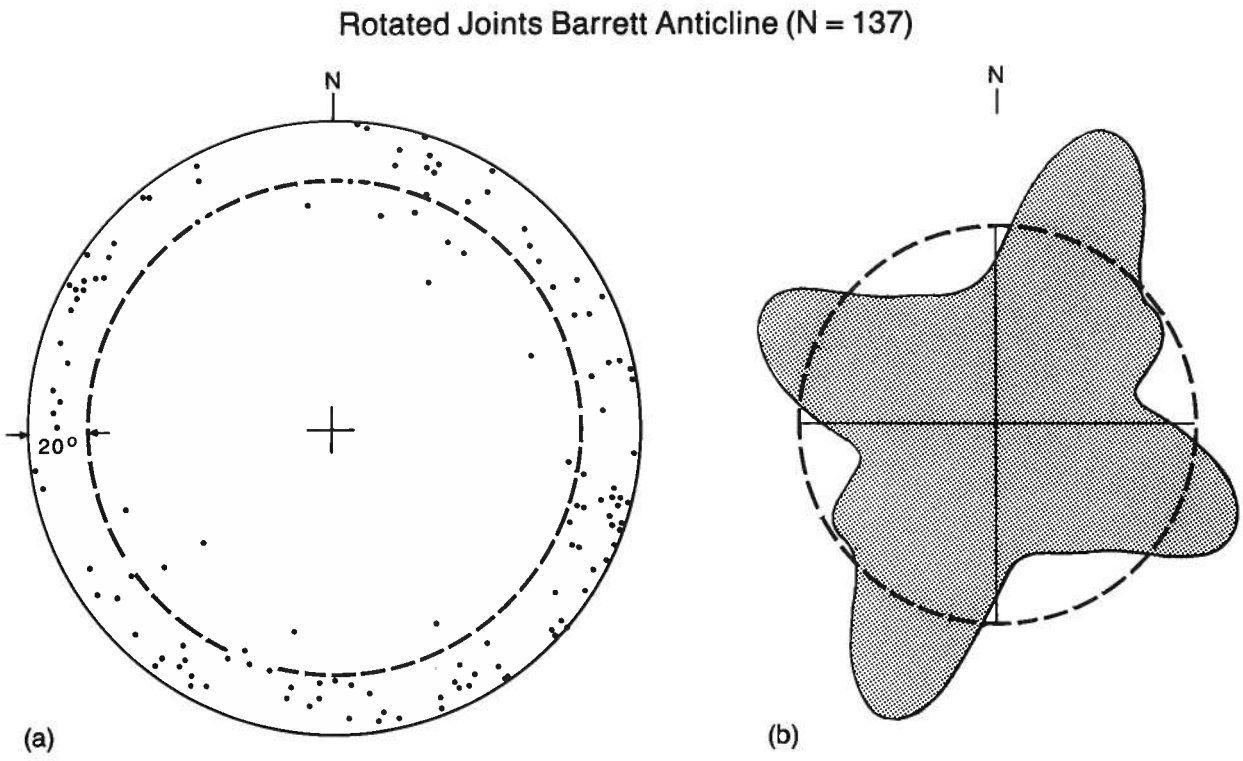

Figure 20. Orientation of 137 joints of the Barrett Anticline in domains 11 and 23 with the bedding rotated towards horizontal. (a) equal area plot of poles to joints. Diagram shows that most joints are within 20° of being normal to bedding. (b) smoothed rose diagram of the strikes of the joints. Smoothing parameter k = 35. The circle represents a uniform distribution.

These directions are probably regional directions of jointing resulting from erosional unloading and uplift as indicated by similar preferred orientations in the central Alberta foothills (Currie and Reik, 1977) and in the plains (Babcock, 1974). The similarity of these orientations is significant because it constitutes field evidence that uplift and erosion are important processes in forming regional joint patterns (Currie and Reik, 1977, pg. 1227). Most of the systematic joints are extensional, occurring in orthogonal systems. Their extensional nature is indicated by the occasional presence of plumes and rib marks on the joints. These observations suggest that most joints did not form with any significant compressive normal stress acting across the fracture surface.

Occasional compressive stress across the fracture plane is indicated by slickensided joint surfaces. The orientation of slickenside striae on 17 surfaces distributed over the whole study area is displayed in figure 22. They show a significantly different movement pattern from that defined by the slickenside striae on bedding and on faults that are displayed in figures 16 and 18. The slipnormals (axes of slip) of the slickensided joints do not indicate a maximum. If we assume that the deformation was homogeneous, then the slickenside striae are traces of the direction in which the area moved. To determine this direction, the common line is found that is contained by all planes defined by each slickenside stria and the associated normal to the plane on which shear took place (Cruden, 1971). So the slipnormals should lie on a great circle and the pole to this great circle is the movement direction. The orientation of this pole is calculated with an eigenvalue method.

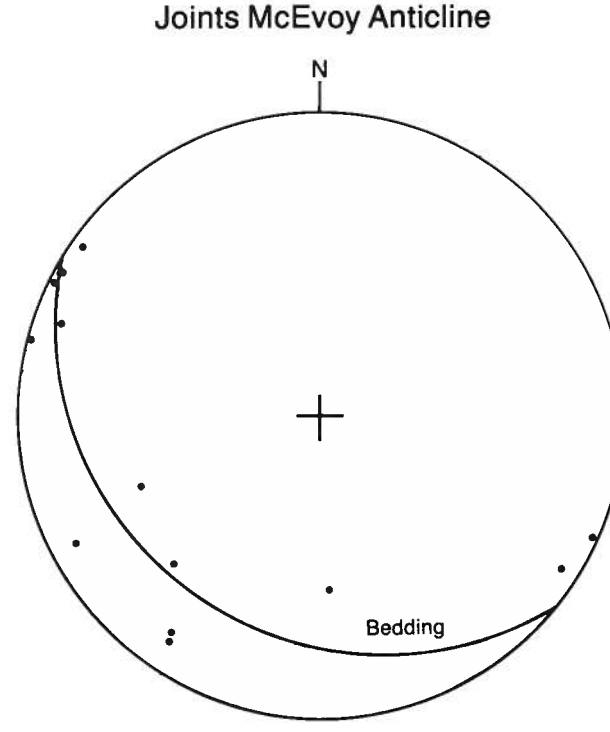

Figure 21. Orientation of joints in the south limb of the McEvoy Anticline in domains 47, 54 and 55 (N = 13). The mean bedding orientation is shown by the solid curve.

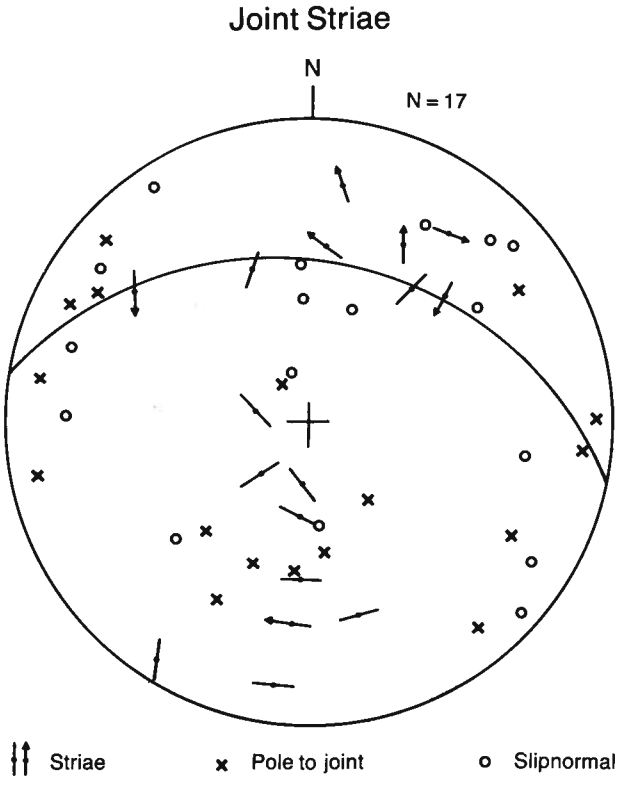

Figure 22. Stereoplot showing the orientation of slickenside striae on joints (N = 17), the joints on which they are present and the slipnormals (axes of slip). The solid curve represents the best fitting plane (great circle) through the slipnormals, which is perpendicular to the slip direction.

Although the great circle is not well defined, its pole is plunging 47 degrees in direction N192°E (figure 21b). This movement direction cannot be easily correlated with the regional deformation responsible for the macroscopic structure, which has a movement direction of N30°E with a shallow plunge. It is suggested that this particular deviating movement pattern is caused by sliding after erosional unloading and uplift. During erosion, sliding can occur toward the valleys as a result of gravitation. This is indicated by several shear joints whose hanging wall moved downward (shown by sense of shear direction in figure 22). Because the orientation of slickensided joints is similar to extensional joints, it is concluded that slickensiding resulted from later stresses across these joint surfaces sufficient for frictional sliding. However, most likely some of the slickensides on joints may represent movements related to folding and thrusting. This applies especially for the ones whose slipnormals conform with those of bedding planes and faults.

Structurally thickened coal

Structurally thickened coal can be found in several places in the study area. It forms important exploration targets for open pit mining. Presently, there are two structural positions identified where thickening occurs—in fold hinges resulting from dilation and in fold limbs resulting from duplex faulting. These two situations will be discussed separately. Coal pods along fold hinges have been known and explored for many years. Coal pods resulting from duplex thrusting have only been recognized recently.

Dilation in fold hinges

The prominent deformation process of the Grande Cache area was flexural slip folding, which resulted in chevron folds. Dilation took place at the fold hinges. The incompetent layers, such as coal, flowed into these dilation zones, with the resulting structure being similar in geometry to a saddle reef.

If a thick competent layer is present in a generally even bedded sequence, the dilation in the hinges is relatively large. This is the case with sandstone overlying No. 4 coal seam (Super 4 sandstone), which is thicker than other nearby sandstone layers. In the case of a thick overlying competent layer, the dilation is larger in an anticline than a syncline (Ramsay, 1974, his figure 7). Consequently, more thickening of coal can be expected in anticlines than in synclines in the Grande Cache area.

The dilation zone can be filled in two ways: either by flow of incompetent material (i.e., coal) into the void, or by hinge collapse. In the Grande Cache area, a combination of these two processes occurs. Good examples of hinge dilations are exposed in the open pits (No. 9 Mine) northwest of Sheep Creek.

At the western end of the main open pit (50600 E -5990000 N) on the crest of the McEvoy Anticline, the No. 4 coal seam is thickened to 10 m from a normal thickness of about 6 m (figure 23). It has, however, not completely filled the dilation space, and, as a result, the hinge has collapsed; this is indicated by steeper dips (up to 55 degrees) of overlying sandstone compared to the footwall (about 25 degrees). The sandstone overlying No. 4 seam forms what has been called a bulbous hinge structure (Ramsay, 1974, pg.1745). These bulbous structures have been formed in plasticene model experiments. Limb thrusts in this exposure are another result of the hinge collapse.

Another good exposure of hinge dilation is on the northeast limb of the McEvoy Anticline, where a sub-

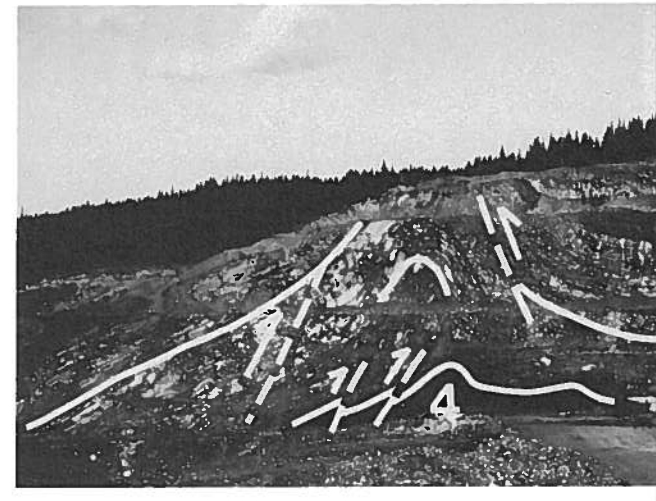

Figure 23. Structural thickening of No. 4 coal seam and accompanying hinge collapse along the McEvoy Anticline in the No. 9 Mine, resulting from hinge dilation in a chevron fold.

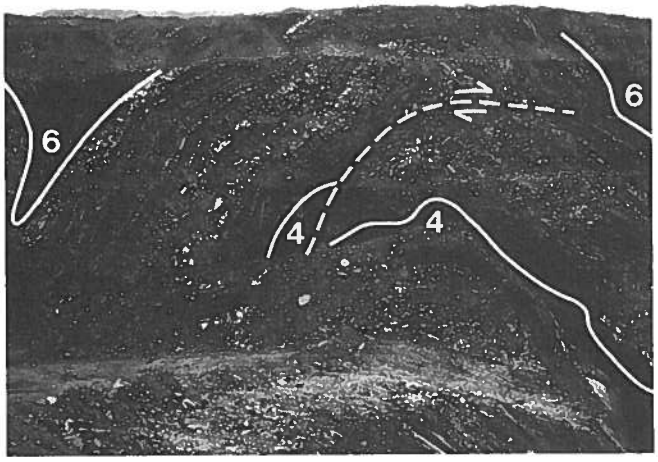

Figure 24. Structural thickening of No. 4 coal seam and accompanying limb thrust along a subsidiary anticline in the northeast limb of the McEvoy Anticline of the No. 9 Mine, resulting from hinge dilation in a chevron fold.

sidiary anticline-syncline pair of No. 4 seam is mined. No. 4 seam coal is thickened in the anticline (figure 24) by flow of coal into the dilation zone. A limb thrust has developed to compensate the folding of the extra thick layer above No. 4 seam (Ramsay, 1974, pg.1745). This minor thrust terminates at the level of the No. 6 seam, and its curved nature shows that it was folded after thrusting. The geometry of this fold is equivalent to the decapitated McEvoy Anticline in domain 10 as described in a previous section. However, the size of the structure is smaller. Consequently, this anticline is a fold-thrust structure.

Duplexes

A duplex is an imbricate thrust system where each subsidiary thrust joins two common thrusts, an upper roof thrust and a lower floor thrust. A good discussion of duplexes has been recently provided by Boyer and Elliott (1982). Charlesworth and Gagnon (1985) give an example of duplexes in a coal seam of the Outer Foothills at Coal Valley (Alberta), where the seam has been thickened to 20 times the stratigraphic thickness.

A good natural exposure of a duplex in the Grande Cache area is at 59500 E-5984300 N. Coal is exposed over a 20-m thick interval between competent sandstones of the footwall and hanging wall of the No. 4 seam. There are many shale intervals between. The thickest coal interval is 2.7 m. In addition, there are two 1 m thick coal intervals and at least 11 intervals with coal 0.1-0.7 m thick. A prominent orange weathering siltstone in the shale intervals is repeated three times by imbricate faulting in the lower part of the exposure (figure 25a). This indicates that the coal intervals are also structural repeats of the same seam. The roof thrust of this duplex is in shale below the overlying sandstone, and the floor thrust is in the shale above the underlying sandstone. These thrusts dip 65 degrees southwest. At 60215 E-5983280 N, 10 m of continuous No. 4 seam coal is exposed on the north limb of the Susa Creek Anticline, indicating that it may have been thickened in a duplex. Both roof and floor thrust must be dipping northeastward, because bedding is oriented in this direction.

Early in 1986, a man-made exposure of a duplex in the No. 4 coal seam was completed for exploration purposes by Smoky River Coal Limited at 50750 E-5986930 N. Because little exposure was present before the recent exploration, the area was left unmapped.

Exposure in the pit (figure 25b) shows that No. 4 seam is thickened three times to 20 m. Coal contains folds and faults indicating that the thickening is tectonic. A slight angular relationship between coal zone and overlying sandstone shows that the roof thrust is at the

(a)

(b)

Figure 25. Structural thickening by duplex thrusting. (a) duplex formed by structural repeats of No. 4 coal, shale and siltstone in the northern limb of Flood Mountain Syncline, 2 km southeast of Smoky River, Station 35. (b) duplex confined to the No. 4 coal seam, resulting in three times normal thickness, in an exploration pit north of Sheep Creek.

top of the coal zone. The floor thrust is assumed to be at the bottom of the coal zone. Nearby drilling showed the presence of rock wedges near the base of the duplex, indicating that the floor thrust is locally situated below the base of No. 4 coal seam (Richard Dawson, pers. comm., 1987). The floor and roof thrusts dip 50 degrees and 60 degrees northeast respectively, indicating that they are backthrusts. This movement pattern is confirmed by minor northeast-dipping upthrusts in the hanging wall sandstone.

Because duplexes have only been recognized recently in the Smoky River coal field, they may become the major exploration target in the near future.

Coal rank

Data collection

As part of the present study, laterally continuous coal seams from the Grande Cache Member were sampled to study in detail the relationship between structural events and coal rank as indicated by mean maximum vitrinite reflectance. In descending order, the seams sampled were No. 11, No. 10 and No. 4 seam (figure 4). In addition, some of the less continuous seams of the Grande Cache Member (Nos. 3, 6, 7 and 8) were analyzed, as were minor seams collected from the overlying Mountain Park Member and from the underlying Nikanassin Formation.

Full seam channel samples were collected from coal seams that were completely exposed. In some instances, channel samples represented upper, middle and lower portions of the same seam; they enabled investigation of vertical reflectance variations within the seams. Grab-samples were taken from partly covered seams and represent variable coal seam thicknesses.

Most of the 157 coal samples were collected from an area straddling the Syncline Hills Thrust in the south and the Muskeg Thrust in the north (figure 26). In addition, a few reference samples were collected at Grande Mountain and Victor Lake to the south and at the No. 9 Mine (McEvoy Anticline) and Copton Creek to the north-

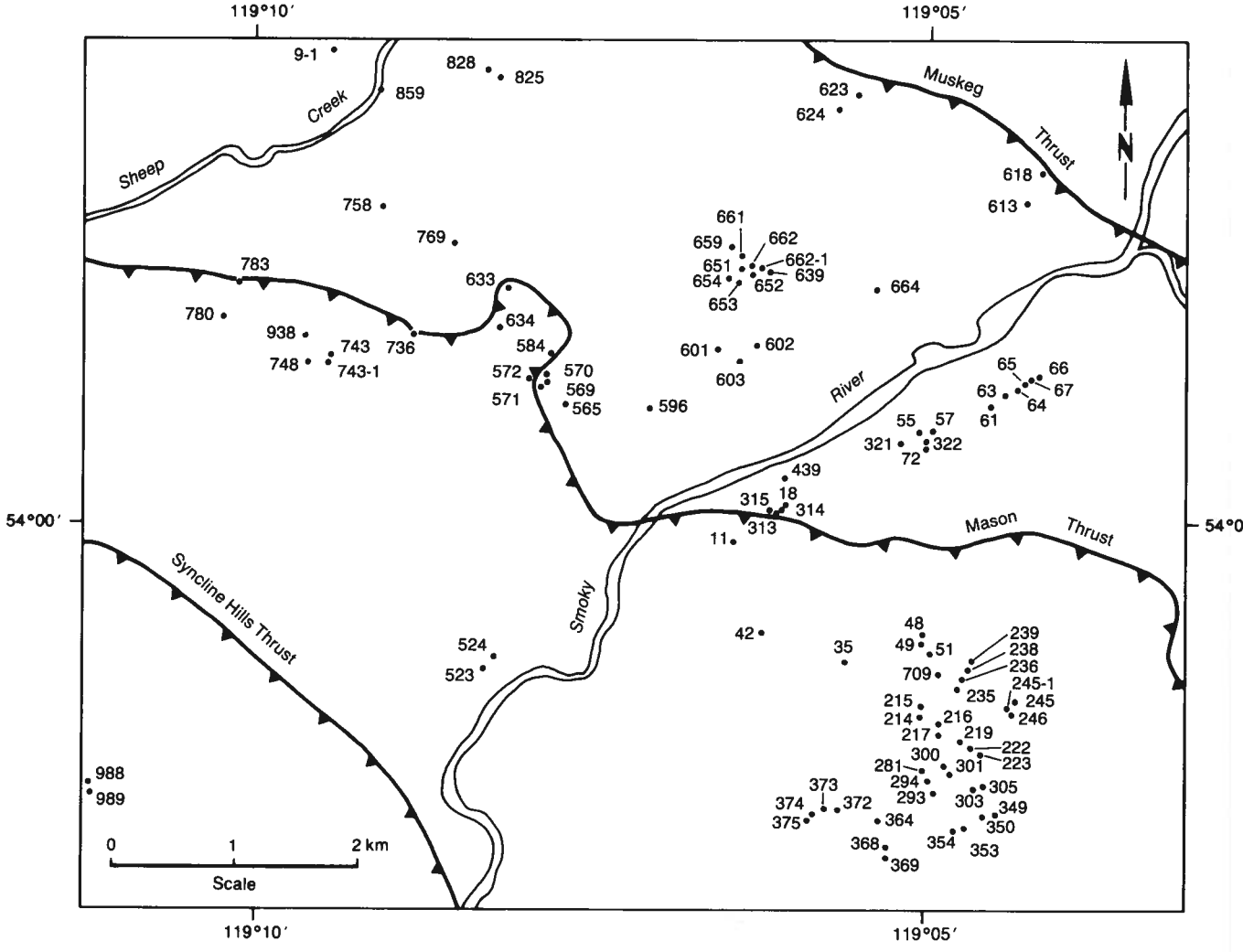

Figure 26. Distribution of coal sample localities with station numbers in part of the study area (from Kalkreuth and Langenberg, 1986).

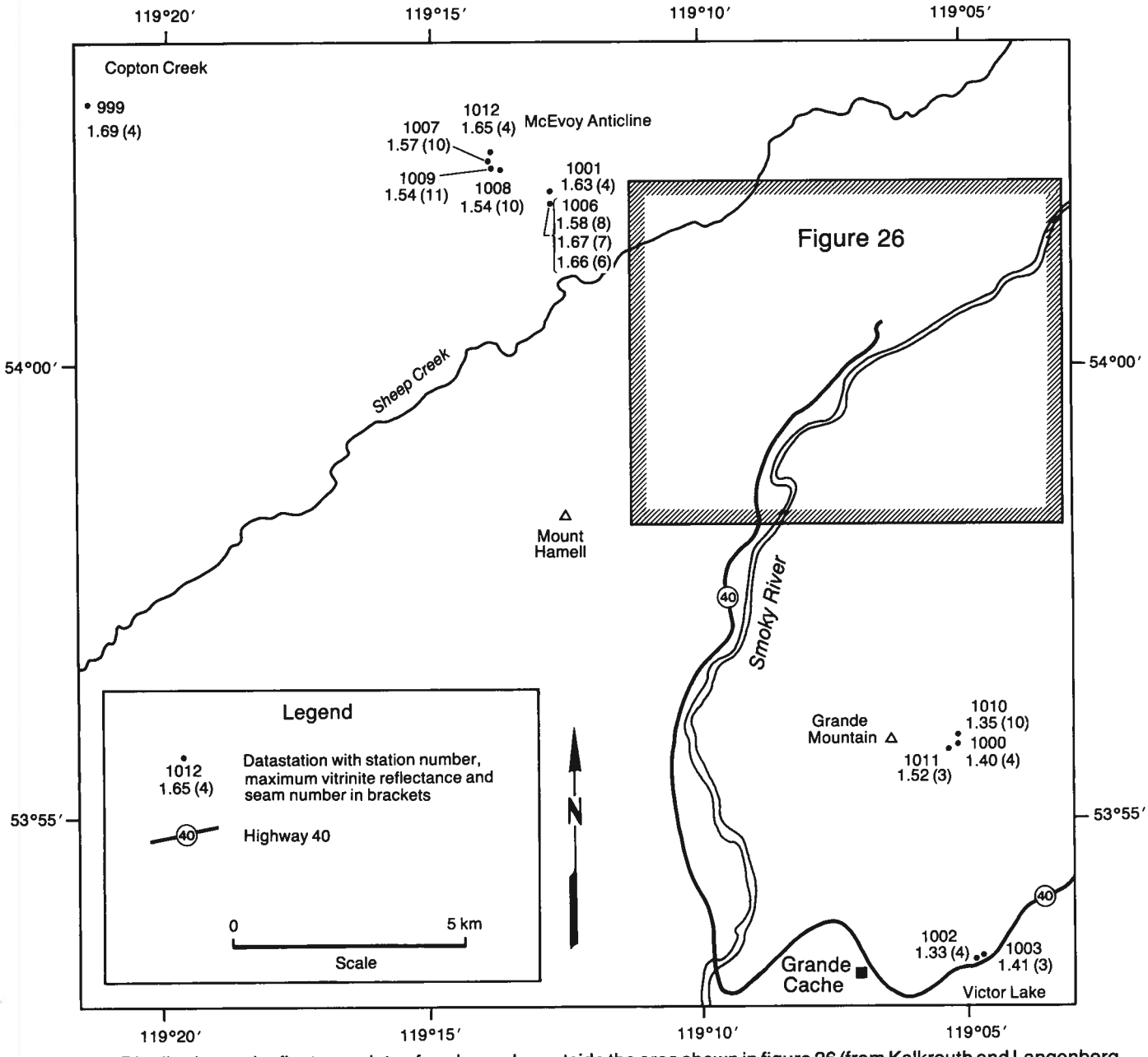

Figure 27. Distribution and reflectance data of coal samples outside the area shown in figure 26 (from Kalkreuth and Langenberg, 1986).

west (figure 27). For the interpretation of regional reflectance changes, averaged values were used for those locations where reflectances had been determined on upper, middle and lower portions of the same seam.

Two sets of samples were taken at decreasing distances from the Mason Thrust. For these samples, the bireflectance (R_{max}-R_{min}) and the ratio R_{max}/R_{min} were determined from the mean values of maximum and minimum reflectance measured on randomly oriented grains. For coals, which are thought to have uniaxial negative reflectance indicatrices, the "true" minimum reflectance can only be determined on samples cut perpendicular to bedding. Therefore, the minimum reflectance determined in the present study represents not the "true" minimum but a value intermediate between the true maximum and minimum (Levine and Davis, 1984).

Rank determination

Rank was determined by calculating the mean and standard deviation of the maximum vitrinite reflectance in oil (see Bustin et al., 1983). American Society for Testing and Materials (ASTM) rank classes were obtained by using the maximum reflectance limits published by Davis (1978). The results have been published previously (Kalkreuth and Langenberg, 1986). In the present publication, the results are summarized and all reflectance data, ASTM rank classes and locations for all samples are listed (appendix C).

Mean maximum vitrinite reflectances range from 1.29 percent in the Mountain Park Member of the Gates Formation to 1.75 percent in a coal from the Nikanassin Formation. In terms of ASTM rank classes, these values indicate medium to low volatile bituminous rank for all coals.

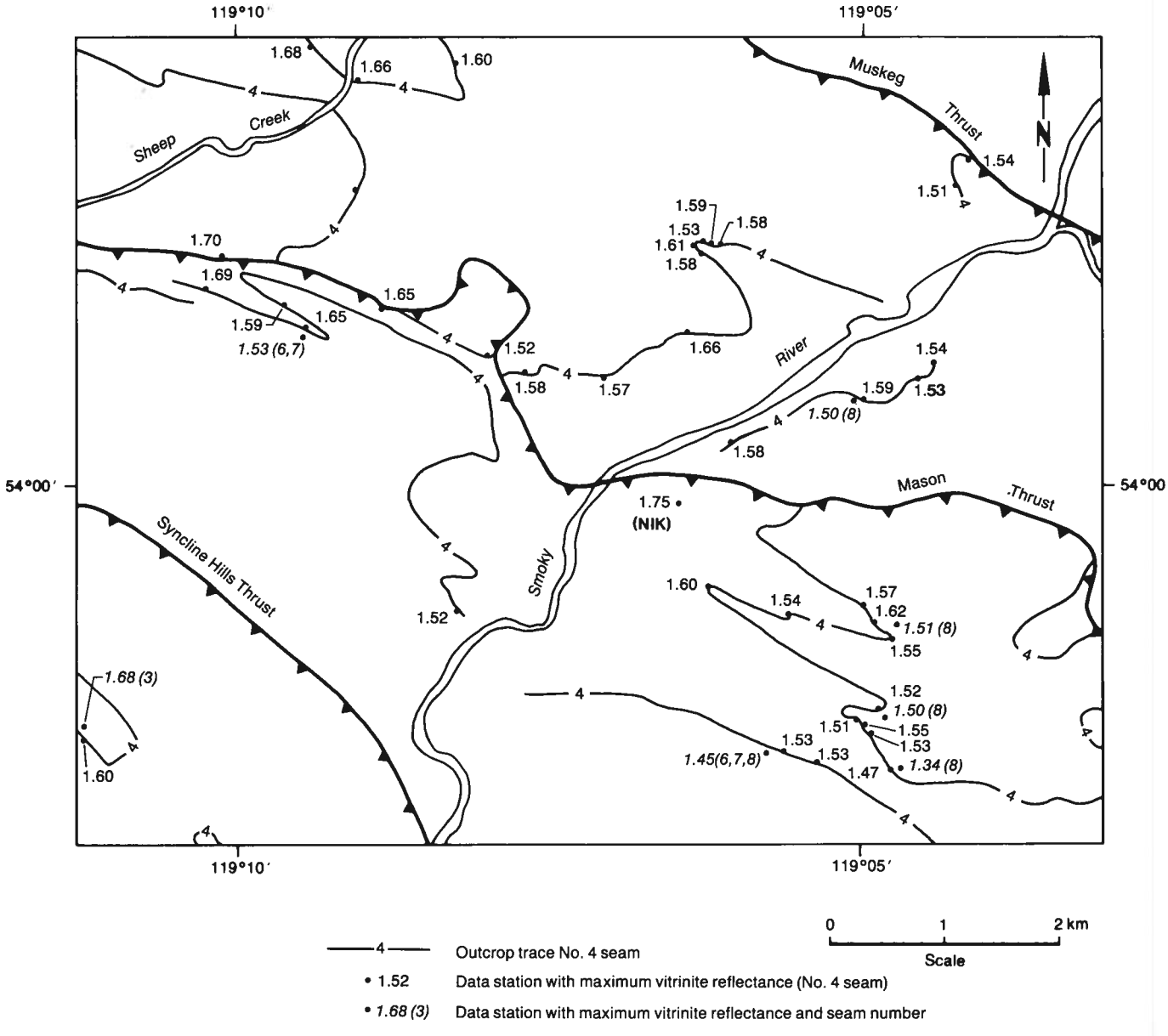

Figure 28. Regional reflectance variations in the lower Grande Cache Member (including the Nos. 3, 4, 6, 7 and 8 seams) and in the Nikanassin (NIK) Formation (from Kalkreuth and Langenberg, 1986).

Vitrinite reflectances in seams from Nikanassin Formation

Two coals from the Nikanassin Formation were analyzed. They were collected at the same location from an uncertain stratigraphic position in the hanging wall of the Mason Thrust. The reflectances of 1.62 and 1.75 percent (the latter value is shown on figure 28) indicate that both samples are low volatile bituminous coals.

Vitrinite reflectances in No. 3 seam, Grande Cache Member, Gates Formation

Three samples were analyzed. The mean maximum vitrinite reflectances range from 1.41 percent at Victor Lake (figure 27) in the south to 1.68 percent near Mount Hamell (in the southwestern part of figure 28). The data are too sparse to allow any regional interpretation.

Vitrinite reflectances in No. 4 seam, Grande Cache Member, Gates Formation

A total of fifty-five samples were analyzed. The mean maximum reflectances range from 1.33 percent at Victor Lake (Station 1002, figure 27) to 1.70 percent in a seam in the contact zone of the Mason Thrust (figure 28). The reflectance data indicate low volatile bituminous coals for most of the samples. Detailed sampling of upper, middle and lower portions of No. 4 seam at five locations indicate that there is a considerable scatter of reflectance values within one seam at one location. In general, there is a trend to a slight increase of reflectance values as one moves from the top of the seam toward the bottom (Kalkreuth and Langenberg, 1986). This variation has to be included in the interpretation of regional rank changes, where data are often obtained from grab samples whose position in the coal seam is not clear.

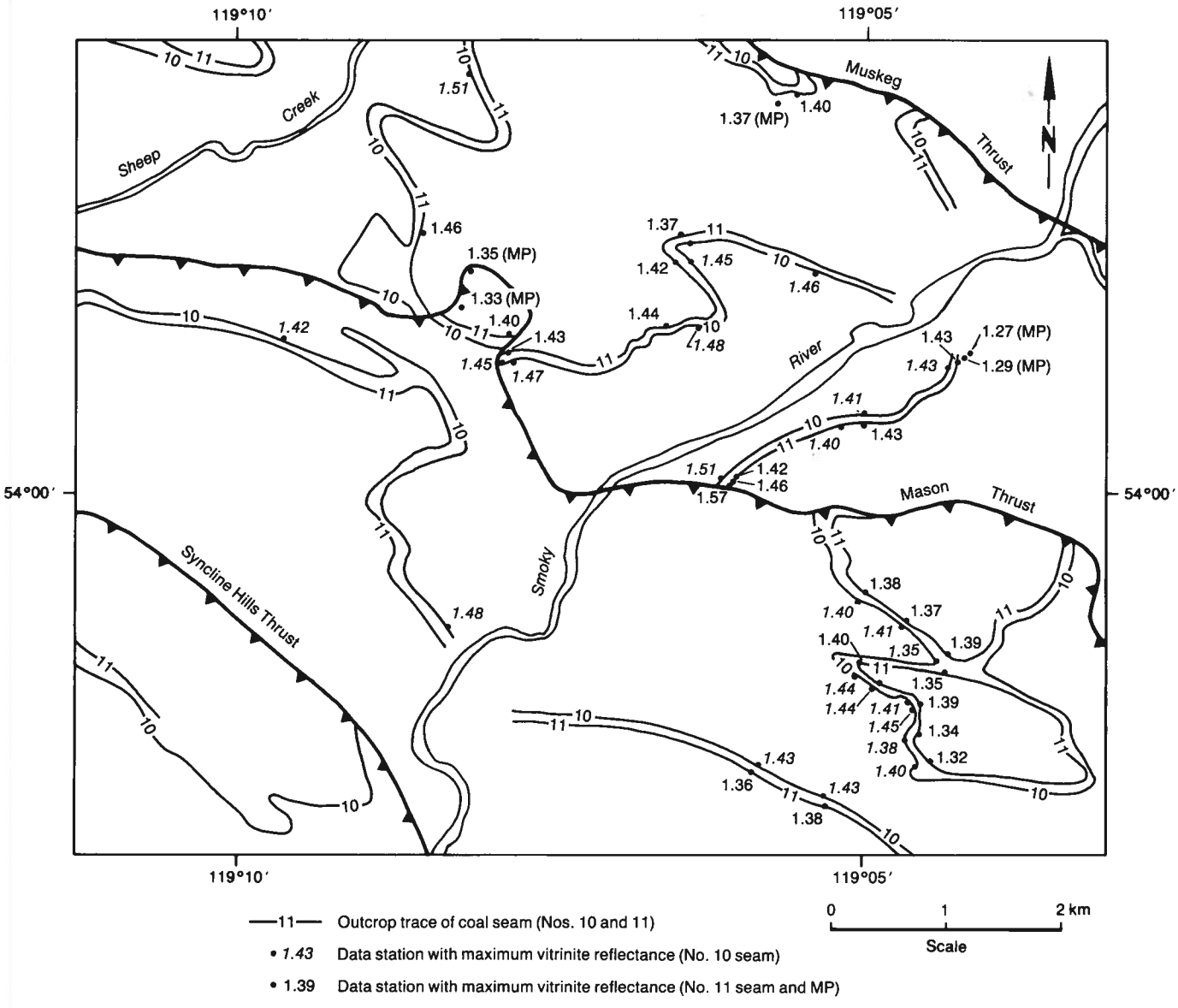

Figure 29. Regional reflectance variations in the upper Grande Cache Member (Nos. 10 and 11 seams) and in the Mountain Park (MP) Member (from Kalkreuth and Langenberg, 1986).

The regional rank variation of the No. 4 seam between the Syncline Hills Thrust and Muskeg Thrust indicates no significant difference with respect to its position in the thrust sheets (figure 28). Only locally might the reflectance of a sample at the contact to the Mason Thrust have been increased slightly to 1.70 percent. There is, however, a trend to somewhat lower reflectance values in the Mason Thrust sheet toward the southeast, in the order of 0.06 percent (averaged). The slight differences in reflectances can easily be explained by slight differences in former depth of burial. Using the coalification gradients (% R_{max}/100 m) determined in the study area (figure 31), it would only require approximately 50 m less overburden in the south to account for the lower reflectance values.

Vitrinite reflectance in Nos. 6, 7 and 8 seam, Grande Cache Member, Gates Formation

Thirteen coal samples were analyzed from the thin, laterally inconsistent No. 6, 7 and 8 seams (figure 28). The reflectance values range from 1.34 percent in No. 8 seam, collected in the southeast, to 1.54 percent in No. 6 seam, from Smoky River No. 8 Mine north of the Smoky River. The sparse data and the discontinuity of the seams allow no regional interpretations.

Vitrinite reflectances in No. 10 seam, Grande Cache Member, Gates Formation

Thirty-two samples were analyzed from the No. 10 seam (figure 29). Between the Syncline Hills Thrust and Muskeg Thrust, the reflectance values range from 1.35 to 1.53 percent, indicating that most samples are medium volatile bituminous coals. Low values (1.35 percent, 1.38 percent and 1.40 percent) are found in the southeastern part of the area, again indicating a possible decrease in depth of burial. The trend to lower values toward the south is also supported by a sample collected at Grande Mountain (1.35 percent at Station 1010, figure 27). By contrast, the highest reflectance on No. 10 seam was determined on a sample collected at

Table 2. Optical properties of vitrinite from No.11 seam at and close to Mason Thrust (station 313)*.

Station	Sample	Distance from Mason Thrust (m)	R_{max} (%)	R_{min} (%)	Bireflectance (R_{max}/R_{min}) (%)	Anisotropy (R_{max}/R_{min})	R_{random} (%)
313	367/83	0.00	1.60	1.20	0.40	1.34	1.40
313	368/83	0.30	1.53	1.18	0.35	1.29	1.35
313	369/83	0.00	1.58	1.23	0.35	1.29	1.40
313	370/83	1.75	1.55	1.29	0.26	1.20	1.42
313	371/83	3.00	1.52	1.18	0.34	1.29	1.35

* Coordinates 58954 E, 5985489 N.

the McEvoy Anticline of the No. 9 Mine (1.57 percent, figure 27). At three locations, the No. 10 seam was sampled in detail to study the vertical reflectance variations within the seam. As in the case of the No. 4 seam, there is a trend to slightly higher reflectances toward the lower part of the seam.

Vitrinite reflectances in No. 11 seam, Grande Cache Member, Gates Formation

Forty-seven coals from the No. 11 seam were analyzed. The reflectance values range from 1.32 percent in the southeast to 1.57 percent in a sample in direct contact with the Mason Thrust. Apart from this locally increased reflectance value, no apparent change in reflectances appears to occur from one thrust sheet to the other (figure 29). The rank of the coal is medium volatile bituminous. Slight differences in reflectances from samples close to each other can be expected if one considers the vertical reflectance variations within the seam at the same location.

Two sets of samples from the No. 11 seam were taken at varying distances from the Mason Thrust. The data suggest that, locally, the mean maximum reflectances are substantially increased in samples at the contact of the fault (table 2). With increasing distances from the contact zone, the mean maximum vitrinite reflectances decrease rapidly in the order of 0.06 percent R_{max} within the decimetre or metre range. Similar observations were reported by Bustin (1983) from the southern Rocky Mountains in British Columbia, where anomalously high reflectances were restricted to narrow films adjacent to shear zones of thrust faults.

It cannot yet be determined whether the increase of reflectances at the contact is due to frictional heating, as suggested by Bustin (1983), or due to preferential orientation of aromatic, graphite-like lamellae in coal, as suggested by Levine and Davis (1984), or a combination of both. The latter authors suggested that maximum reflectance and the degree of anisotropy in tectonically disturbed coals is related to aromatic, graphite-like lamellae, which develop preferentially in the direction of minimum compressive stress. The few measurements of maximum and minimum reflectances and the calculation of bireflectance and anisotropy for the set of samples in the contact zone to the Mason Thrust show a weak trend of increasing anisotropy in the coal with decreasing distance to the thrust (table 2). Current investigations on oriented samples at and near the thrust zones are aimed to give a better insight into the effects of tectonic stress upon vitrinite reflectance.

Vitrinite reflectances in seams from Mountain Park Member, Gates Formation

Five coals from the Mountain Park Member of the Gates Formation were analyzed. The reflectance values range from 1.27 to 1.35 percent (figure 29). The data are too sparse to allow regional interpretations.

Vertical rank changes within seams

Preliminary observations suggest that vertical rank changes within seams are related to differences in petrographic composition of the samples and are also influenced by varying degrees of weathering. Weathering tends to decrease the vitrinite reflectances of these coals by up to 0.1 percent (Marchioni, 1983). In general, the reflectances increase from top to bottom of the seam. The vertical rank variations may explain minor irregularities in reflectances across the study area because samples were collected from various positions within the seams.

Relationships of coal rank to deformation

Previous work on coal rank in and near the study area (Hacquebard and Donaldson 1974; Kalkreuth and McMechan 1984; Ting 1984) suggests that the rank of the coals was established prior to folding. Kalkreuth and McMechan (1984) showed that coal rank in the Inner Foothills northwest of Grande Cache has been largely controlled by former depth of burial and by the timing of the Laramide deformation. This is in contrast to results from coalification studies by Pearson and Grieve (1985) to the south, where, in the Crowsnest Coalfield, a substantial amount of coalification was post-orogenic.

The relationships between rank and folding are illustrated by two cross sections (figure 30). The cross sections were selected from those of figure 2 (in pocket) on the basis of available nearby rank data. The projected reflectance data from Nos. 4, 10 and 11 seams indicate that rank is independent of structural position. The iso-reflectance lines run parallel to the bedding of the folded strata, indicating pre-folding coalification. This is evident particularly in the Barrett Anticline (section EE′) and at Goat Cliffs (section GG″), where no substantial reflectance changes occur in samples collected from hinges of synclines and anticlines, despite more than 1100 m of vertical relief in their present position. This is also evident from a coal sample collected from the thickened hinge of the McEvoy Anticline (station 1012, figure 27), which shows a regional reflec-

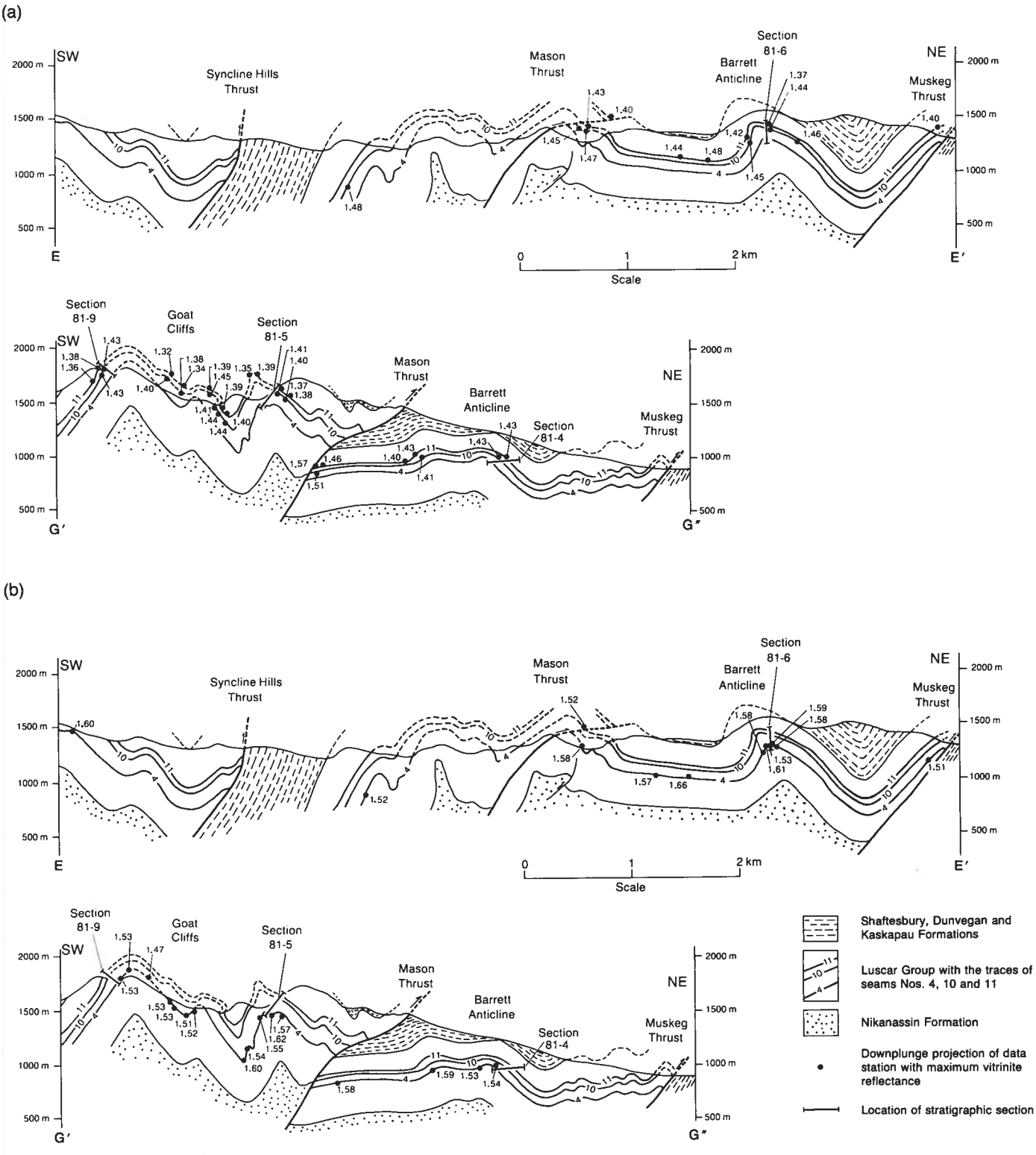

Figure 30. Cross sections, modified from Kalkreuth and Langenberg (1986), illustrating relationship of coal rank to deformed strata (E-E′ and G′-G″ in figure 1 denote lines of sections). (a) data from the Nos. 10 and 11 seams. (b) data from the No. 4 seam.

tance value of 1.65 percent; consequently, the rank has not been affected by the deformation to any large extent. The rank of the seams is clearly a function of their stratigraphic position. Therefore, No. 4 seam exhibits the highest reflectances, No. 10 seam intermediate and No. 11 seam the lowest reflectances.

Because the coalification pattern of No. 4, No. 10 and No. 11 seams shows no substantial change in rank from one thrust sheet to the other (figures 28 and 29), it can be concluded that coalification of the seams was established before thrusting started. However, it should be realized that, during coalification in the Grande Cache

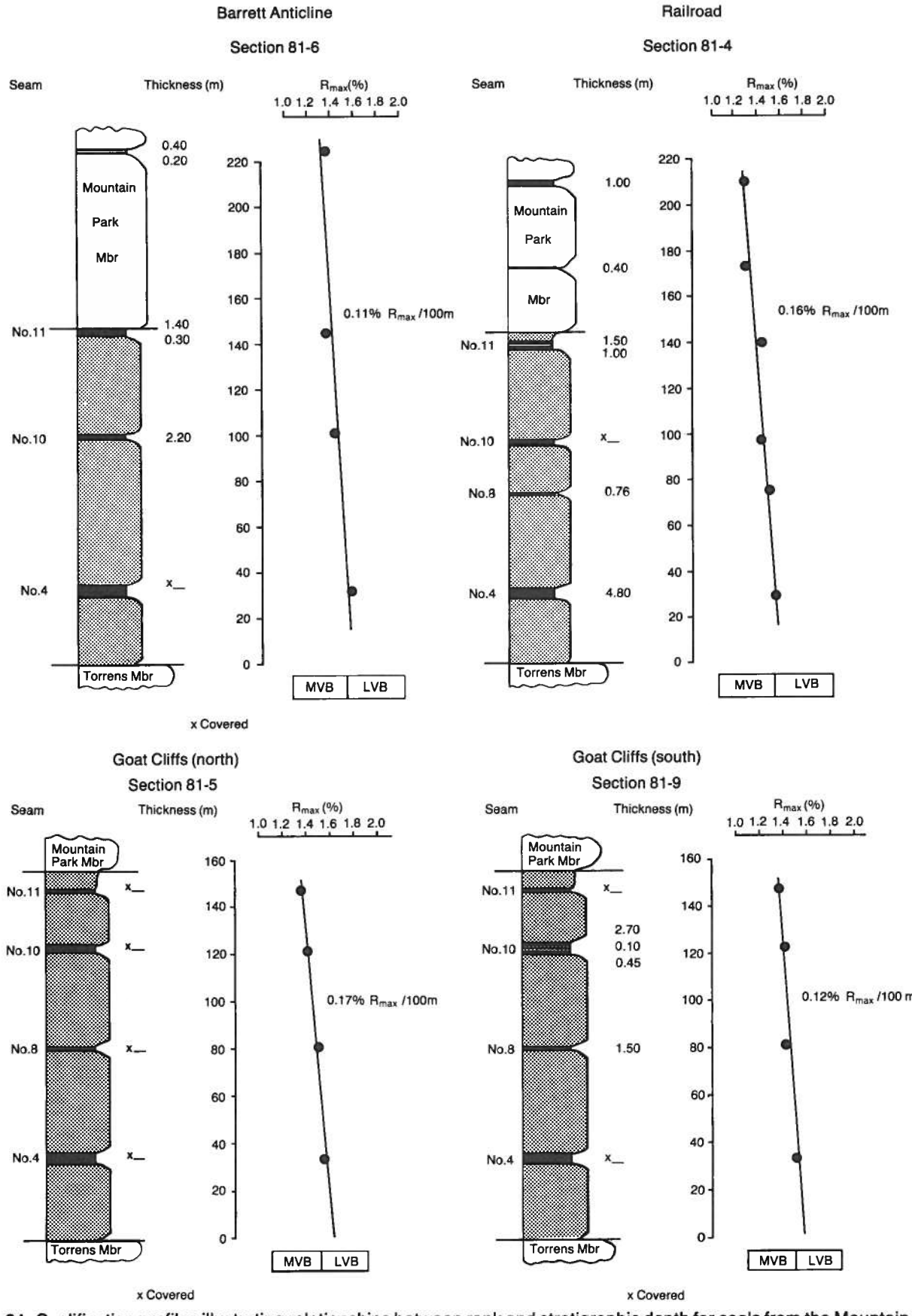

Figure 31. Coalification profiles illustrating relationships between rank and stratigraphic depth for coals from the Mountain Park and Grande Cache Members based on measured stratigraphic sections. The locations of stratigraphic sections 81-4, 81-5 and 81-6 are shown on figure 1. Section 81-9 is located 1.5 km southsouthwest of section 81-5 (from Kalkreuth and Langenberg, 1986).

area, overthrusting was taking place farther to the west. This thrusting and resulting uplift caused the westward decrease of thermal maturation as documented by Kalkreuth and McMechan (1984).

The relationships between stratigraphic depth and coal rank are illustrated in four coalification profiles, which are based on measured stratigraphic sections (figure 31). In all profiles, the reflectance values increase regularly with increasing stratigraphic depth. Rank in these coals is apparently a function of former depth of burial and has not been overprinted by subsequent coalification. Differences in coalification gradients may be due to differences in paleogeothermal gradients. The similarity of coalification gradients in the study area (figure 31), ranging from 0.11 to 0.17 % R_{max}/100 m, suggests that similar geothermal gradients occurred throughout the area. Kalkreuth and McMechan (1984) assumed, on the basis of measured and calculated reflectances, a paleogeothermal gradient of 2.7°C/100 m for the study area, which is similar to the present day geothermal gradient. Using this gradient, the maximum temperatures for the base of the Gates Formation, obtained at the time of maximum burial, would be approximately 170°C based on an overburden of 5500 m and an average annual surface temperature of 20°C.

Based on the coalification pattern of No. 4, No. 10 and No. 11 seam, it can be concluded that the coal rank was largely established during burial between Albian and late Paleocene times (from 100 Ma to 60 Ma ago), before folding and thrusting started. However, locally in the footwall of the Mason Thrust, mean maximum vitrinite reflectance and bireflectance have been increased above regional values. Deformation in the Grande Cache area resulted in displacement and uplift of strata at the end of the Paleocene, after which rapid erosion started. These events essentially ended coalification of the Lower Cretaceous coals of the Grande Cache area.

Concluding remarks

A detailed map and cross sections of the Grande Cache area depict a deformational model that comprises a series of fold-thrust structures with cylindrical chevron folds, which become conical at their tapering ends. This model can be used for exploration in the Grande Cache area and may well be applicable in other areas along Alberta's deformed belt.

Dilation in hinges of chevron folds resulted in thickened coal. In the case of a thick, overlying competent unit, such as the sandstone on top of the No. 4 seam, dilation is larger in an anticline than a syncline. Consequently, in the Grande Cache area, more structural thickening can be expected in anticlines than in synclines. This conclusion is supported by the location of existing open pits, which are generally situated along anticlines. Thickening of coal by duplex thrusting is sometimes present in the limbs of folds. It is not yet understood why it forms in some locations and not in others. The recognition of displacement transfer between folds and thrusts may assist in finding locations of coal seams.

The geometric solution of an area is the foundation of any good geological work (Dahlstrom, 1970). Numerical techniques, such as described in this bulletin, are strong tools for unravelling the geometry of deformed rocks. Most of these techniques are now part of the TRIPOD software (Charlesworth, et al., 1987). This methodology has been successfully applied by the staff of Smoky River Coal Limited, substantially adding to their coal reserves (R. Dawson, pers. comm., 1986). The availability of a microcomputer version of TRIPOD has greatly added to the applicability of this software. Because they are relatively new techniques, they are not yet widely used; however, the future will almost certainly see increased use.

Detailed studies in the Grande Cache area have greatly added to understanding the geometry of the foothills strata and made it possible to start looking at coal quality parameters (coal rank data in particular). Similar studies of coal-bearing strata are needed for other parts of the deformed belt to properly develop Alberta's coal resources.

References

Babcock, E.A. (1974): Jointing in central Alberta; Canadian Journal of Earth Sciences, vol. 11, pp. 1181-1186.

Bally, A.W., Gordy, P.L. and Stewart, G.A. (1966): Structure, seismic data, and orogenic evolution of southern Canadian Rocky Mountains; Bulletin of Canadian Petroleum Geology, vol. 14, pp. 337-381.

Boyer, S. and Elliott, D. (1982): Thrust systems; Bulletin American Associatin of Petroleum Geologists, v. 66, pp. 1196-1230.

Bustin, R. (1983): Heating during thrust faulting in the Rocky Mountains: friction or fiction?; Tectonophysics, 95, pp. 308-328.

Bustin, R., Cameron, A., Grieve, D. and Kalkreuth, W. (1983): Coal petrology: its principles, methods and applications; Geological Association of Canada, Short Course Notes, vol. 3, 273 pages.

Cant, D.J. (1983): Spirit River Formation—A stratigraphic diagenetic gas trap in the deep basin of Alberta; Bulletin American Association of Petroleum Geologists, v. 67, pp. 577-587.

Chapman, T.J. and Williams, G.D. (1984): Displacement distance method in the analysis of fold-thrust structures and linked-fault systems; Journal of the Geological Society, London, v. 141, pp. 121-128.

Charlesworth, H.A.K. and Gagnon, L.G. (1985): Intercutaneous wedges, the Triangle Zone and structural thickening of the Mynheer coal seam at Coal Valley in the Rocky Mountain Foothills of central Alberta; Bulletin of Canadian Petroleum Geology, v. 33, pp. 22-30.

Charlesworth, H.A.K., Langenberg, C.W. and Ramsden, J. (1976): Determining axes, axial planes, and section of macroscopic folds using computer-based methods; Canadian Journal of Earth Sciences, v. 13, pp. 54-65.

Charlesworth, H.A.K., Gold, C., Wynne, D. and Guidos, J. (1987): A microcomputer-based system for collecting, storing, retrieving and processing structural, stratigraphic and positional data from outcrops and drillholes; Computer Manual; University of Alberta, 65 pages.

Cruden, D.M. (1971): Traces of a lineation on random planes; Bulletin Geological Society of America, v. 82, pp. 2302-2306.

Cruden, D.M. and Charlesworth, H.A.K. (1966): The Mississippian-Jurassic unconformity near Nordegg, Alberta; Bulletin of Canadian Petroleum Geology, v. 14, pp. 266-272.

Currie, J.B. and Reik, G.A. (1977): A method of distinguishing regional directions of jointing and of identifying joint sets associated with individual geologic structures; Canadian Journal of Earth Sciences, v. 14, pp. 1211-1228.

Dahlstrom, C.D.A. (1969): Balanced cross sections; Canadian Journal of Earth Sciences, v. 6, pp. 743-757.

—— (1970): Structural geology in the eastern margin of the Canadian Rocky Mountains; Bulletin of Canadian Petroleum Geology, v. 18, pp. 332-406.

Davis, A. (1978): The measurement of reflectance of coal macerals—its automation and significance. The Pennsylvania State University, University Park, PA, Technical Report 88.

Dott, R.H. (1964): Wacke, graywacke and matrix—what approach to immature sandstone classification; Journal of Sedimentary Petrology, v. 34, pp. 625-632.

Dubey, A.K. and Cobbold, P.R. (1977): Noncylindrical flexural-slip folds in nature and experiment; Tectonophysics, v. 38, pp. 223-229.

Eisbacher, G.H., Carrigy, M.A. and Campbell, R.B. (1974): Paleodrainage pattern and late orogenic basins of the Canadian Cordillera; *in* Tectonics and sedimentation, edited by W.R. Dickson: Society of Economic Paleontologists and Mineralogists, Special Publication 22, pp. 143-166.

Elliot, D. (1983): The construction of balanced cross sections; Journal of Structural Geology, v. 5, p. 101.

Gardner, D.A.C. and Spang, J.H. (1973): Model studies of displacement transfer associated with overthrust faulting; Bulletin of Canadian Petroleum Geology, v. 21, pp. 534-552.

Hacquebard, P. and Donaldson, J. (1974): Rank studies of coals in the Rocky Mountains and inner Foothills Belt, Canada; *in* Carbonaceous materials as indicators of metamorphism; edited by R. Dutcher, P. Hacquebard, J. Schopf and J. Simon: Geological Society of America, Special Paper 153, pp. 75-94.

Hossack, J.R. (1979): The use of balanced cross-sections in the calculation of orogenic contraction: a review; Journal of the Geological Society, London, v. 136, pp. 705-711.

Irish, E.J.W. (1951): Pierre Greys Lakes, Alberta; Geological Survey of Canada, Map 996A.

—— (1955): Copton Creek, Alberta; Geological Survey of Canada, Map 1041A.

—— (1965): Geology of the Rocky Mountain Foothills, Alberta; Geological Survey of Canada, Memoir 334, 241 pages.

Irish, E.J.W. and Thorsteinsson, R. (1957): Grande Cache, Alberta; Geological Survey of Canada, Map 1049A.

Kalkreuth, W. and Langenberg, C.W. (1986): The timing of coalfication in relation to structural events in the

Grande Cache area, Alberta; Canadian Journal of Earth Sciences, v. 23, pp. 1102-1116.

Kalkreuth, W. and McMechan, M.E. (1984): Regional pattern of thermal maturation as determined from coal rank studies, Rocky Mountain Foothills and Front Ranges north of Grande Cache, Alberta—implications for petroleum exploration; Bulletin of Canadian Petroleum Geology, v. 32, pp. 249-271.

Kelker, D. and Langenberg, C.W. (1982): A mathematical model for orientation data from macroscopic conical folds; Journal of the International Association of Mathematical Geology, v. 14, pp. 289-307.

Kilby, W.E. (1985): Tonstein and bentonite correlations in northeast British Columbia; Geological Fieldwork 1984, B.C. Ministry of Mines, Paper 1985-1, pp. 257-277.

Landes, K. (1963): Exploration report, Smoky River area; McIntyre Mines, internal report.

Langenberg, C.W. (1984): Structural and sedimentological framework of Lower Cretaceous coal-bearing rocks in the Grande Cache area, Alberta; *in* The Mesozoic of Middle North America, edited by D.F. Stott and D.J. Glass: Canadian Society of Petroleum Geologists, Memoir 9, pp. 533-540.

—— (1985): The geometry of folded and thrusted rocks in the Rocky Mountain Foothills near Grande Cache, Alberta; Canadian Journal of Earth Sciences, v. 22, pp. 1711-1719.

Langenberg, C.W. and McMechan, M.E. (1985): Lower Cretaceous Luscar Group (revised) of the northern and north central Foothills of Alberta; Bulletin of Canadian Petroleum Geology, v. 33, pp. 7-77.

Leckie, D.A. (1986): Petrology and tectonic significance of Gates Formation (early Cretaceous) sediments in northeast British Columbia; Canadian Journal of Earth Sciences, v. 23, pp. 129-141.

Levine, J. and Davis, A. (1984): Optical anisotropy of coals as an indicator of tectonic deformation, Broad Top coal Field, Pennsylvania; Geological Society of America Bulletin, v. 95, pp. 100-108.

MacKay, B.R. (1929a): Mountain park, Alberta; Geological Survey of Canada, Map 208A.

—— (1929b): Cadomin, Alberta; Geological Survey of Canada, Map 209A.

—— (1930): Stratigraphy and structure of the bituminous coal fields in the vicinity of Jasper Park, Alberta; Canadian Institute of Mining and Metallurgy, Bulletin No. 222, Transaction Section, pp. 1306-1342.

MacVicar, J. (1917): Foothills coal areas north of the Grand Trunk Pacific Railway, Alberta; Geological Survey of Canada; Summary Report 1916, pt. C, pp. 85-93.

—— (1920): Coal areas northwest of Brule Lake, Alberta; Geological Survey of Canada, Summary Report 1919, pt. C, pp. 8-13.

—— (1924): Preliminary investigations of coal deposits on Smoky, Hay and Berland Rivers, Alberta; Geological Survey of Canada, Summary Report, 1923, pt. B, pp. 21-62.

Marchioni, D.L. (1983): The detection of weathering in coal by petrographic, rheologic and chemical methods; International Journal of Coal Geology, v. 2, pp. 231-259.

Mardia, K.B. (1972): Statistics of directional data; Academic Press, 357 pages.

McEvoy, J. (1925): The Smoky River coal field, Alberta; The Dominion Fuel Board, Publication no. 7. Geological Survey of Canada, Publication no. 2055, 15 pages.

McLean, J.R. (1977): The Cadomin Formation: stratigraphy, sedimentology and tectonic implications; Bulletin of Canadian Petroleum Geology, v. 25, pp. 792-827.

—— (1982): Lithostratigraphy of the Lower Cretaceous coal-bearing sequence, Foothills of Alberta; Geological Survey of Canada, Paper 80-29, 46 pages.

McLean, J.R. and Wall, J.H. (1981): The early Cretaceous Moosebar sea in Alberta; Bulletin of Canadian Petroleum Geology, v. 29, pp. 334-377.

McLearn, F.H. (1923): Peace River Canyon coal area, British Columbia; Geological Survey of Canada, Summary Report 1922, pt. B, pp. 1-46.

Mellon, G.B. (1967): Stratigraphy and petrology of the Lower Cretaceous Blairmore and Mannville groups, Alberta Foothills and Plains; Alberta Research Council, Bulletin 21, 270 pages.

Miall, A.D. (1977): A review of the braided river depositional environment; Earth Science Reviews, v. 13, pp. 1-62.

Mountjoy, E.W. (1978): Mount Robson; Geological Survey of Canada, Map 1499A.

Pearson, D. and Grieve, D. (1985): Rank variation, coalification pattern and coal quality in the Crowsnest Coalfield, British Columbia, Canada; CIM Bulletin, v. 78, no. 881, pp.39-46.

Pearson, G.R. (1960): Evaluation of some Alberta coal deposits; Alberta Research Council, Earth Sciences Report 60-1, 61 pages.

Pettijohn, F.J. (1975): Sedimentary rocks, third edition; Harper & Row, 628 pages.

Price, R.A. (1981): The Cordilleran foreland thrust and fold belt in the southern Canadian Rocky Mountains; *in* Thrust and nappe tectonics, edited by K.R. McClay and N.J. Price: Geological Survey of London, Special Publication 9. pp.427-448.

Price, R.A. and Mountjoy, E.W. (1970): Geologic structure of the Canadian Rocky Mountains between Bow and Athabasca Rivers—a progress report; *in* Structure of the southern Canadian Cordillera, edited by J.O. Wheeler: Geological Association of Canada, Special Paper 6, pp. 7-25.

Ramsay, J.G. (1967): Folding and fracturing of rocks; McGraw-Hill, 568 pages.

Ramsay, J.G. (1974): Development of chevron folds; Bulletin Geological Society of America, v. 85, pp. 1741-1754.

Ramsay, J.G. and Huber, M. (1983): The techniques of modern structural geology. v. 1: Strain Analysis; Academic Press, 307 pages.

Ramsden, J. (1975): Numerical methods in fabric analysis; unpublished Ph.D. thesis, University of Alberta, 434 pages.

Sampson, R.J. (1985): Surface II Graphics System; Computer Manual, Kansas Geological Survey, 240 pages.

Spears, P.A. and Duff, P. McL.D. (1984): Kaolinite and mixed-layer illite-smectite in Lower Cretaceous bentonites from the Peace River coalfield, British Columbia; Canadian Journal of Earth Sciences, v. 21, pp. 465-476.

Stott, D.F. (1968): Lower Cretaceous Bullhead and Fort St. John groups, between Smoky and Peace Rivers, Rocky Mountain Foothills, Alberta and British Columbia; Geological Survey of Canada, Bulletin 152, 279 pages.

——(1982): Lower Cretaceous Fort St. John Group and Upper Cretaceous Dunvegan Formation of the Foothills and Plains of Alberta; British Columbia, District of Mackenzie and Yukon Territory; Geological Survey of Canada, Bulletin 328, 124 pages.

Suppe, J. (1985): Principles of structural geology; Prentice-Hall, 537 pages.

Taylor, D.R. and Walker, R.G. (1984): Depositional environments and paleogeography in the Albian Moosebar Formation and adjacent fluvial Gladstone and Beaver Mines Formations, Alberta; Canadian Journal of Earth Sciences, v. 21, p. 698-714.

Thompson, R.I. (1981): The nature and significance of large 'blind' thrusts within the northern Rocky Mountains of Canada; *in* Thrust and nappe tectonics, edited by K.R. McClay and N.J. Price: Geological Society of London, Special Publication 9, pp. 449-462.

Ting, F.T.C. (1984): Paragenetic relationship of thermal maturation (coalification) and tectonic framework of some Canadian Rocky Mountain coals; Organic Geochemistry, v. 5, pp. 279-281.

Williams, G.D. and Chapman, T.J. (1983): Strains developed in the hanging wall of thrusts due to their slip/propagation rate: a dislocation model; Journal of Structural Geology, v. 5, pp. 563-571.

Wrightson, C.B. (1979): Structure and stratigraphy of Campbell Flats Anticlinorium near Grande Cache, Alberta; unpublished University of Alberta M.Sc. thesis, 116 pages.

Wrightson, C.B. and Gold, C.M. and Charlesworth, H.A.K. (1979): Structure-contour maps computer constructed from orientational, stratigraphic, and positional outcrop data (abstract); American Association of Petroleum Geologists Bulletin, v. 63, p. 555.

Appendix A. Stratigraphic sections of the Grande Cache area.

Locations are shown on Figure 1 (in pocket).

Legend

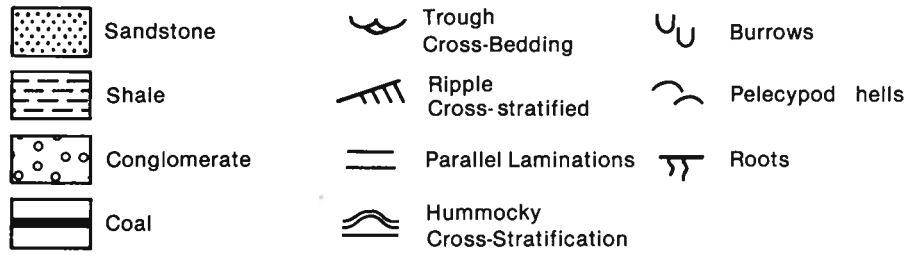

Section 81-1

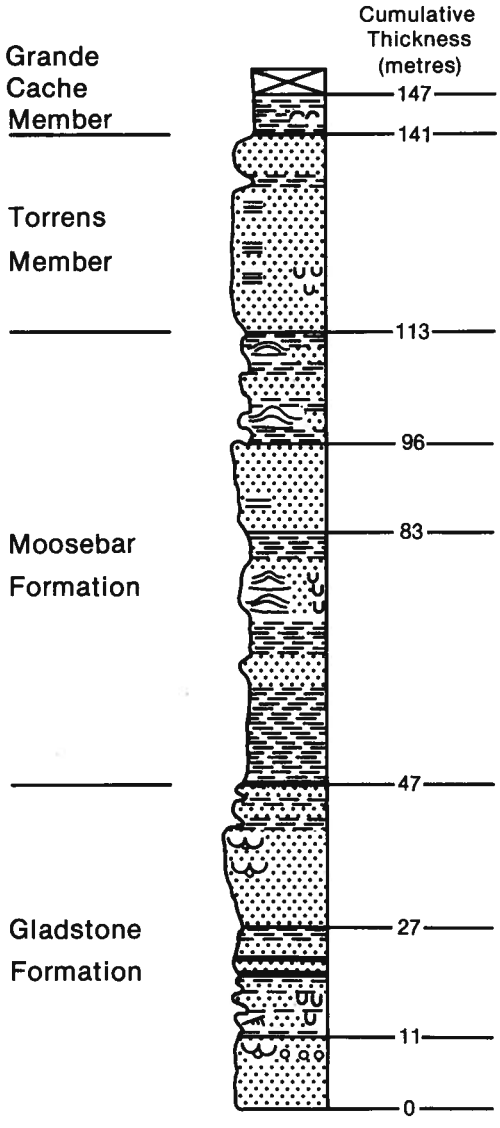

Unit	Thickness (metres)	Description
8	6	Carbonaceous shales, dark gray with minor ironstone layers. Some conspicuous layers with pelecypod-shells.
7	28	Fine-grained sandstone, grayish orange weathering, very thick-bedded with parallel laminations. In lower part some burrowed layers, indicative of a suspension feeding fauna.
6	17	Interbedded very fine-grained sandstone and shales. Sandstones show hummocky cross-stratification. Some burrows.
5	13	Coarsening upward succession with medium-grained sandstone on top; lower down very fine-grained sandstones with minor shale. Some parallel laminations.
4	36	Dark gray shale, some ironstone layers. Toward top interbedded very fine-grained sandstone and shale. Sandstones show hummocky cross-stratification. Burrows are indicative of a deposit feeding fauna.
3	20	Sandstones, very fine-to medium-grained, grayish orange weathering. Trough cross-bedded. At the top some shales and at the very top a 10 cm thick coal seam.
2	16	Interbedded fine-grained sandstones and shales. Burrowed. Ripple cross-stratification. Two thin coal seams; the upper one 20 cm thick.
1	11	Fine-grained sandstone, moderate reddish brown weathering. Thick-to very thick-bedded. Some shale interlayers. Some minor coal seams and a 10 cm thick chert conglomerate layer.

Appendix A. (continued)

Section 81-2

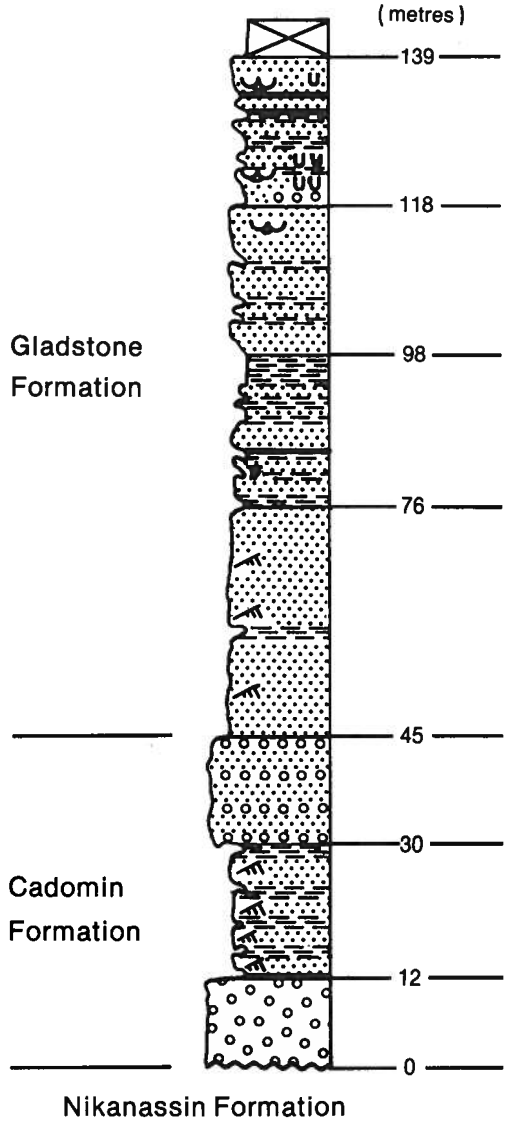

Unit	Thickness (metres)	Description
7	21	Interbedded very fine-to fine-grained sandstones and shales. Trough cross-bedding, some extensively burrowed layers. Two 30 cm thick coal seams. A 5 cm thick chert pebble conglomerate.
6	20	Fine grained sandstones, grayish orange weathering. Trough cross-bedded. Some minor shale.
5	22	Interbedded fine-grained sandstones and shales. Sandstone pale reddish brown weathering. Two minor coal seams, the lower one 20 cm thick.
4	31	Fine-grained, ripple cross-stratified sandstone. Light brown to moderate reddish brown weathering. Some minor shale.
3	15	Interbedded pebble conglomerate and medium-grained sandstone, cross bedded.
2	18	Fine-grained sandstone, cross-bedded. Minor shale. A 40 cm thick coal seam at bottom.
1	12	Pebble and cobble conglomerate. Very thick bedded.

Appendix A. (continued)

Section 81-3 (bottom)

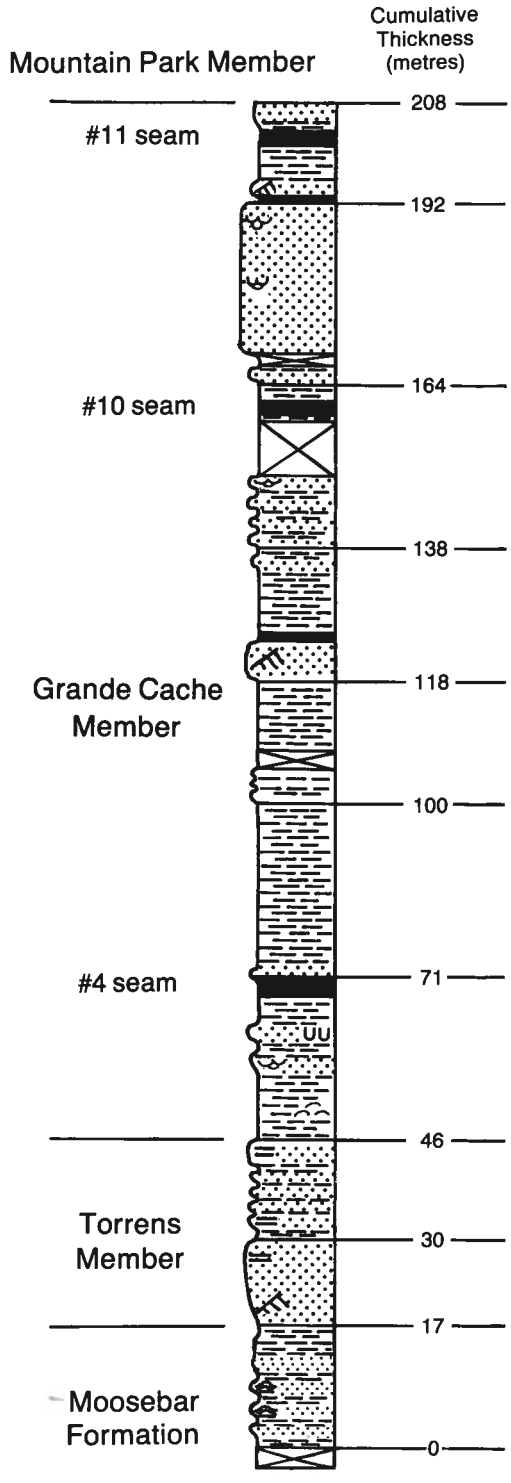

Unit	Thickness (metres)	Description
10	16	Shale and very fine-grained sandstone. A 2 m thick coal seam (#11 seam). At the bottom of this unit a 1 m thick coal seam.
9	28	Medium-grained very thick-bedded sandstone, pale brown weathering. Trough cross-bedded. At bottom same fine-grained sandstone.
8	26	Interbedded fine-grained sandstone and shale. Coal 1.5 m thick (#10 seam).
7	20	Shale and a 1 m thick coal seam. At the bottom fine-grained cross-bedded grayish orange weathering sandstone.
6	18	Carbonaceous shale with ironstone and interbedded very fine-grained shaly sandstone and shale.
5	29	Dark gray shale, in places carbonaceous. At bottom 1 m thick fine-grained grayish orange weathering sandstone.
4	25	Shale, fine-grained sandstone and coal (3m thick - #4 seam). Sandstone below coal is burrowed. Pelecypod shells at 3 m from base.
3	16	Fine-grained sandstone and interbedded shale and sandstone.
2	13	Medium- and fine-grained sandstone. Very thick-bedded, moderate brown weathering. Parallel laminations and some cross-bedding.
1	17	Interbedded shales and very fine-grained sandstone with hummocky cross-stratification.

Appendix A. (continued)

Section 81-3 (top)

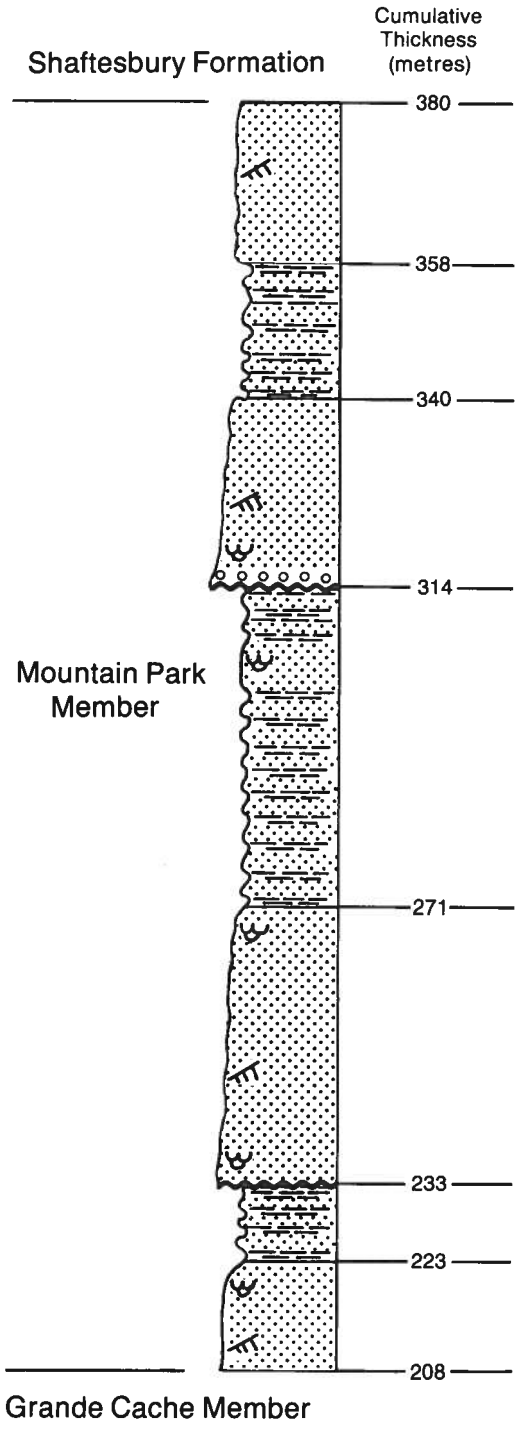

Unit	Thickness (metres)	Description
17	22	Fine-grained moderate reddish orange weathering sandstone, ripple cross-stratified.
16	18	Interbedded fine-grained sandstone and shale, in places carbonaceous.
15	26	Medium-grained pale yellowish orange weathering sandstone. Very thick-bedded, ripples and trough cross-bedding. Scouring into unit 14 with an ironstone conglomerate at the base.
14	43	Interbedded fine-grained sandstone and shale. Near the top 5 m thick massive trough cross-bedded sandstone, which is thick-bedded.
13	38	Medium-grained pale yellowish orange weathering sandstone, very thick-bedded, through cross-bedded. Scouring into unit 12 with an ironstone conglomerate at the base.
12	10	Interbedded very fine-grained sandstone and shale. Minor ironstone.
11	15	Medium-grained pale yellowish orange weathering sandstone, very thick-bedded and cross-bedded.

Appendix A. (continued)

Section 81-4 (bottom)

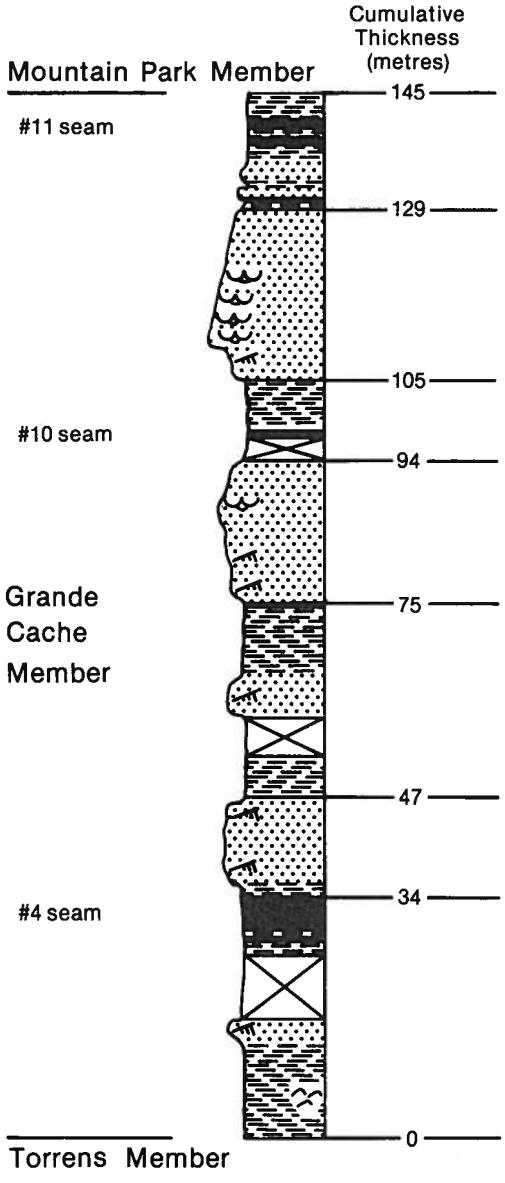

Unit	Thickness (metres)	Description
7	16	Shales and coal, minor very fine-grained sandstone. Composite thickness of coal 4.5 m (#11 seam).
6	24	Fine-to medium-grained sandstone, trough cross-bedded. Pale brown weathering. Rip up clasts and ripple cross-stratification in lower part.
5	11	Shales and 1.5 m of coal exposed (#10 seam).
4	19	Fine-grained shaley sandstone, minor medium-grained sandstone. Yellowish gray weathering. Ripple cross-stratification.
3	28	Gray shales, some fine-grained rippled sandstone. A 40 cm thick coal seam at top.
2	13	Fine-grained sandstone, moderate yellowish brown weathering. Ripple cross-stratified.
1	34	Dark gray carbonaceous shale and coal. 5 m thick coal bed (#4 seam). At 5 m from base, conspicuous pelecypods layers.

Appendix A. (continued)

Section 81-4 (top)

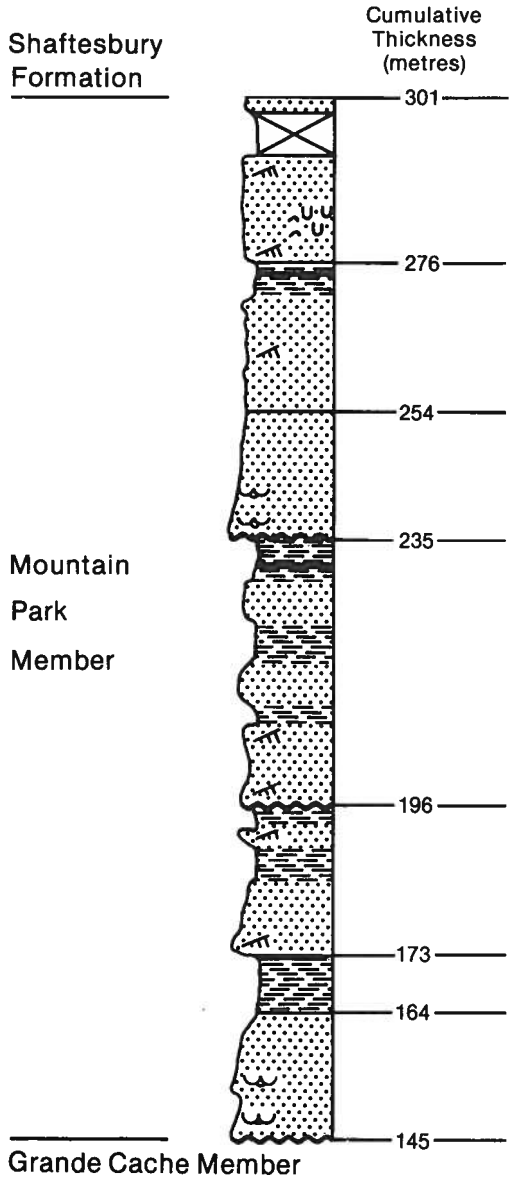

Unit	Thickness (metres)	Description
14	25	Fine-grained sandstone, ripple cross-stratified. Reddish brown weathering. Some burrowing in a zone with gastropod and pelecypod fossils.
13	22	Interbedded fine-grained sandstone and shale. Sandstone ripple cross-stratified. At top, shale and minor coal (coal up to 20 cm thick).
12	19	Fine-to medium-grained sandstone. Grayish orange weathering. Trough cross-bedding. Scour surface at bottom.
11	39	Fine-grained sandstone, shaley sandstone and shale. Sandstone show ripple cross-stratification. Light olive gray weathering. Scour surface at bottom. Near top, 1 m thick coal and shaley coal.
10	23	Medium-to fine-grained sandstone and shale. Sandstone ripple cross-stratified and grayish orange weathering.
9	9	Shale and minor sandstone. A 40 cm thick coal seam at the top.
8	19	Fine-to medium-grained sandstone. Trough cross-bedded. Moderate brown weathering. Scouring into Grande Cache Member at bottom.

Appendix A. (continued)

Section 81-5 (bottom)

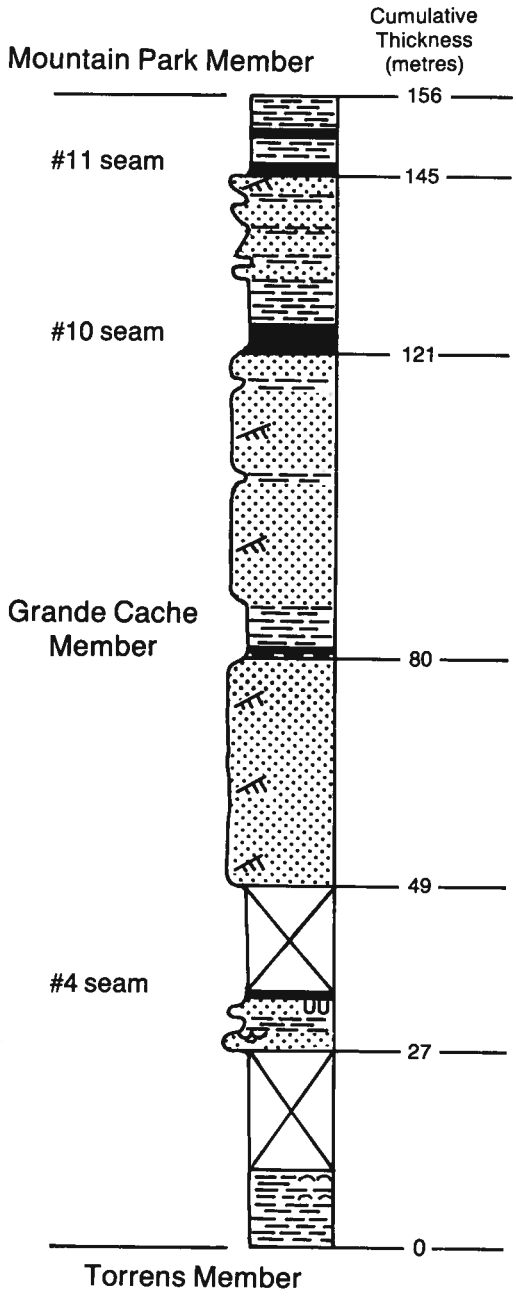

Unit	Thickness (metres)	Description
6	11	Gray shale and coal. The lower of the two coal seams is 1.5 m thick (#11 seam).
5	24	Fine-grained dark yellowish orange weathering sandstone, shale and coal. The coal is 2.9 m thick (#10 seam).
4	41	Fine-grained sandstone, shaly sandstone (light brown and dark yellowish orange weathering) and shale. Sandstone medium bedded and ripple cross-stratified. Near bottom 50 cm thick coal seam.
3	31	Fine-grained light brown and dark yellowish brown weathering sandstone, ripple cross-stratified. Medium to thick bedded.
2	22	Largely covered unit of fine-to medium-grained sandstone, shale and coal (50 cm exposed of #4 seam). Sandstone below coal is burrowed.
1	27	Largely covered unit of shale. At 6 m and 10 m from bottom pelecypod shells.

Appendix A. (continued)

Section 81-5 (top)

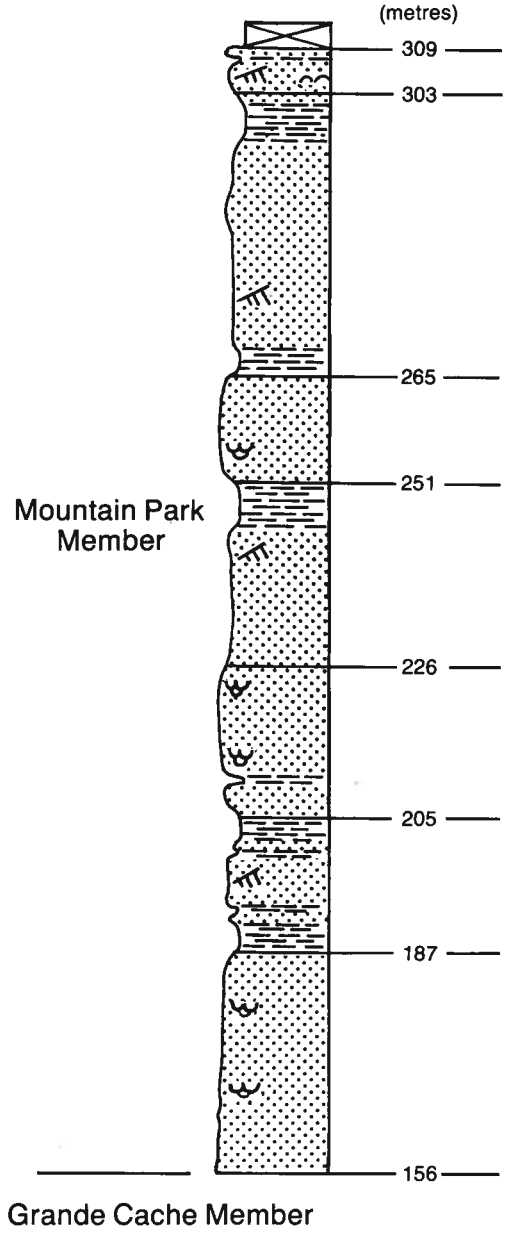

Unit	Thickness (metres)	Description
13	6	Fine-grained moderate reddish brown weathering sandstone, ripple cross-stratified. Some gastropod and pelecypod casts.
12	38	Fine-grained light olive-gray weathering shaly sandstone and shale. In the middle medium-grained very thick-bedded sandstone (5 m thick).
11	14	Medium-grained moderate yellowish brown weathering sandstone. Trough cross-bedded in very thick beds.
10	25	Fine-grained light olive gray weathering rippled shaly sandstone and shale.
9	21	Medium-grained moderate yellowish brown weathering sandstone. Trough cross-bedded in very thick beds.
8	18	Shale and fine-grained ripple cross-stratified sandstone, pale yellowish brown weathering.
7	31	Medium-grained grayish orange weathering sandstone. Trough cross-bedded in very thick beds. Some ironstone pebbles at the bottom of troughs.

Appendix A. (continued)

Section 81-6

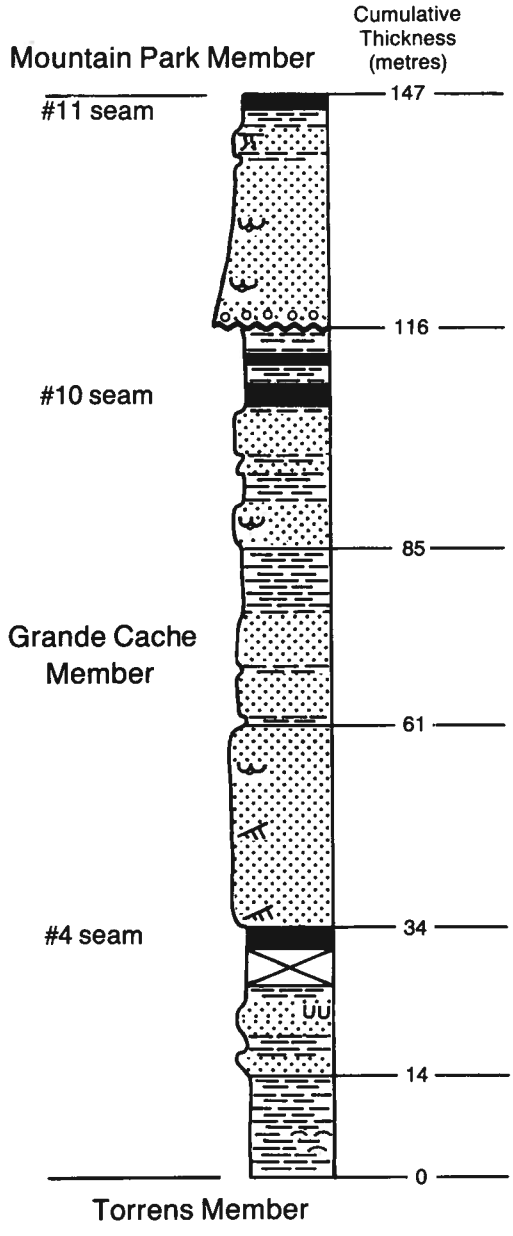

Unit	Thickness (metres)	Description
6	31	Medium- to fine-grained light brown weathering sandstone. An ironstone pebble conglomerate at the bottom. Some shales and a 2 m thick coal seam at top (#11 seam).
5	31	Shale and interbedded fine-grained sandstone and shale. Trough cross-bedded grayish orange weathering fine-grained sandstone at bottom. Near top 2.5 m thick coal (#10 seam).
4	24	Shale and dark yellowish orange weathering shaly sandstone, medium-bedded.
3	27	Fine-grained medium- to thick-bedded sandstone. Trough cross-bedded. Ripple cross-stratification. Grayish orange weathering.
2	20	Very fine-grained bioturbated gray sandstone and shales. At top coal seam of which 2 m is exposed (#4 seam).
1	14	Dark gray carbonaceous shale. At 5 m from bottom pelecypod layers.

Appendix A. (continued)

Section 81-7

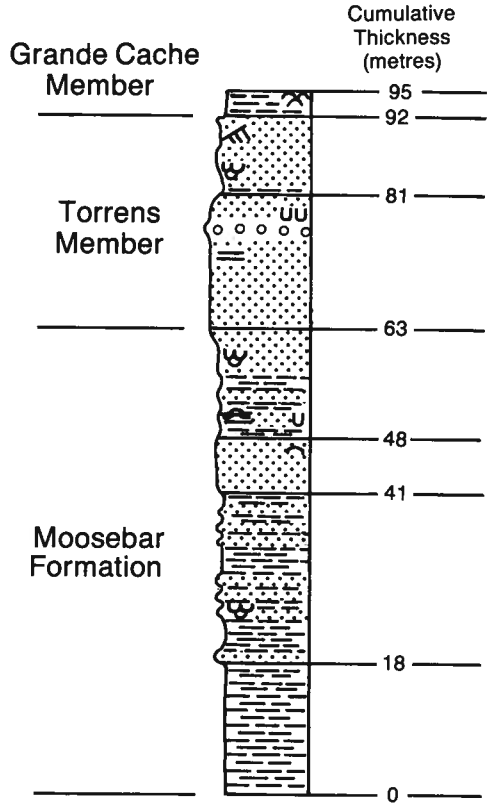

Unit	Thickness (metres)	Description
7	3	Gray carbonaceous shales with pelecypod layers.
6	11	Very fine- and fine-grained sandstone and shaly sandstone, ripple cross-stratified. Some trough cross-beds, light brown weathering.
5	18	Fine-grained light brown weathering sandstone, very thick-bedded with parallel laminations. Some burrowed layers and a 20 cm thick chert pebble conglomerate.
4	15	Very fine- and fine-grained shaly sandstone at top. Interbedded very fine sandstone and shale at bottom. These sandstones show hummocky cross-stratification and some burrows.
3	7	Light brown weathering fine-grained shaly sandstone with a lot of carbonaceous material. Some pelecypod shells at 47 m.
2	23	Shale and interbedded grayish orange very fine-grained sandstone and shale.
1	18	Medium gray and light olive gray weathering shale with some ironstone.

Appendix A. (continued)

Section 81-8 (bottom)

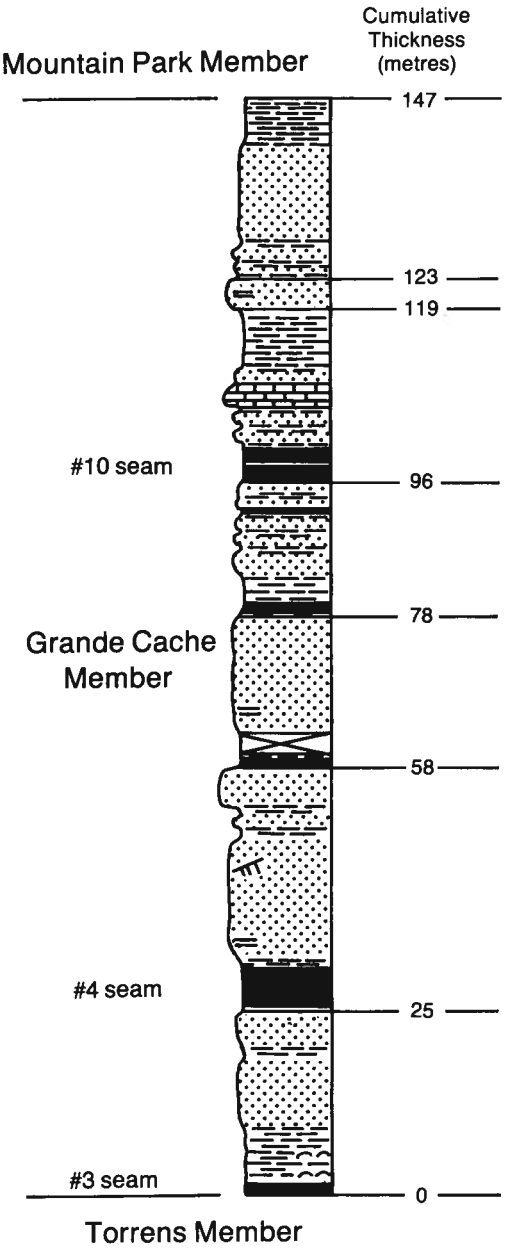

Unit	Thickness (metres)	Description
7	24	Very fine-grained grayish orange weathering shaly sandstone, shale and minor ironstone.
6	4	Fine-grained light gray weathering shaly sandstone with parallel laminations.
5	23	Shale, interbedded shale and fine-grained sandstone, limestone and coal. The coal (#10 seam) is 4.3 m thick and has a shale split.
4	18	Interbedded fine-grained moderate yellowish brown weathering sandstone and shale. At bottom carbonaceous shale and 1.5 m thick coal seam.
3	20	Very fine-grained pale yellowish orange weathering sandstone with parallel laminations. At bottom 75 cm thick coal.
2	33	Very fine-grained rippled dark yellowish orange weathering sandstone. At top medium-grained sandstone, at bottom 5 m thick coal (#4 seam).
1	25	Fine-grained and very fine-grained sandstone, shale and 1.5 m thick coal (#3 seam). Above coal are pelecypod layers.

Appendix A. (continued)

Section 81-8 (top)

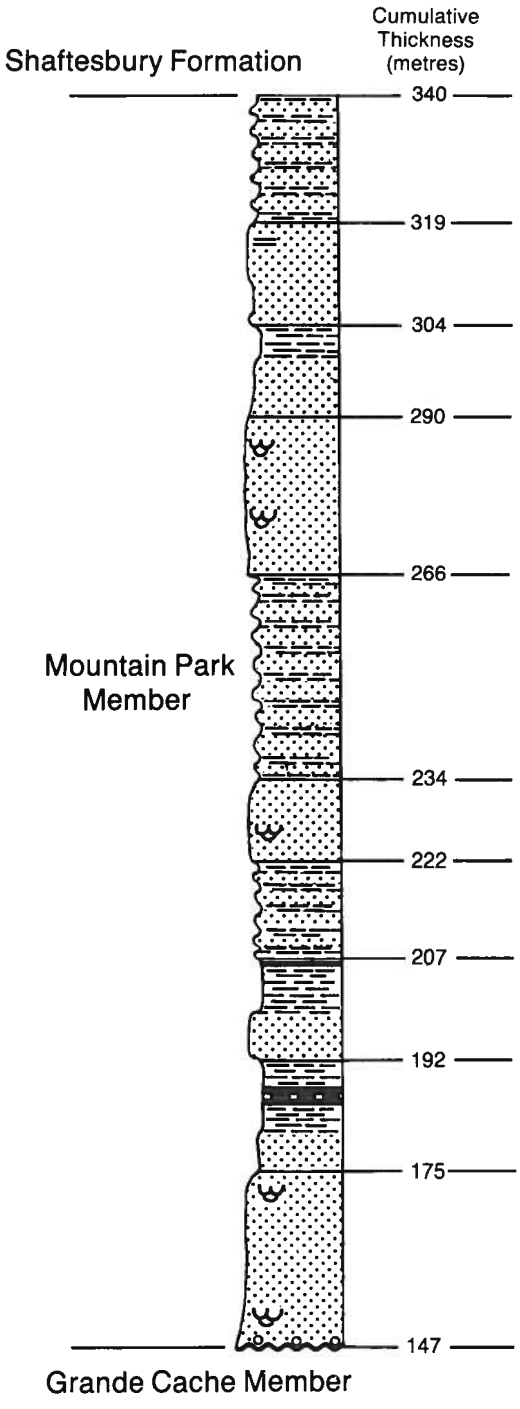

Unit	Thickness (metres)	Description
17	21	Interbedded fine-grained moderate brown weathering sandstone and shale.
16	15	Fine-grained very light gray weathering sandstone with parallel laminations. At bottom very fine-grained shaly sandstone.
15	14	Fine-grained shaly sandstone and shale.
14	24	Fine-grained moderate yellowish brown weathering sandstone. Trough cross-bedded in thick beds.
13	32	Interbedded fine-grained dark yellowish brown weathering sandstone and shale.
12	12	Fine-grained sandstone and shaly sandstone. Trough cross-bedded and grayish orange weathering.
11	15	Interbedded fine-grained light olive gray weathering shaly sandstone and shale.
10	15	Fine-grained sandstone and minor shaly sandstone, pale yellowish orange weathering. At the top shales with minor ironstone and minor discontinuous coal (30 cm thick).
9	17	Very fine-grained shaly sandstone, shale and two coal seams (60 and 70 cm thick).
8	28	Medium-grained very light gray weathering sandstone. Trough cross-bedded. At top some orange weathering sandstone, at bottom a thin ironstone pebble conglomerate.

Appendix B. Listing of domains, fold axes, eigenvalues and test statistics.

Domain	Fold axis		N	Minimum eigenvalue /N	Maximum eigenvalue /N	K	F-test
	Trend	Plunge					
1	124	4	73	0.0159	0.7421	230	0.72
2	118	1	39	0.0101	0.6802	205	0.46
3	129	14	32	0.0218	0.6504	160	3.85
4	109	6	66	0.0137	0.5963	229	1.89
5	295	10	62	0.0111	0.8322	206	0.50
6	297	5	69	0.0147	0.5250	271	1.11
7	104	4	42	0.0252	0.6135	176	1.91
8	302	10	26	0.0182	0.6798	184	1.53
9	295	5	38	0.0181	0.5976	183	2.90
10	118	1	41	0.0127	0.7063	215	0.59
11	125	3	44	0.0067	0.5940	236	1.54
12	121	1	36	0.0216	0.6799	182	0.08
13	301	1	10	0.0152	0.5557	-	-
14	119	2	20	0.0177	0.7759	307	3.12
15	124	4	43	0.0184	0.6665	201	0.12
16	123	1	36	0.0345	0.6266	209	0.70
17	117	3	37	0.0267	0.6406	183	1.00
18	299	9	28	0.0267	0.5566	137	4.39
19	304	6	29	0.0067	0.7612	208	1.58
20	118	4	20	0.0420	0.5463	-	-
21	120	3	22	0.0245	0.7282	219	1.58
22	321	2	21	0.0341	0.6516	169	0.43
23	122	5	46	0.0057	0.6743	216	2.27
24	123	9	59	0.0207	0.5671		
25	124	8	9	0.0465	0.6702	168	1.24
26	300	4	20	0.0178	0.7768		
27	126	7	25	0.0221	0.8060	210	1.89
28	125	1	21	0.0169	0.6665	174	0.07
29	133	9	38	0.0123	0.5483	207	2.75
30	128	5	39	0.0099	0.6165	179	2.05
31	130	6	33	0.0117	0.6607	-	-
32	127	16	39	0.0110	0.6547	-	1.12
33	320	0	56	0.0160	0.8889	-	-
34	316	2	80	0.0167	0.5340	-	1.00
35	119	7	44	0.0274	0.6577	-	0.58
36	123	2	31	0.0046	0.8192	-	2.02
37	314	1	26	0.0285	0.5601	-	0.96
38	309	0	8	0.0171	0.7297	-	-
39	311	0	103	0.0228	0.7737	-	-
40	312	5	19	0.0097	0.6353	-	1.60
41	316	2	19	0.0249	0.7216	-	-
42	143	7	18	0.0145	0.6139	-	0.89
43	134	4	97	0.0087	0.7597	-	2.94
44	148	11	30	0.0302	0.6475	-	4.03
45	134	0	80	0.0137	0.8468	-	1.97
46	308	4	22	0.0049	0.6069	-	0.82
47	299	2	25	0.0120	0.7693	306	1.33
48	118	3	-	-	-	-	-
49	300	3	-	-	-	-	-
50	300	3	-	-	-	-	-
51	300	3	13	0.0723	0.6513	-	0.12
52	120	4	11	0.0195	0.5127	154	2.53
53	110	5	-	-	-	-	-
54	297	1	24	0.0117	0.7712	-	0.23
55	302	3	37	0.0061	0.6512	366	1.15
56	299	4	21	0.0123	0.6114	185	0.01
57	304	2	14	0.0213	0.6045	129	1.39
58	122	5	8	0.0350	0.9072	267	2.53
59	295	3	10	0.0262	0.7072	160	2.57
60	303	5	-	-	-	-	-

N - number of stations (generally 5 repeated measurements of bedding were taken at each station)
K - concentration parameter of the Fisher distribution calculated from stations where repeated measurements of bedding were taken

Appendix C. Coal rank data

Vitrinite reflectances, ASTM rank classes, locations and thicknesses, for No. 3 and No. 4 coal seams

Station	Seam	Thickness (m)	Sample	Type	Maximum Reflectance (%)			ASTM rank	Easting	Northing
					Mean	S	N			
9-1	4	4.00+	505/83	g	1.68	0.06	50	Low volatile bituminous	55388	5989225
35	4	2.70	381/83	c,u	1.52	0.05	50	Low volatile bituminous	59500	5984297
35	4	0.70	380/83	c,u	1.53	0.06	50	Low volatile bituminous	59500	5984297
35	4	1.00	379/83	c,m	1.47	0.03	50	Medium volatile bituminous	59500	5984297
35	4	1.00	378/83	c,l	1.54	0.04	50	Low volatile bituminous	59500	5984297
35	4	0.50	377/83	c,l	1.62	0.05	50	Low volatile bituminous	59500	5984297
42	4	2.05+	375/83	g,s	1.60	0.05	50	Low volatile bituminous	58842	5984553
51	4	*--	530/83	g	1.57	0.04	50	Low volatile bituminous	60183	5984376
57	4	0.95	338/83	c,u	1.54	0.04	50	Low volatile bituminous	60198	5986165
57	4	1.70	339/83	c,m	1.60	0.06	50	Low volatile bituminous	60198	5986165
57	4	2.15	340/83	c,l	1.62	0.06	50	Low volatile bituminous	60198	5986165
61	4	*--	344/83	g,m	1.53	0.06	50	Low volatile bituminous	60673	5986363
63	4	1.15	345/83	c,u	1.53	0.06	50	Low volatile bituminous	60801	5986455
63	4	3.00	346/83	c,m	1.53	0.05	50	Low volatile bituminous	60801	5986455
63	4	1.35	347/83	c,l	1.57	0.04	50	Low volatile bituminous	60801	5986455
235	4	*--	528/83	g	1.55	0.06	50	Low volatile bituminous	60414	5984105
281	4	*--	397/83	g	1.51	0.04	50	Low volatile bituminous	60137	5983446
293	4	*--	399/83	g	1.53	0.04	50	Low volatile bituminous	60216	5983279
294	4	*--	398/83	g	1.55	0.06	50	Low volatile bituminous	60195	5983325
300	4	*--	396/83	g	1.52	0.06	50	Low volatile bituminous	60305	5983474
354	4	*--	518/83	g,m	1.47	0.08	50	Medium volatile bituminous	60424	5982940
364	4	8.00+	510/83	g	1.53	0.05	50	Low volatile bituminous	59759	5983041
372	4	7.00+	511/83	g	1.53	0.06	50	Low volatile bituminous	59436	5983108
439	4	*--	354/83	g,m	1.58	0.05	50	Low volatile bituminous	59018	5985790
524	4	1.10	444/83	c,u	1.53	0.05	50	Low volatile bituminous	56678	5984336
524	4	2.14	445/83	c,m	1.45	0.06	50	Medium volatile bituminous	56678	5984336
524	4	5.25	446/83	c,l	1.57	0.06	50	Low volatile bituminous	56678	5984336
565	4	2.00+	547/83	g,u	1.58	0.03	50	Low volatile bituminous	57251	5986394
572	4	3.00+	540/83	g	1.52	0.04	50	Low volatile bituminous	56991	5986583
596	4	1.00+	452/83	g,u	1.57	0.06	50	Low volatile bituminous	57930	5986357
603	4	1.30+	451/83	g,m	1.66	0.05	50	Low volatile bituminous	58659	5986738
613	4	0.30+	486/83	g,u	1.51	0.04	50	Low volatile bituminous	60975	5988015
618	4	*--	487/83	g	1.54	0.04	50	Low volatile bituminous	61094	5988244
639	4	2.00+	481/83	g,l	1.58	0.04	50	Low volatile bituminous	58842	5987476
662	4	2.70+	479/83	c,u	1.53	0.05	50	Low volatile bituminous	58732	5987506
662-1	4	1.00+	480/83	c,u	1.59	0.05	50	Low volatile bituminous	58787	5987489
709	4	*--	529/83	g	1.62	0.05	50	Low volatile bituminous	60256	5984227
736	4	*--	504/83	g	1.65	0.04	50	Low volatile bituminous	56031	5986964
743	4	*--	536/83	g	1.65	0.05	50	Low volatile bituminous	55364	5986778
758	4	*--	499/83	g	1.65	0.04	50	Low volatile bituminous	55778	5987973
780	4	6.00+	502/83	g	1.69	0.04	50	Low volatile bituminous	54486	5987089
783	4	*--	503/83	g	1.70	0.04	50	Low volatile bituminous	54644	5987378
828	4	2.50	491/83	c,u	1.55	0.06	50	Low volatile bituminous	56617	5989061
828	4	0.50	492/83	c,u,s	1.62	0.05	50	Low volatile bituminous	56617	5989061
828	4	1.30	493/83	c,m	1.62	0.05	50	Low volatile bituminous	56617	5989061
828	4	0.30	494/83	c,l,s	1.62	0.05	50	Low volatile bituminous	56617	5989061
828	4	0.90	495/83	c,l,s	1.61	0.05	50	Low volatile bituminous	56617	5989061
859	4	*--	500/83	g	1.66	0.06	50	Low volatile bituminous	55754	5988915
938	4	*--	501/83	g	1.59	0.04	50	Low volatile bituminous	55157	5986952
989	4	*--	700/83	g	1.60	0.05	50	Low volatile bituminous	53428	5983254
999 (Copton Creek)	4	3.00+	468/83	g	1.69	0.06	50	Low volatile bituminous	42351	5990975

*-- seam partly covered
** - severely weathered

g - grab sample
c - channel sample
s - sheared coal

u - upper portion
m - middle portion
l - lower portion

S - standard deviation
N - number of measurements

Appendix C. (continued)

Vitrinite reflectances, ASTM rank classes, locations and thicknesses, for No. 3 and No. 4 coal seams

Station	Seam	Thickness (m)	Sample	Type	Maximum Reflectance (%)			ASTM rank	Easting	Northing
					Mean	S	N			
1000 (Grande Mtn)	4	*--	549/83	g	1.40**	0.09	50	Medium volatile bituminous	59924	5977789
1001 (McEvoy Anticline)	4	7.48	462/83	g	1.63	0.06	50	Low volatile bituminous	51739	5989130
1002 (Victor Lake)	4	1.40+	467/83	c	1.33**	0.08	50	Medium volatile bituminous	60320	5973400
1012 (McEvoy Anticline)	4	6.00+	698/83	g	1.65	0.05	50	Low volatile bituminous	50592	5989941
988	3	*--	699/83	g	1.68	0.07	50	Low volatile bituminous	53422	5983309
1003 (Victor Lake)	3	1.25+	466/83	c	1.41	0.05	50	Medium volatile bituminous	60350	5973409
1011 (Grande Mtn)	3	*--	548/83	g	1.52	0.04	50	Low volatile bituminous	59771	5977707

*-- - seam partly covered
** - severely weathered
g - grab sample
c - channel sample
s - sheared coal
u - upper portion
m - middle portion
l - lower portion
S - standard deviation
N - number of measurements

Vitrinite reflectances, ASTM rank classes, locations and thicknesses, for Nos. 6, 7 and 8 coal seams, Grande Cache Member, and some coals collected from overlying Mountain Park Member and underlying Nikanassin Formation

Station	Formation/ Seam No.	Thickness (m)	Sample	Type	Maximum Reflectance (%)			ASTM rank	Easting	Northing
					Mean	S	N			
11	NIK	0.40	372/83	c	1.75	0.05	50	Low volatile bituminous	58610	5985266
11	NIK	0.20	373/83	c	1.62	0.06	50	Low volatile bituminous	58610	5985266
55	GC No.8	0.76	402/83	c	1.50	0.05	50	Low volatile bituminous	60107	5986147
66	MP	1.00	352/83	c	1.27	0.04	50	Medium volatile bituminous	61051	5986604
67	MP	0.40	351/83	c	1.29	0.03	50	Medium volatile bituminous	60987	5986577
236	GC No.8	*--	527/83	g	1.51	0.04	50	Low volatile bituminous	60451	5984175
301	GC No.8	*--	395/83	g	1.50	0.04	50	Low volatile bituminous	60375	5983425
353	GC No.8	0.50	519/83	g	1.34	0.07	50	Medium volatile bituminous	60463	5982956
373	GC No.8	0.75	512/83	c	1.40	0.05	50	Medium volatile bituminous	59341	5983114
373	GC No.7	0.75	513/83	c	1.48	0.04	50	Medium volatile bituminous	59341	5983114
373	GC No.6	0.60	514/83	c	1.53	0.05	50	Low volatile bituminous	59341	5983114
373	GC ?	0.50	515/83	c	1.39	0.05	50	Medium volatile bituminous	59341	5983114
624	MP	0.60	490/83	g	1.37	0.06	50	Medium volatile bituminous	59436	5988762
633	MP	0.60	534/83	g	1.35	0.04	50	Medium volatile bituminous	56787	5987324
634	MP	0.50	535/83	g	1.33	0.04	50	Medium volatile bituminous	56729	5987013
743-1	GC No.7	0.15	539/83	c	1.52	0.05	50	Low volatile bituminous	55364	5986778
743-1	GC No.6	0.40	538/83	c	1.54	0.04	50	Low volatile bituminous	55364	5986778
1006 (McEvoy Anticline)	GC No.8	0.50	456/83	c	1.58	0.06	50	Low volatile bituminous	51771	5988926
1006 (McEvoy Anticline)	GC No.7	0.40	457/83	c	1.67	0.06	50	Low volatile bituminous	51771	5988926
1006 (McEvoy Anticline)	GC No.6	0.60	458/83	c	1.66	0.05	50	Low volatile bituminous	51771	5988926

GC - Grande Cache Mbr
MP - Mountain Park Mbr
NIK - Nikanassin Fm
c - channel sample
g - grab sample
*-- - seam partly covered
S - standard deviation
N - number of measurements

ppendix C. (continued)

itrinite reflectances, ASTM rank classes, locations and thicknesses, for No. 10 coal seam

Station	Seam	Thickness (m)	Sample	Type	Maximum Reflectance (%)			ASTM rank	Easting	Northing
					Mean	S	N			
49	10	*--	531/83	g	1.40	0.04	50	Medium volatile bituminous	60122	5984471
64	10	*--	348/83	g	1.43	0.05	50	Medium volatile bituminous	60875	5986501
214	10	*--	385/83	g	1.44	0.04	50	Medium volatile bituminous	60116	5983891
217	10	2.00+	386/83	g	1.44	0.05	50	Medium volatile bituminous	60259	5983757
219	10	1.00	392/83	c,u	1.39	0.05	50	Medium volatile bituminous	60439	5983672
219	10	2.40	391/83	c,l	1.43	0.05	50	Medium volatile bituminous	60439	5983672
222	10	1.00+	393/83	c,l	1.45	0.04	50	Medium volatile bituminous	60552	5983608
238	10	*--	526/83	g	1.41	0.04	50	Medium volatile bituminous	60450	5984266
245-1	10	*--	523/83	g	1.35	0.05	50	Medium volatile bituminous	60856	5983986
303	10	*--	400/83	g	1.38	0.04	50	Medium volatile bituminous	60472	5983303
315	10	*--	374/83	g	1.51	0.06	50	Low volatile bituminous	58918	5985510
322	10	*--	341/83	g	1.41	0.04	50	Medium volatile bituminous	60152	5986092
350	10	*--	520/83	g	1.40	0.05	50	Medium volatile bituminous	60618	5983065
368	10	0.45	508/83	c,u	1.42	0.05	50	Medium volatile bituminous	59835	5982788
368	10	0.10	507/83	c,m	1.42	0.04	50	Medium volatile bituminous	59835	5982788
368	10	2.70	506/83	c,l	1.45	0.05	50	Medium volatile bituminous	59835	5982788
374	10	*--	516/83	g	1.43	0.06	50	Medium volatile bituminous	59262	5983090
523	10	*--	443/83	g	1.48	0.05	50	Medium volatile bituminous	56595	5984242
569	10	4.00+	546/83	g	1.47	0.04	50	Medium volatile bituminous	57104	5986586
571	10	*--	541/83	g,u	1.47	0.06	50	Medium volatile bituminous	57019	5986549
571	10	1.50	542/83	g,l	1.43	0.04	50	Medium volatile bituminous	57019	5986549
602	10	*--	450/83	g,u	1.48	0.05	50	Medium volatile bituminous	58738	5986869
653	10	2.75	469/83	c	1.45	0.06	50	Medium volatile bituminous	58631	5987391
661	10	2.20+	482/83	c,m + l	1.44	0.05	50	Medium volatile bituminous	58659	5987589
664	10	*--	485/83	g	1.46	0.05	50	Medium volatile bituminous	59747	5987314
748	10	*--	537/83	g	1.42	0.06	50	Medium volatile bituminous	55187	5986726
825	10	3.30	497/83	c,m	1.50	0.05	50	Low volatile bituminous	56714	5989018
825	10	1.10	496/83	c,l	1.53	0.04	50	Low volatile bituminous	56714	5989018
1007	10	1.40	453/83	c,u	1.59	0.06	50	Low volatile bituminous	50505	5989763
1007 (McEvoy Anticline)	10	1.80	455/83	c,l	1.56	0.05	50	Low volatile bituminous	50505	5989763
1008 (McEvoy Anticline)	10	1.20	463/83	c	1.54	0.05	50	Low volatile bituminous	50755	5989584
1010 (Grande Mtn)	10	*--	550/83	g	1.35	0.05	50	Medium volatile bituminous	59954	5977994

*-- - seam partly covered
s - sheared coal

g - grab sample
c - channel sample

l - lower portion
m - middle portion
u - upper portion

S - standard deviation
N - number of measurements

Appendix C. (continued)

Vitrinite reflectances, ASTM rank classes, locations and thicknesses, for No. 11 seam

Station	Seam	Thickness (m)	Sample	Type	Maximum Reflectance (%)			ASTM rank	Easting	Northing
					Mean	S	N			
18.1	11	1.25	358/83	c,u	1.44	0.04	50	Medium volatile bituminous	58997	5985531
18.1	11	1.15	357/83	c,u	1.38	0.05	50	Medium volatile bituminous	58997	5985531
18.1	11	0.20	356/83	c,m	1.42	0.05	50	Medium volatile bituminous	58997	5985531
18.1	11	0.75	355/83	c,l	1.46	0.05	50	Medium volatile bituminous	58997	5985531
18.2	11	1.30	362/83	c,u	1.50	0.04	50	Low volatile bituminous	58997	5985531
18.2	11	1.10	361/83	c,u	1.46	0.04	50	Medium volatile bituminous	58997	5985531
18.2	11	0.20	360/83	c,m	1.42	0.06	50	Medium volatile bituminous	58997	5985531
18.2	11	1.30	359/83	c,l	1.49	0.04	50	Medium volatile bituminous	58997	5985531
48	11	*--	532/83	g	1.38	0.04	50	Medium volatile bituminous	60122	5984489
65	11	1.50	349/83	c,u	1.42	0.07	50	Medium volatile bituminous	60957	5986562
65	11	1.00	350/83	c,l	1.44	0.05	50	Medium volatile bituminous	60957	5986562
72	11	0.40	343/83	c,u	1.45	0.04	50	Medium volatile bituminous	60149	5986062
72	11	0.68	342/83	c,l	1.42	0.05	50	Medium volatile bituminous	60149	5986062
215	11	0.45	382/83	c,u	1.40	0.05	50	Medium volatile bituminous	60131	5983928
215	11	0.40	383/83	c,m	1.40	0.04	50	Medium volatile bituminous	60131	5983928
215	11	0.50	384/83	c,l	1.39	0.05	50	Medium volatile bituminous	60131	5983928
216	11	1.25	387/83	c,u	1.40	0.04	50	Medium volatile bituminous	60268	5983791
216	11	1.50	388/83	c,l	1.40	0.04	50	Medium volatile bituminous	60268	5983791
216	11	0.40	389/83	c,l	1.36	0.05	50	Medium volatile bituminous	60268	5983791
216	11	1.00	390/83	c,l	1.38	0.04	50	Medium volatile bituminous	60268	5983791
223	11	*--	394/83	g	1.39	0.04	50	Medium volatile bituminous	60594	5983587
239	11	*--	525/83	g	1.37	0.04	50	Medium volatile bituminous	60518	5984291
245	11	*--	524/83	g	1.39	0.04	50	Medium volatile bituminous	60862	5983965
246	11	*--	522/83	g	1.35	0.05	50	Medium volatile bituminous	60853	5983907
305	11	*--	401/83	g	1.34	0.04	50	Medium volatile bituminous	60533	5983315
321	11	1.20	353/83	g,m	1.40	0.05	50	Medium volatile bituminous	59954	5986062
349	11	*--	521/83	g,l	1.32	0.04	50	Medium volatile bituminous	60704	5983078
369	11	*--	509/83	g	1.38	0.04	50	Medium volatile bituminous	59841	5982755
375	11	*--	517/83	g	1.36	0.06	50	Medium volatile bituminous	59223	5983035
570	11	*--	544/83	g	1.43	0.05	50	Medium volatile bituminous	57080	5986626
570	11	*--	545/83	g	1.43	0.05	50	Medium volatile bituminous	57080	5986626
584	11	*--	543/83	g	1.40	0.05	50	Medium volatile bituminous	57132	5986790
601	11	1.24	448/83	c,u	1.39	0.05	50	Medium volatile bituminous	58448	5986839
601	11	0.95	449/83	c,l	1.50	0.05	50	Low volatile bituminous	58448	5986839
623	11	1.40	488/83	c,u	1.39	0.04	50	Medium volatile bituminous	59604	5988890
623	11	0.85	489/83	c,l	1.41	0.05	50	Medium volatile bituminous	59604	5988890
654	11	1.15	470/83	c,u	1.43	0.04	50	Medium volatile bituminous	58583	5987412
654	11	0.15	472/83	c,l	1.42	0.04	50	Medium volatile bituminous	58583	5987412
659	11	1.40	483/83	c,u	1.34	0.05	50	Medium volatile bituminous	58586	5987644
659	11	0.30	484/83	c,l	1.41	0.05	50	Medium volatile bituminous	58586	5987644
769	11	*--	498/83	g	1.46	0.04	50	Medium volatile bituminous	56367	5987692
1009 (McEvoy Anticline)	11	1.50	459/83	g,u	1.54	0.10	50	Low volatile bituminous	50565	5989647

*-- - seam partly covered
g - grab sample
c - channel sample
s - sheared coal

u - upper portion
m - middle portion
l - lower portion

S - standard deviation
N - number of measurements

Appendix D. Fossil localities

Fauna species	Formation/Member	Easting	Northing
Dunveganoceras sp.	Kaskapau	57848	5982151
Inoceramus athabaskensis	Dunvegan	57430	5987635
Elliptio sp. *Unio* sp.	Mountain Park	56525	5987699
Lioplacodes bituminus	Mountain Park	59357	5982383
Unio douglassi *Murraia (?)*	Grande Cache	60216	5983117
Murraia naiadiformis *Unio (?)*	Grande Cache	58637	5984571
Murraia naiadiformis *Unio douglassi*	Grande Cache	57348	5983712
Ostrea sp.	Torrens	58061	5990006
Protocardium sp. *Melania* sp. *Eupera onesta*	Gladstone	58516	5985105
Pentacrinus sp.	Nikanassin	50335	5985184

Flora species	Formation/Member	Easting	Northing
Ptilophylum sp. *Elatides curvifolia*	Grande Cache	63173	5982953
Elatides sp. *Pityophyllum nordenskjoldi* *Nilsonia canadensis*	Grande Cache	56855	5986570

Trace fossil species	Formation/Member	Stratigraphic section	Distance from base of section
Teichichnus sp. *Palaeophycus* sp. *Thalassinoides* sp. *Lockeia* sp. *Rhizocorallium* sp. *Muensteria* sp. *Diplocraterion* sp. *Arenicolites* sp. *Planolites* sp. *Skolithos* sp.	Gladstone	81-2	122 m
Diplocraterion sp. *Palaeophycus* sp. *Skolithos* sp. *Planolites* sp.	Gladstone	81-1	13 m
Arenicolites sp. *Skolithos* sp. *Planolites* sp.	Moosebar	81-1	75 m
Arenicolites variabilis *Diplocraterion* sp. *Teichichnus* sp. *Skolithos* sp.	Torrens	81-1	120 m
Diplocraterion sp. *Skolithos* sp.	Mountain Park	81-4	282 m

Appendix D. (continued)

Microfossil species	Environment	Formation/Member	Stratigraphic section	Distance from base of section
Foraminifera:				
Hippocrepina (?) sp.	Shallow	Grande Cache	81-8	115 m
Miliammina (?) sp.	brackish marine			
Miliammina (?) sp.	Shallow brackish marine	Grande Cache	81-3	83 m
Ostracoda:				
Cytheridea bonaccordensis Loranger (?)	Shallow brackish marine	Grande Cache	81-3	48 m
Cytheridea bonaccordensis Loranger	Shallow brackish marine	Grande Cache	81-1	142 m
Foraminifera:				
Saccammina sp.	Marine	Moosebar	81-3	40 m
Haplophragmoides sp.				
Haplophragmoides sp.				
Gaudryina tailleuri (Tappan)	Marine	Moosebar	81-1	51 m
Discorbis norrisi Mellon and Wall				
Haplophragmoides sp.A.	Marine	Moosebar	81-1	81 m
Haplophragmoides sp.A.				
Dentalina sp.	Marine	Moosebar	81-1	107 m
Saracenaria trollopei Mellon and Wall				
Hippocrepina (?) sp.	Possibly fresh to brackish marine	Gladstone	81-1	11 m
Thecamoebians:				
Thecamoebian (?) A				

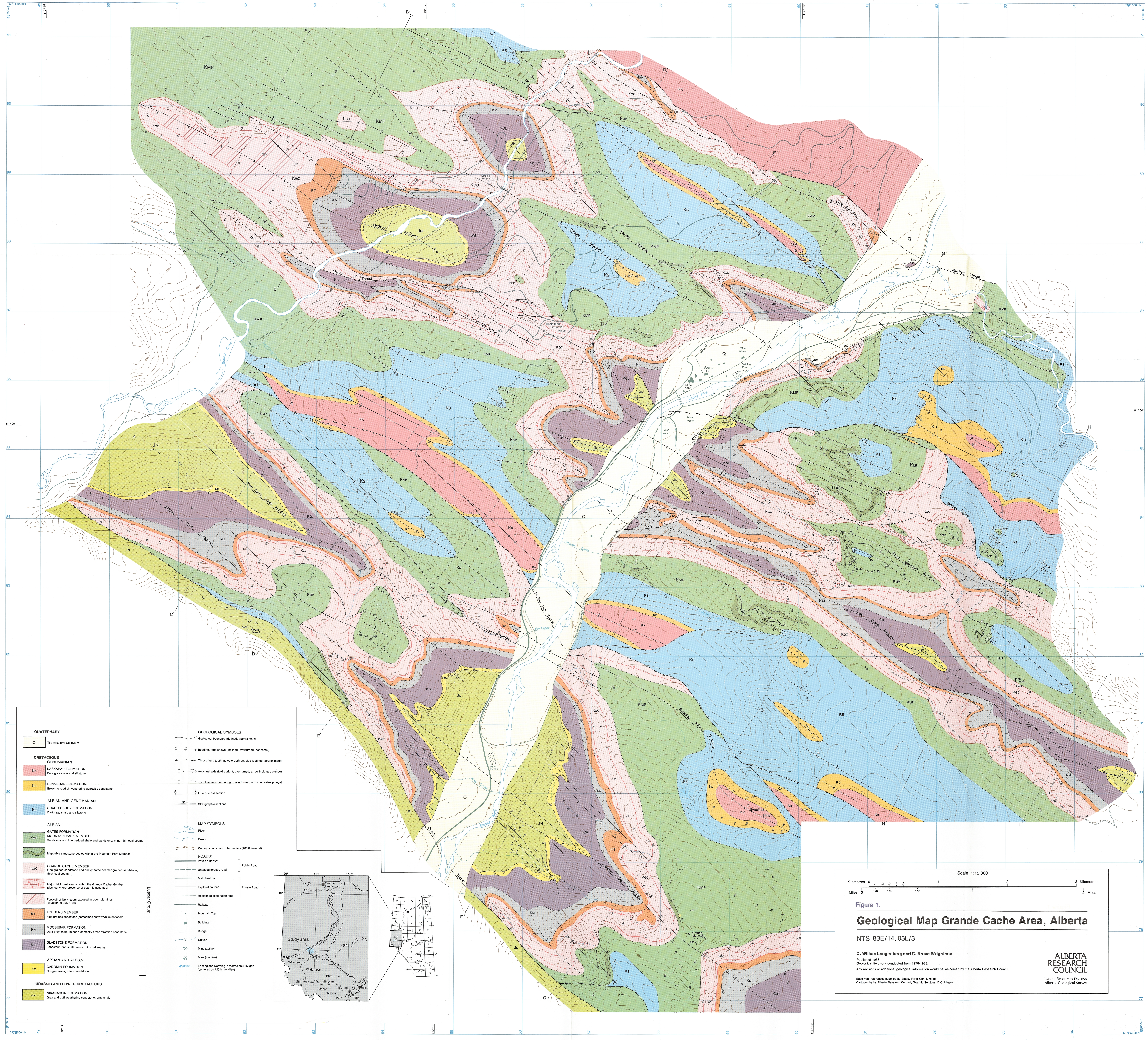

Figure 1.

Geological Map Grande Cache Area, Alberta

NTS 83E/14, 83L/3

C. Willem Langenberg and C. Bruce Wrightson

Published 1986
Geological fieldwork conducted from 1978-1983.

Any revisions or additional geological information would be welcomed by the Alberta Research Council.

Base map references supplied by Smoky River Coal Limited.
Cartography by Alberta Research Council, Graphic Services, D.C. Magee.

ALBERTA RESEARCH COUNCIL
Natural Resources Division
Alberta Geological Survey

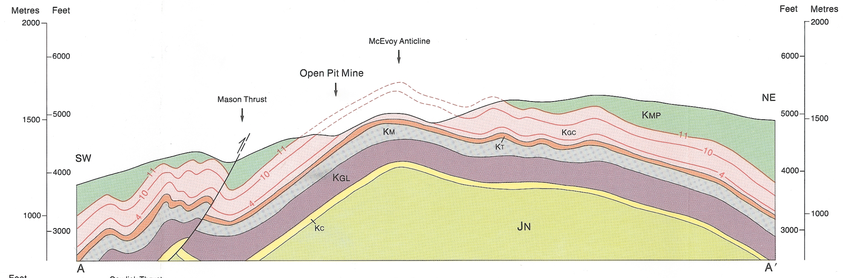

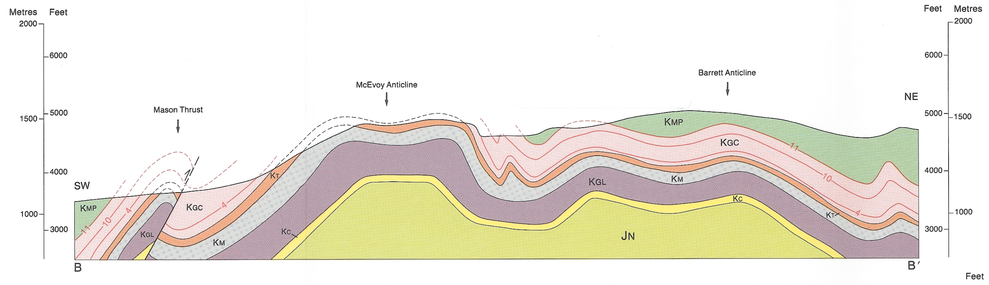

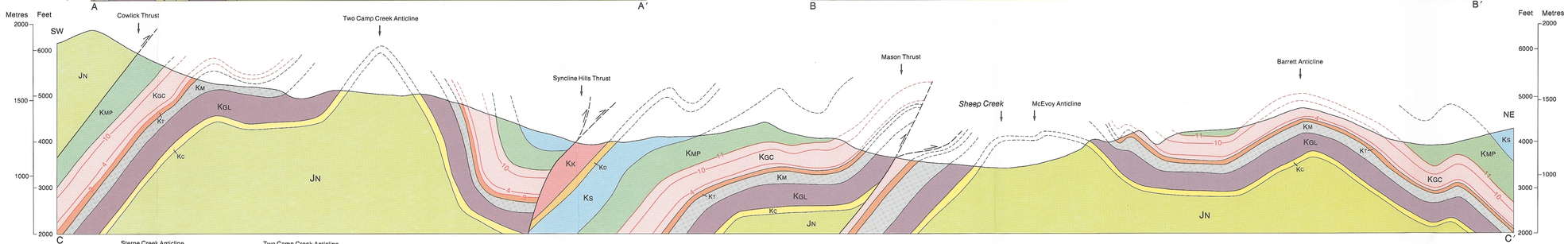

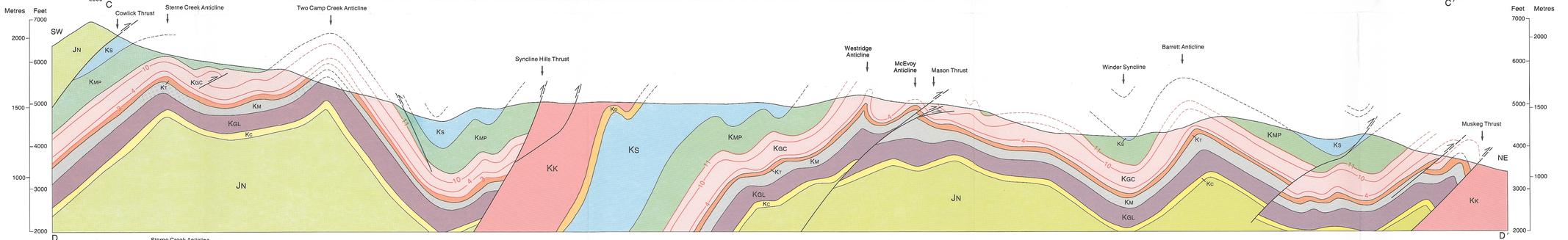

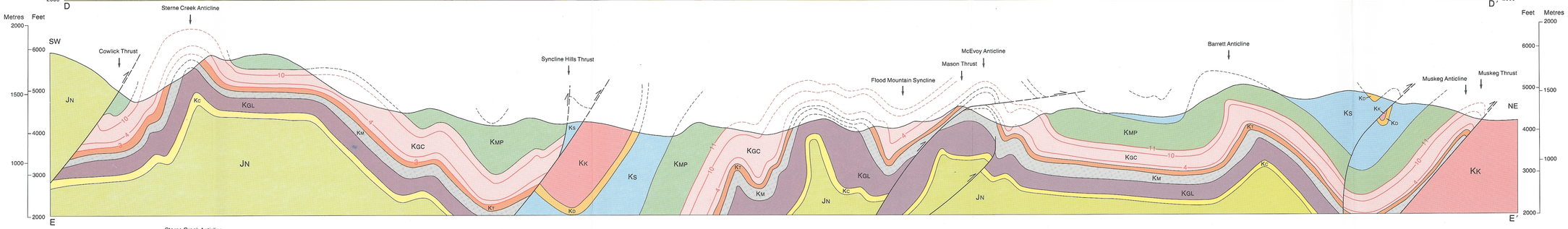

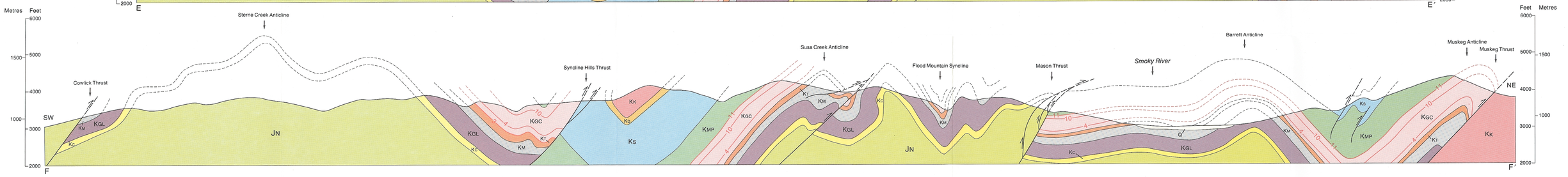

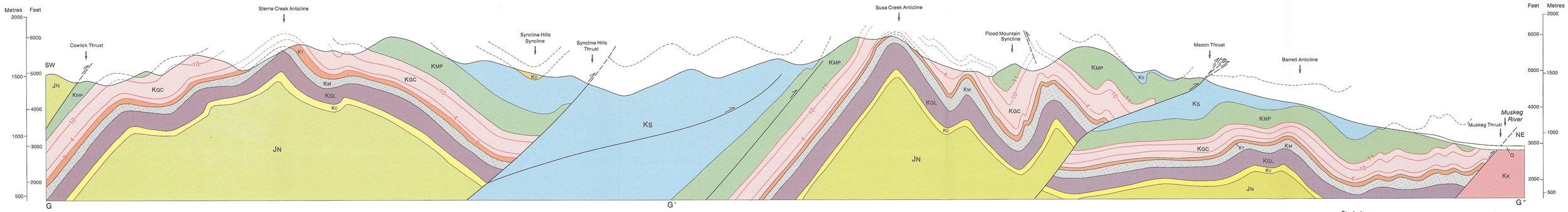

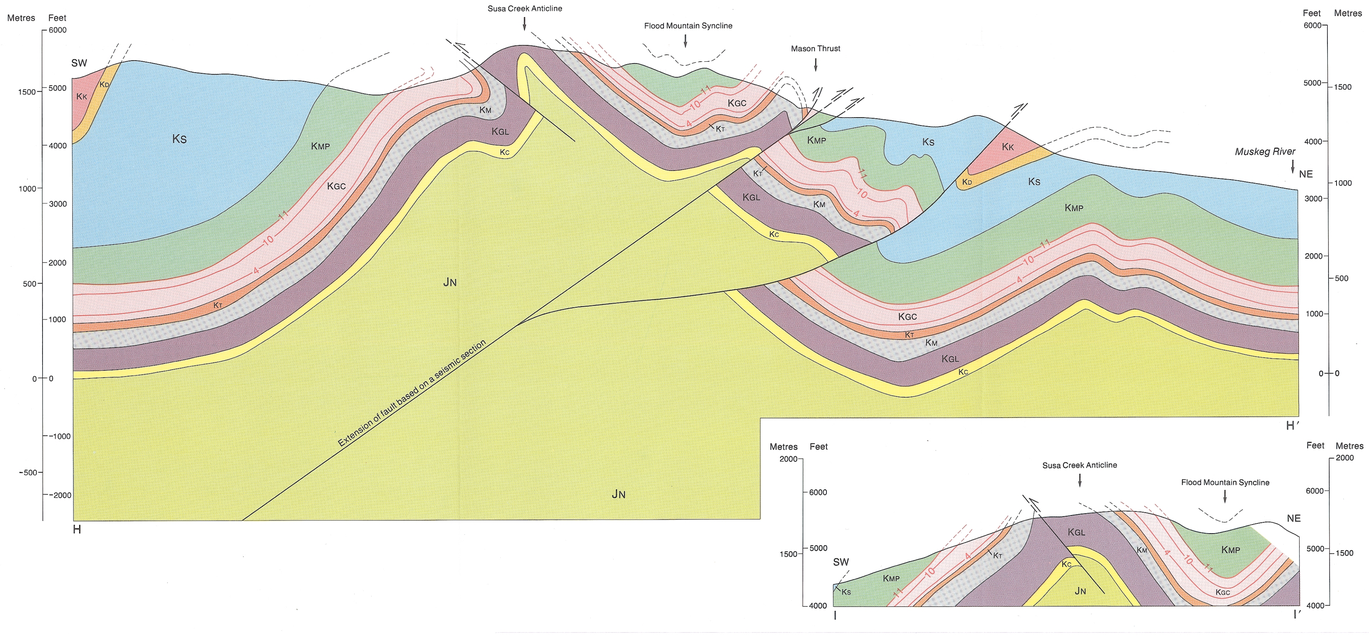

Q Quaternary

KK Kaskapau Formation

KD Dunvegan Formation

KS Shaftesbury Formation

KMP Mountain Park Member

11 10 4 3 Grande Cache Member (including numbers 3, 4, 10 and 11 coal seams)

KT Torrens Member

KM Moosebar Formation

KGL Gladstone Formation

KC Cadomin Formation

JN Nikanassin Formation (may include parts of the Fernie Formation)

Fault with sense of movement

Study Area

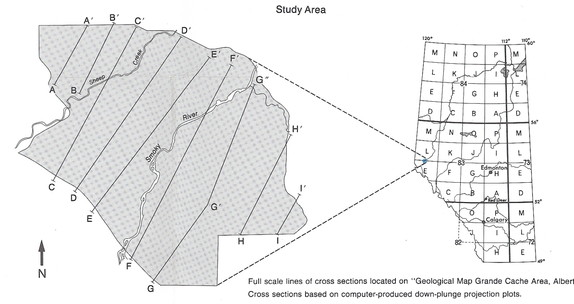

Full scale lines of cross sections located on "Geological Map Grande Cache Area, Alberta."
Cross sections based on computer-produced down-plunge projection plots.

Scale 1:15,000

Kilometres 0 .1 .2 .3 .4 .5 1 2 3 Kilometres

Miles 0 1/8 1/4 1/2 1 2 Miles

Figure 2.

Cross Sections, Grande Cache Area, Alberta

NTS 83E/14, 83L/3

C. Willem Langenberg and C. Bruce Wrightson

Published 1986
Geological fieldwork conducted from 1978-1983

Base map references supplied by Smoky River Coal Limited.
Cartography by Alberta Research Council, Graphic Services, D.C. Magee.

ALBERTA RESEARCH COUNCIL
Natural Resources Division
Alberta Geological Survey

Scale 1:30,000

Kilometres 0 .2 .4 .6 .8 1 2 3 Kilometres

Miles 0 1/4 1/2 1 2 Miles

- 4 — Outcrop trace of number 4 coal seam (dashed where presence of seam is assumed)
- 5000 — Structure contours: index and intermediate (200′ interval)
- 4000 — Structure contour below thrust fault
- Anticlinal axis
- Synclinal axis
- Outcrop trace of thrust fault (defined, approximate)
- Location of drill hole collar
- ▲ Mountain top
- Footwall of Number 4 coal seam in open pit mines (situation in July 1983)
- Location of underground mines in Number 4 coal seam
- 65000mE — Easting and Northing in metres on 3TM grid. (centered on 120th meridian).

Subsurface information supplied by Smoky River Coal Company Limited.

Study Area

Figure 3.

Structure of Top of Number 4 Coal Seam, Grande Cache Area, Alberta

NTS 83E/14, 83L/3

C. Willem Langenberg and C. Bruce Wrightson

Published 1986
Geological fieldwork conducted from 1978-1983.

Any revisions or additional geological information would be welcomed by the Alberta Research Council.

Base map references supplied by Smoky River Coal Limited.
Cartography by Alberta Research Council, Graphic Services, D.C. Magee.

ALBERTA RESEARCH COUNCIL

Natural Resources Division
Alberta Geological Survey